UNIVERSIDADE DE COIMBRA

FACULDADE DE CIÊNCIAS E TECNOLOGIA

DEPARTAMENTO DE CIÊNCIAS DA VIDA

APPROACHES TO IMPROVE THE DIFFERENTIATION, MATURATION AND BIOLOGICAL ACTIVITY OF VASCULAR CELLS DERIVED FROM STEM CELLS

HELENA SOFIA ESMERALDO DE CAMPOS VAZÃO

DOUTORAMENTO EM BIOLOGIA

(ESPECIALIDADE EM BIOLOGIA CELULAR)

2012

UNIVERSIDADE DE COIMBRA

FACULDADE DE CIÊNCIAS E TECNOLOGIA

DEPARTAMENTO DE CIÊNCIAS DA VIDA

APPROACHES TO IMPROVE THE DIFFERENTIATION, MATURATION AND BIOLOGICAL ACTIVITY OF VASCULAR CELLS DERIVED FROM STEM CELLS

HELENA SOFIA ESMERALDO DE CAMPOS VAZÃO

DOUTORAMENTO EM BIOLOGIA

(ESPECIALIDADE EM BIOLOGIA CELULAR)

2012

Supervisor: **Doutor Lino da Silva Ferreira**

Co- Supervisor: **Doutor João Ramalho de Sousa Santos**

Este trabalho foi realizado ao abrigo da bolsa de doutoramento SFRH / BD / 40077 / 2007, concedida a Helena Vazão pela Fundação para a Ciência e a Tecnologia, comparticipado pelo Fundo Social Europeu e por fundos nacionais do MCTES.

Os trabalhos apresentados nesta tese de doutoramento foram ainda apoiados pelas seguintes instituições:

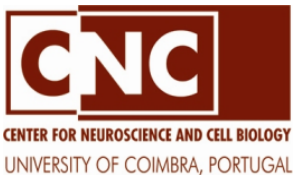

NOTAS PRÉVIAS

Para a elaboração da presente tese de doutoramento foram usados como capítulos artigos científicos publicados, ou em preparação para posterior publicação, em revistas científicas internacionais indexadas. Tendo sido estes trabalhos realizados em colaboração com outros investigadores, esclareço que participei integralmente na concepção e execução do trabalho experimental, na interpretação dos resultados e na redacção dos manuscriptos. Relativamente ao **capítulo 5** participei na concepção, execução, interpretação e redação dos resultados resultantes de todas as figuras; à excepção das figuras **1C, 1D, 8** e **Tabela 2.**

CONTENTS

Agradecimentos 9

Resumo 11

Abstract 13

Acronyms and Abbreviations 15

Chapter 1 - Aims and Outline of the thesis 17

Chapter 2- Introduction 19

1. Human pluripotent stem cells 19

2. Vascular differentiation 20

2.1 Embryonic vascular differentiation 20

2.2 Vascular differentiation of hESCs 22

2.2.1- EC differentiation 22

2.2.1.1 - Differentiation methodologies: yields and kinetics 22

2.2.1.2 - Inductive signals 24

2.2.1.3 - Maturation and functionality of hESC-derived ECs 25

2.2.1.4 - Therapeutic potential of hESC-derived ECs 25

2.2.2 - SMC differentiation 26

2.2.2.1 - Differentiation methodologies: yields and kinetics 26

2.2.2.2 - Inductive signals 27

2.2.2.3 - Maturation and functionality of hESC-derived SMCs 27

2.2.2.4 - Therapeutic potential of SMCs 28

2.3. Vascular differentiation of hiPSCs 31

2.3.1 - EC differentiation 31

2.3.1.1 - Differentiation methodologies: yields and kinetics 31

2.3.1.2 - Therapeutic potential of hiPSC-derived ECs 31

2.3.2- SMC differentiation 32

2.3.2.1 - Differentiation methodologies: yields and kinetics 32

2.3.2.2 - Therapeutic potential of hiPSC-derived SMCs 32

2.4 Tissue engineering applications of vascular cells derived from hPSCs 32

2.5. Future of pluripotent stem cells 33

3. Vascular modulation /applications 37

3.1 Vascular specification plasticity ……..……**37**
3.2 Vascular mechanobiology ……..……**38**
3.2.1 Endothelial cells response to fluid shear stress ……..……**38**
3.2.2 Shear stress in endothelial differentiation ……..……**40**
3.2.3 Shear stress in arterial and in venous endothelial phenotype ……..……**41**
3.2.4 Microfluidic technology in vascular research ……..…**41**
4. Stem cells-derived vascular cells as building blocks for regenerative medicine ……**42**
4.1 Role of VEGF in vascular tissues ..……..……**43**
4.2 VEGF signaling activation pathways …..…… **44**
Bibliography ……..……**45**

Chapter 3 - Towards the maturation and characterization of smooth muscle cells derived from human embryonic stem cells ……**57**

Chapter 4 - Combining pluripotent stem cell-derived endothelial cells with dynamic technology to assess vascular toxicity..……...**91**

Chapter 5 – VEGF-functionalized dextran has longer intracellular bioactivity than VEGF in endothelial cells ……..**117**

Chapter 6 - General conclusions and perspectives……**151**

Agradecimentos

Gostaria de agradecer em primeiro lugar ao Doutor Lino Ferreira, supervisor deste trabalho de doutoramento, pela sua contribuição essencial na idealização, realização, análise e discussão de todos os resultados aqui apresentados. Agradeço toda a disponibilidade e ainda a oportunidade de colaborar como membro do seu grupo desde o início da formação do seu laboratório de Biomaterials and Stem Cell-Based Therapeutics. Muito obrigada pela pronta e eficiente ajuda na revisão desta tese. Quero também agradecer ao meu co-orientador Doutor João Ramalho de Sousa Santos pela sua disponibilidade para me ajudar.

Agradeço aos colegas de grupo, colaboradores do Biocant e do Centro de Neurociências e Biologia Celular que de uma forma ou outra foram relevantes para a criação de condições para o desenvolvimento deste trabalho.

A todos os meus Amigos de sempre ou adquiridos nestes últimos 4 anos, o meu muito obrigada pela presença constante na minha vida. A amizade que recebi foi essencial durante as várias fases deste percurso.

Obrigada aos meus pais, Alice e Levi. A relevância do vosso amor e apoio incondicional ao longo da minha vida é imensurável e mais uma vez foi a base de tudo. Tenho muito orgulho em vocês e estarei para sempre em dívida! Obrigada.

Resumo

As células estaminais embrionárias humanas (hESCs) podem ser uma fonte ilimitada de células endoteliais e de músculo liso para medicina regenerativa, rastreio de compostos farmacológicos e ensaios de toxicologia. Nos últimos 10 anos têm sido feitos avanços significativos na diferenciação de hESC em células vasculares e algumas das estratégias têm sido implementadas recentemente na diferenciação de células estaminais pluripotentes induzidas (hiPSCs). Um dos objectivos desta tese de doutoramento é desenvolver plataformas de diferenciação mais eficientes para obter células de músculo liso (SMC) e células endoteliais (EC) a partir de hESCs. A primeira parte deste trabalho (capítulo 3) demonstra que células $CD34^+$ derivadas de hESC têm maior potencial em se diferenciar em SMCs que células $CD34^-$. Das várias moléculas indutoras testadas, o ácido retinóico (RA) e o factor de crescimento derivado de plaquetas ($PDGF_{BB}$) mostraram ser os mais eficientes no direccionamento da diferenciação de células $CD34^+$ em células progenitoras de músculo liso (SMPCs), caracterizadas pela expressão de genes e proteínas de SMC, secreção de citoquinas de SMC, contracção em resposta a agentes despolarizantes e péptidos vasoactivos e ainda à expressão de genes específicos de SMC em ambiente tri-dimensional. Essas células apresentavam baixa organização das proteínas contrácteis e a resposta contráctil mostrou ser mediada por Ca^{2+}, envolvendo a activação das vias dependentes das cinases Rho A/Rho e Ca^{2+}/calmodulina (CaM) /cadeia leve da miosina (MLCK). As SMPCs obtidas da diferenciação de células $CD34^+$ com RA podem ser maturadas em meio suplementado com endotelina-1, mostrando no final filamentos contrácteis completamente individualizados e organizados. Na segunda parte do trabalho (capítulo 4), mostrou-se que hESCs cultivadas na presença de timosina $\beta 4$, $VEGF_{165}$ e o inibidor da via de sinalização TGF-β (SB431542), adicionados em diferentes fases do processo de diferenciação, dão origem a células precursoras endoteliais que podem amadurecer em células endoteliais arteriais. As células expressam genes arteriais tais como JAG1, ephrin B1 e Hey-2 e a proteína arterial EphB2. As células respondem a fluxo arterial, alinhando-se na sua direcção e aumentando a expressão de genes arteriais. O processo provavelmente envolve o proteoglicano heparano sulfato (HSPG), um componente do glicocalix, o qual é activado pelo efeito de corte do fluido. Os resultados mostram que células endoteliais derivadas de hESCs possuem maior sensibilidade à terbinafine, uma droga antifungica, que células somáticas endoteliais. Células cultivadas em condições fisiológicas de efeito de corte possuem maior sensibilidade que células cultivadas em condições estáticas. Na terceira parte desta tese

(capítulo 5) estudámos também novas abordagens de modulação de actividade vascular, através do factor de crescimento vascular endotelial (VEGF). Neste trabalho demonstrámos que VEGF conjugado ao dextrano (dexOx-VEGF) tem maior bioactividade intracellular em células endoteliais, quando comparado com VEGF livre. O dexOx-VEGF prolonga a fosforilação do receptor 2 de VEGF (VEGFR-2). Tanto o dexOx-VEGF como o VEGF livre activam VEGFR-2 e os complexos são internalizados nos endossomas primários (vesículas $EEA1^{+}$) e depois transportados para os lisossomas (vesículas $Rab7^{+}$). No entanto, após activação celular o dexOx-VEGF é preferencialmente co-localizado nos endossomas primários, onde a sinalização de VEGF ainda está activa; enquanto que o VEGF livre é preferencialmente transportado para os lisossomas. Os resultados mostram ainda que o dexOx-VEGF após a fosforilação do VEGFR-2 induz um aumento do Ca^{2+} intracelular e activa vias a jusante, tais como AKT e ERK1/2. O DexOx-VEGF pode ser integrado num gel de forma a ser incorporado em géis de fibrina que por sua vez contêm células endoteliais (derivadas de células do sangue de cordão umbilical humano), de modo a modular a sua actividade.

Palavras chave: células estaminais embrionárias humanas, células vasculares, células endoteliais, células de músculo liso, RA, $PDGF_{BB}$, TGF-β, Tβ4, $VEGF_{165}$, tensão de corte, mecanotransdução, arterial, venoso, ensaios toxicológicos, engenharia de tecidos, medicina regenerativa.

Abstract

Human embryonic stem cells are an unlimited source of endothelial and smooth muscle cells for regenerative medicine, drug screening and toxicology assays. Significant advances have been made in the last 10 years in driving the differentiation of human embryonic stem cells (hESCs) into vascular cells and some of the approaches have been implemented recently in the differentiation of induced pluripotent stem cells (iPSCs). One of the aims of the PhD thesis was to develop more efficient differentiation platforms to obtain smooth muscle (SMC) and endothelial cells (EC) from hESCs. The first part of this thesis (chapter 3) shows that $CD34^+$ cells derived from hESCs have higher SMC potential than $CD34^-$ cells. From all inductive signals tested, retinoic acid (RA) and platelet derived growth factor ($PDGF_{BB}$) are the most effective agents in guiding the differentiation of $CD34^+$ cells into smooth muscle progenitor cells (SMPCs) characterized by the expression of SMC genes and proteins, secretion of SMC-related cytokines, contraction in response to depolarization agents and vasoactive peptides and expression of SMC-related genes in a 3D environment. These cells are also characterized by a low organization of the contractile proteins and the contractility response is mediated by Ca^{2+}, which involves the activation of Rho A/Rho kinase- and Ca^{2+}/calmodulin (CaM) /myosin light chain kinase (MLCK)-dependent pathways. SMPCs obtained from the differentiation of $CD34^+$ cells with RA, can be maturated in medium supplemented with endothelin-1 showing at the end individualized contractile filaments. In the second part of this thesis (chapter 4), our results show that vascular endothelial growth factor ($VEGF_{165}$), thymosin β4 (Tβ4), and TGF-β inhibitor administered at different times over a 18 day-differentiation protocol can give rise to endothelial precursor cells that have the ability to differentiate into arterial ECs. The cells express arterial genes such as JAG1, ephrin B1 and Hey-2 and the arterial protein EphB2. The cells respond to arterial flow by aligning in the direction of the flow and further up-regulating the expression of arterial genes. The process is likely mediated by heparan sulfate proteoglycan (HSPG), a component of glycocalyx, which is activated by fluidic shear stress. Our results show that hESC-derived ECs have higher sensitivity to terbinafine, an antifungal drug, than somatic human umbilical arterial endothelial cells. Cells cultured under physiologic shear stress have higher sensitivity to terbinafine than cells cultured in static conditions. In the third part of the thesis (chapter 5) we also investigated new approaches to modulate vascular cell activity, through vascular endothelial growth factor. Our results show that VEGF functionalized dextran (dexOx-VEGF) has longer intracellular bioactivity in endothelial cells when compared to free VEGF. It prolongs the phosphorylation of VEGF receptor 2 (VEGFR-2). Both dexOx-VEGF and

free VEGF activate VEGFR-2 and the complexes are internalized into early endosomes ($EEA1^+$ vesicles) and then transported to lysosomes ($Rab7^+$ vesicles). However, after cell activation dexOx-VEGF is preferentially co-localized in early endosomes where VEGF signaling is still active while soluble VEGF is preferentially transported to late endosomes or lysosomes. The results further show that dexOx-VEGF after phosphorylation of VEGF receptor 2 induces an increase of intracellular Ca^{2+} and activates VEGF downstream effectors such as Akt and extracellular signal-regulated kinase (ERK1/2) proteins. Under specific conditions the activation level is different from the one observed for soluble VEGF, thus suggesting mechanistic differences, which is illustrated by functional cell migration studies. DexOx-VEGF can be crosslinked with adipic acid dihydrazide to form a degradable gel, which in turn can be incorporated in a fibrin gel containing endothelial cells (derived from human cord blood) to modulate their activity.

Keywords: human embryonic stem cells, vascular cells, endothelial cells, smooth muscle cells, RA, $PDGF_{BB}$, TGF-β, Tβ4, $VEGF_{165}$, shear stress, mechanotransduction, arterial, venous, toxicology assays, tissue engineering, regenerative medicine.

Acronyms and abbreviations

3D	tri-dimensional
α-SMA	smooth muscle α-actin
ADMA	asymmetric dimethyl arginine
bFGF	basic fibroblast growth factor
BSA	bovine serum albumin
CALP	calponin
cDNA	complementar desoxiribonucleic acid
ct	cycle threshold
DAPI	4', 6'-diamidino-2-phenylindole
dexOx-VEGF	VEGF functionalized dextran
DiI-Ac-LDL	DiI-labeled acetylated low-density lipoprotein
DMEM	cell culture basal medium
DMSO	dimethyl sulfoxide
EBs	embryoid bodies
ECM	extracelular matrix
EGM-2	endothelial growth medium-2
ELISA	enzyme-linked immunoabsorbent assay
End-1	endothelin-1
FACS	fluorescence activated cell sorting
FBS	fetal bovine serum
Flk-1/KDR	vascular endothelial growth factor receptor 2
G-CSF	granulocyte colony-stimulating factor
GM-CSF	granulocyte/macrophage colony-stimulating factor
hESCs	human embryonic stem cells
hiPSCs	human induced pluripotent stem cells
hPSCs	human pluripotent stem cells
HUAECS	umbilical artery endothelial cells
hVSMCs	human vascular smooth muscle cells
HUVEC	human umbilical endothelial cells
IFN-γ	interferon gama
IgG1/ IgG2A	isotype controls

IL	interleukin-1
M199	basal medium
MACS	magnetic cell sorting
MCP-1/MCAF	monocyte chemotactic protein
MEF	mouse embryonic fibroblast
MIP-1β	macrophage inflammatory protein
mRNA	messenger RNA
PBS	phosphate buffered saline
PCR	polimerase chain reaction
$PDGF_{BB}$	platelet derived growth factor
qRT-PCR / qPCR	quantitative real time polimerase chain reaction
RA	retinoic acid
RNA	ribonucleic acid
SMCs	smooth muscle cells
SMGM-2	smooth muscle growth medium-2
SMLCs	smooth muscle-like cells
SM-MHC	smooth muscle myosin heavy chain
SMPCs	smooth muscle progenitor cells
Tβ4	thymosin beta4
TBS	tris buffered saline
$TGF_{\beta\text{-}1}$	transforming growth factor beta 1
TNF-α	tumor necrosis factor
VeCad	vascular endothelial cadherins
VEGF	vascular endotelial growth factor
VSMCs	vascular smooth muscle cells
vWf	von Willebrand factor
vWfpp	von Willebrand factor pro-peptide

CHAPTER 1 – Aims and thesis outline

The present work aims at developing new differentiation/maturation protocols of human embryonic stem cells (hESCs) into vascular cells and to identify new strategies to modulate vascular cell activity. The application of hESC-derived vascular cells in regenerative medicine, drug screening and toxicology studies requires the use of mature and functional cells. The results described in this thesis show for the first time part of the mechanism underlining the maturation process of hESC-derived smooth muscle cells and the specialization of hESCs into arterial endothelial cells. A particular innovative aspect of the thesis is related to the use of hESC-derived endothelial cells for drug screening/toxicology assessment under physiologic shear stress. Another significant contribution of the present work is to identify a new strategy to manipulate vascular cells by the use of a new conjugate of vascular endothelial growth factor (VEGF).

The specific goals of this thesis can be summarized as follows.

In chapter 2, to review the vascular potential of human pluripotent stem cells, the mechanobiology in cells cultured under fluidic shear stress and the role of VEGF in vascular cells.

In chapter 3, to develop an efficient differentiation platform of hESCs into smooth muscle cells (SMCs) and to characterize the maturation and functionality of the derived cells.

In chapter 4, to develop an efficient differentiation platform of hESCs into endothelial cells (ECs) and to characterize the maturation process, sub-phenotype and functionality of the derived cells; to study the effect of shear stress in the phenotype specification of hESC-derived ECs; to use hESC-derived cells cultured under physiologic shear stress for drug screening/toxicology assessment.

In chapter 5, to develop a new approach to control the bioactivity of VEGF by conjugating the biomolecule to a polysaccharide; to incorporate the VEGF conjugate in a three-dimensional matrix for endothelial cell transplantation.

In chapter 6, to highlight the general conclusions and discuss future opportunities arising from this thesis.

CHAPTER 2 - Introduction

1. Human pluripotent stem cells

Human pluripotent stem cells (hPSCs) including human embryonic stem cells (hESCs) and human induced pluripotent stem cells (hiPSCs) are promising sources of vascular cells for regenerative medicine, drug discovery and toxicology assays. hESCs derived from the inner cell mass of blastocysts were originally isolated by James Thomson and co-workers [1]. hiPSCs derived by the transfection of adult skin cells (fibroblasts) with four pluripotency genes were isolated and characterized for the first time by Shinya Yamanaka and James Thompson labs in 2007 [2,3]. hiPSCs have similar properties to hESCs including similar morphology, karyotype, high level of telomerase, expression of characteristic genes and proteins, ability to give rise to cells of the three germ layers; endoderm, ectoderm and mesoderm, and can be maintained *in vitro* for several months without losing their properties [1,4] .

hPSCs are an important system to study embryonic vasculogenesis, being vasculogenesis the process by which blood vessels are formed *de novo*. In mammals, vasculogenesis occurs in parallel with hematopoiesis, the formation of blood cells [5]. In addition, hPSCs represent an unlimited source of vascular cells for regenerative medicine. hPSC-derived vascular cells can be useful to both initiating vasculogenesis and angiogenesis in clinical ischemic conditions [6,7,8,9,10]. Angiogenesis stimulation by hPSC-derived vascular cells can be induced from their secretion of pro-angiogenic and pro-survival growth factors and cytokines as well as from the physical contact with pericytes or smooth muscle cells [11]. Finally, although less explored, hPSC-derived vascular cells can be an important model for drug screening and toxicology assays [12]. The establishment of hPSC cell lines from patients with inherited diseases presenting vascular abnormality should enable the identification of new drugs to treat the disease.

Several methodologies have been reported in the differentiation of human pluripotent stem cells (both human embryonic stem cells and induced pluripotent stem cells) into vascular cells and these achievements have been recently reviewed elsewhere [11,13,14,15]. A major challenge in this field is to develop more efficient protocols (in terms of differentiation yield and kinetics) for the differentiation of hPSCs, and in conditions that might be suitable for clinical translation (i.e., in serum-free conditions). Another challenge is related to the development of methodologies that are conducive to the full maturation of vascular cells.

2. Vascular differentiation

2.1 Embryonic vascular differentiation

During embryonic development, there are four key steps in vasculogenesis: (i) the establishment of the angioblasts from mesoderm, (ii) the assembly of angioblasts into vascular structures, (iii) the formation of vascular lumens, and (iv) the organization of continuous vascular networks. Vasculogenesis occurs at two distinct embryonic locations during development: the extraembryonic and intraembryonic tissues [16], [5]. Extraembryonic vasculogenesis precedes intraembryonic vascular development, and in mammals appears as blood islands assembling within the mesodermal layer of the yolk sac. Endocardium and great vessels are the first intraembryonic endothelial structures formed during development [17].

Some of the steps in vasculogenesis have been reproduced and identified in the hESC differentiation system [18,19]. It has been shown that hESC-derived hemangioblast (a precursor of endothelial and hematopoietic cells) expresses KDR and develops within 72 to 96 hours of EB differentiation, the stage during which KDR and CD117 are expressed on distinct populations, prior to the expression of CD31 and CD34. These human hemangioblasts generate distinct blast colonies that display hematopoietic and endothelial potential [18] **(Figure 1)**.

The molecular regulation in the vascular development has been clarified by several studies in the last decade (reviewed in ref. [16].). Fibroblast growth factor (FGF), bone morphogenetic protein (BMP) and Wnt signaling pathways seem to be key components required for hematovascular differentiation in differentiating embryonic stem cells [20] [16]. The vascular endothelial growth factor (VEGF) is the first secreted molecule with specificity for the endothelium during development. Cells that respond to VEGF must first express its receptors, Flk-1/KDR and Flt-1 (VEGFR2 and VEGFR1) [21]. Therefore, the appearance of Flk-1/KDR expression is a marker for hemangioblasts during early development [18]. In addition to the early events, there are regulatory factors required for blood vessels to assemble. For example some paracrine factors have an important role in endothelial cell survival and remodeling of the capillary complex (e.g.: angiopoietin) [22].

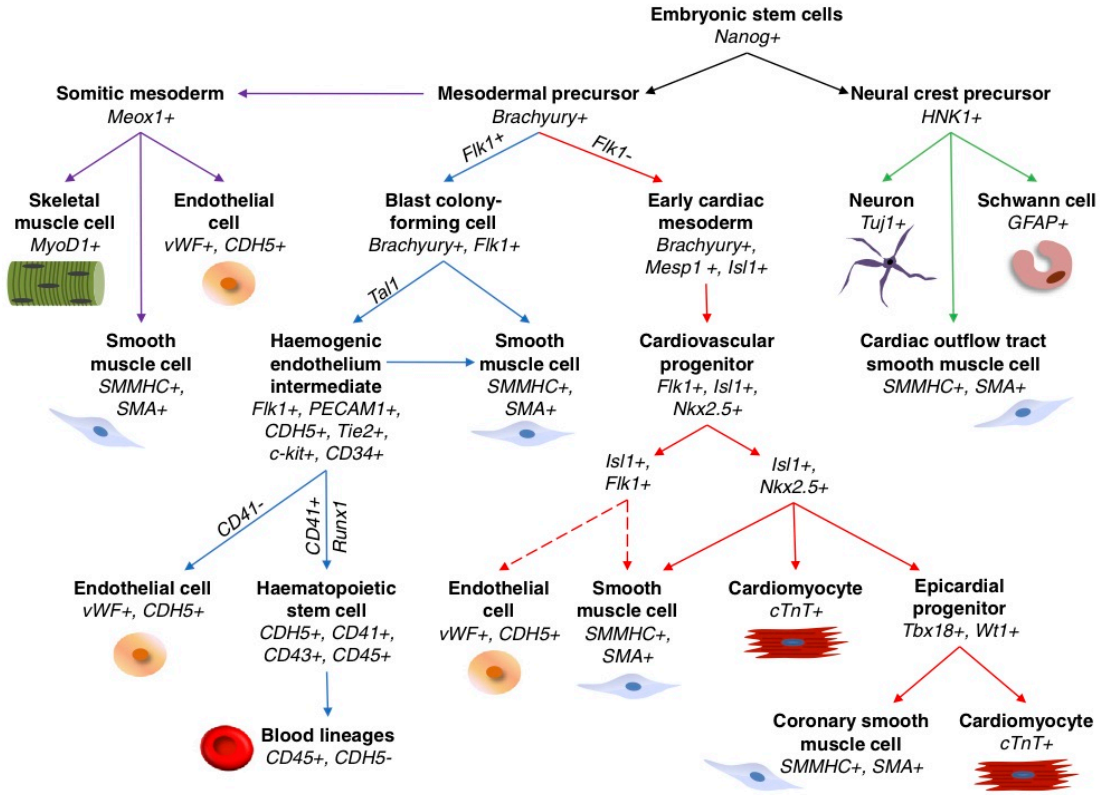

Figure 1: Schematic diagram showing the generation of smooth muscle and endothelial cells from embryonic stem cells. The differentiation pathways were obtained from embryological and embryonic stem cell differentiation studies. Positive and/or negative expression of phenotypic markers for the particular cell types are represented in italic. Derivatives of cardiac mesoderm, haemangioblast, somitic mesoderm and neural crest are indicated by red, blue, purple and green arrows respectively. Dotted arrows denote speculative differentiation pathways where there is still insufficient evidence at present. Figure and legend adapted from [23].

After the vasculogeneis and angiogenesis, primordial vascular smooth muscle cells (VSMCs) are recruited to the endothelium to form a multilayered vessel wall. Platelet-derived growth factors are required for recruitment of pericytes and smooth muscle cells to invest in developing arteries and establish vasomotor tone [24]. As VSMCs become associated with the vascular endothelium, they produce and organize extracellular matrix (ECM) molecules within the vessel wall [25]. Primordial VSMCs also proliferate shortly after association with the nascent endothelium [26]. As the vasculature matures, the presence of VSMCs provides for vascular tone, control of peripheral resistance, and for distribution of blood flow throughout the developing organism [26].

Most of the VSMCs derive from mesoderm, with the exception of VSMCs from the great vessels (ascending aorta and branchial arches) that are derived from the cranial neural crest and VSMCs of the coronary artery, which are derived from cells that have migrated from the epicardium (reviewed in ref. [27]). Although the molecular basis for phenotypic modulation of VSMCs is poorly understood, specific cytoskeletal and

contractile proteins such as α-smooth muscle actin (α-SMA), calponin, caldesmon, smooth muscle myosin heavy chain (SM-MHC) and smoothelin have been found to characterize VSMC differentiation [28,29]. In contrast to α-SMA, which may also be also expressed by other cells, the smooth-muscle-specific isoforms of myosin heavy chains, SM-1 and SM-2, appear to be specific markers for VSMCs [30]. Smoothelin, a protein identified from adult chicken gizzard smooth muscle, is expressed in all vertebrates and is purported to be a very late marker for differentiated, contractile SMCs [30].

2.2 Vascular differentiation of hESC

2.2.1- EC differentiation

2.2.1.1 - Differentiation methodologies: yields and kinetics

Several methodologies have been used for the vascular differentiation of hESCs such as embryoid bodies (EBs) which recapitulates *in vivo* embryogenesis [9,31], a mixture of EBs with 2D or 3D culture systems [10], [7,8], [7], [32] and co-culture with cell lines [33,34,35,36] (**Figure 2**). Typically, EB differentiation protocols, where cells are allowed to spontaneously differentiate into all the germinative cell layers, are relatively inefficient in driving the vascular differentiation of the cells (yields below 5%) [9], [8]. Although, recent studies have used different approaches to ameliorate the efficiency of system by using inductive agents (e.g. TGFβ-1 inhibitor [37] and $VEGF_{165}$ [38]), bioengineering approaches (including scaffolds [39] or micro- and nanoparticles [40]), or specific culture conditions (e.g. hypoxia) [41], the yield (with few exceptions, the yield is generally below 5-10%) is relatively low. Methodologies using co-culture systems might be more efficient, in terms of yield, in the vascular differentiation of hESCs. Several types of feeder layers have been used including mouse embryonic fibroblasts [35], OP9 stromal cells [36,42] M2-10B4 stromal cells [43] and S17 stromal cells [34].

Endothelial cells (ECs) can be isolated from a heterogeneous cell population by fluorescence activated cell sorting or magnetic activated cell sorting. A marker that has often been used to isolate ECs is CD31 [9,44]. In some cases (either in methodologies comprising EB or co-culture with cell lines), the protocols involve the isolation of hemangioblasts (cells that have the capacity to give rise to endothelial and hematopoietic cells; e.g. $CD31^+$/KDR/$VE\text{-}cad^+$ cells isolated at day 10 of EB differentiation [31], KDR^+ cells isolated at day 4 of EB differentiation [18], or $CD34^{bright}CD31^+KDR^+$ cells isolated at day 14 of a co-culture differentiation system [34]), or vascular progenitor cells (progenitor

cells that have the ability to give rise to endothelial and smooth muscle cells; e.g. $CD34^+$ cells isolated from EBs at day 10 [8], $CD34^+$ cells isolated from hESCs co-cultured with M2-10B4 stromal cells or Wnt1 expressing M2-10B4 for 13–15 days [43], $KDR^+/TRA1\text{-}60^-$ cells isolated at day 8 of a co-culture differentiation system [33]). In both cases, hemangioblasts or vascular progenitor cells are then cultured in medium conditions that drive their differentiation into ECs. Although the isolation of these progenitor cells are important to understand issues related to developmental biology and their therapeutic effect, the percentage of these cells is relatively low (below 5%). A recent study has reported an efficient methodology to derive functional hESC-derived $CD34^+$ progenitor cells (vascular progenitor cells) by both inhibition of MEK/ERK signaling and activation of BMP4 signaling [45]. hESC-derived $CD34^+$ cells were differentiated into functional endothelial cells and contributed to blood perfusion and limb salvage through neovasculogenesis in hind limb ischemic mice.

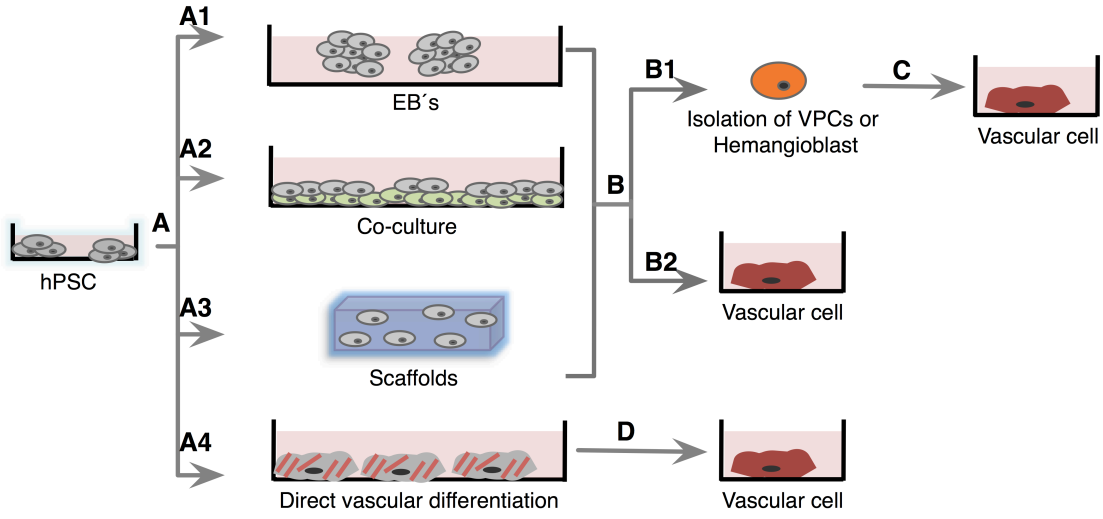

Figure 2: Schematic diagram of the differentiation protocols used in the vascular differentiation of human pluripotent stem cells. (A1): Differentiation through an EBs stage; (A2): differentiation in a co-culture system with feeder cells; (A3): differentiation in 3D scaffolds; (A4): differentiation in 2D cultures using biomolecules. The differentiation process can include (B1) isolation of VPCs or hemanglioblats or the direct differentiation of the cells into vascular cells (B2, C, D). *hPSC*: human pluripotent stem cells; *EB´s*: embryoid bodies; *VPCs*: vascular progenitor cells.

Few of the protocols reported so far have been carried out in serum-free conditions [37], [46], [32]. Kane and co-workers have expanded hESCs in feeder-free conditions using pluripotency medium that was then replaced by endothelial growth medium [46]. In these conditions, 82% of the cells co-express vascular endothelial-cadherin (VE-cad) and

CD31 at day 21 of differentiation. Although it is necessary to show that the same efficacy can be obtained for several cell lines of hESCs and the phenotype is preserved after several cell passages, the results are very encouraging for the potential clinical application of these cells. In a separate study, Rafii and co-workers developed a methodology for the long-term expansion of hESC-derived ECs in serum-free conditions [37]. They have identified TGFβ1 inhibitor SB431542 as a key molecule for human endothelial differentiation and proliferation in serum-free conditions.

2.2.1.2 - Inductive signals

The differentiation of hESCs into vascular progenitor cells and then into ECs is largely dependent on the modulation of several intracellular signaling pathways including BMP4, Wnt and VEGF. BMP4 (and also BMP2 or 7, but not BMP9), VEGF and FGF2 were shown to be critical for the induction of hESCs into vascular progenitor cells ($CD34^+CD31^+$ cells) [47]. Using a 12-day protocol relying on a stromal cell co-culture and defined media formulations, Bai and colleagues achieved 10% efficiency and showed that BMP4, acting through the Smad1/5/8 pathway, is required at an early stage of differentiation (days 1 to 6), whereas VEGF and FGF2 are necessary at later stages (day 4 up to day 12). The early requirement for BMP4 is thought to be related with the blocking of pluripotency and the induction into mesodermal lineages. ECs could be further differentiated from the $CD34^+CD31^+$ subpopulation with good efficiency, since approximately $1.3x10^4$ ECs were obtained from $1x10^4$ $CD34^+CD31^+$ cells, which in turn had been achieved from 1×10^5 hESCs.

Wnt signaling has been also investigated to enhance the differentiation of hESCs into vascular progenitor cells with the capacity to further differentiate into ECs. Wnt1 (and Wnt5, to a lesser extent), expressed and putatively secreted by Wnt1- (or Wnt5-) overexpressing stromal cells used in a stromal-hESC co-culture system, increased the efficiency of hESC differentiation into $CD34^+$ cells between 3 to 4 fold, as compared to the effect of the unmodified feeder cells [34,43]. Canonical (Wnt1) signaling pathway seems to be the most important for the endothelial differentiation of hESCs [34]; however it is unclear the signaling events occurring downstream of Wnt.

The differentiation of vascular progenitor cells into ECs is mediated by VEGF signaling. Vascular progenitor cells ($CD34^+$ cells) can be differentiated into cells with mature and functional features of ECs (both *in vitro* and *in vivo*), by stimulation with VEGF [8]. It was later shown that the presence of VEGF at the EB differentiation stage increases the presence of vascular progenitor cells with potential to differentiate into ECs [38],

suggesting that VEGF plays an inductive role at various stages of hESC-derived ECs differentiation.

2.2.1.3 - Maturation and functionality of hESC-derived ECs

Several studies have shown that hESC-derived ECs are functional since they are able to synthesize nitric oxide, form vascular network *in vitro* when cultured on top of Matrigel, metabolize acetylated low-density lipopoprotein (DiI-Ac-LDL), and produce extracellular matrix for developing a basal lamina [8], [7,9] [10] [31,32] [37]. Furthermore, *in vivo* studies have shown that hESC-derived ECs form microvessels that anastomose with animal vasculature [48] [43] [9] [10], enhancing blood flow [9] [33] [7] [45]. Unfortunately, to the best of our knowledge, there is no report showing the specification of the human hPSC-derived ECs into arterial, venous, lymphatic or brain-like phenotype either *in vitro* or after transplantation in animal models. A recent study has shown that mouse ESC-derived ECs have a preferential venous phenotype [49,50], and this might be due to the fact that venous is the default EC phenotype during development [50]. During embryonic development, specification into arterial-, venous-, lymphatic- or brain-derived ECs is defined at gene level and is mediated by several signaling pathways including VEGF, Notch and ephrin before circulation begins [51,52]. Studies in mouse have shown that ephrinB2 and its receptor EphB4 are differentially expressed in arterial and venous endothelial cells, respectively, before the onset of circulation in the developing embryo [53]. After the onset of the circulation, the distinct hemodynamic forces found in arteries and veins, such as blood flow rate, direction and pressure, can be a major driver in the specification of the endothelial cells [51,52]. Further research is needed to evaluate the effect of these parameters in the phenotype of hESC-derived ECs.

2.2.1.4 - Therapeutic potential of hESC-derived ECs

The therapeutic potential of hESC-derived ECs has been evaluated in animal models of hind limb [46] [7] [32] [33] [42], myocardial infarction [6] [10] [32] and after subcutaneous transplantation in immunodefficient rodents [8] [9] (**Table 1**). Most studies have demonstrated that the transplanted hESC-derived ECs could be successfully incorporated into the host vasculature and significantly accelerate local blood flow [33] [42] [54] [7]. Importantly, mature ECs (not derived from hESCs) had not the same therapeutic effect when transplanted in the same animal models and thus suggesting that the hESC-derived ECs have high pro-angiogenic properties [46] [33]. Indeed, these cells express several angiogenic growth factors including VEGF, bFGF, HGF, and PDGF-BB [33]. Recent

studies indicate that a key player for the enhanced therapeutic effect of hESC-derived ECs is Sirt1, a nicotinamide adenine dinucleotide (NAD^+)-dependent histone deacetylase [55]. Inhibition of Sirt1 attenuates the differences in functionality between hESC-derived ECs and adult ECs.

Several variables affect the final therapeutic outcome of the ECs derived from hPSCs. For example, the combined transplantation of hESC-derived ECs with hESC-derived SMCs has higher therapeutic effect than each cell type administered alone [42]. Both cells injected intra-arterially can augment neovascularization in an animal model of hindlimb ischemia. In addition, co-implantation of hESC-derived ECs with mouse embryonic fibroblasts form durable blood vessels *in vivo* [35]. At the moment, it is unclear whether the improvement is due to cell-cell interactions or soluble factors released by the mural cells. The differentiation stage of hESC-derived ECs also affects their therapeutic outcome. Highly differentiated [33] or very immature (KDR^+/TRA1-60^-) [33] hESC- derived ECs do not improve local blood flow in murine hindlimb ischemia model. However, hESC-derived ECs after moderate differentiation (10 days) produce nitric oxide, express angiogenesis-associated mature miRNAS (miR-126, 130a, 1331 and b, and 210), and augment neovascularization in hindlimb ischemia [46].

2.2.2 - SMC differentiation

2.2.2.1 - Differentiation methodologies: yields and kinetics

Different strategies have been reported to differentiate hESCs into smooth muscle like cells (SMLCs) by exposing a monolayer of undifferentiated hESCs to retinoic acid [56] or a combination of cell culture medium and extracellular matrix environment [57] [12] [8] either in single-hESC- [58], embryoid bodies (EBs)- [8] or stromal cell- [43] culture conditions (**Fig.2**). Most of the protocols reported so far have high efficiencies (i.e., high yields) in the differentiation of hESCs into SMLCs. For example, more than 90% of hESCs treated with basal medium supplemented with retinoic acid (10 μM) for 15 days express α-SMA. However, only 65% of the cells express mature markers such as SM-MHC. We [8] [59] and others [42] have also reported efficient (above 90% of the cells expressed α-SMA) differentiation protocols comprising the isolation of vascular progenitor cells ($CD34^+$ [8] [59]) or KDR^+/$TRA1^-$ [42] followed by their differentiation in specific medium. We found that vascular progenitor cells ($CD34^+$ cells) have higher SMC potential than $CD34^-$ cells and $PDGF_{BB}$ and RA were the most effective agents to drive the differentiation of hESCs into SMLCs [59]. We have further demonstrated that the SMLCs cells contract and relax in response to SMC agonists or inhibitors, respectively, and the effect is mediated by Rho

A/Rho kinase- and Ca^{2+}/ CaM / MLCK-dependent pathways. Recent studies demonstrated an essential role of microRNAs in SMC differentiation – for example, miR-145 can regulate the fate of ES-pre-SMCs as they become differentiated SMCs [60].

2.2.2.2 - Inductive signals

Three types of differentiation protocols have been adopted so far for the differentiation of hESCs into SMCs: (i) single-step protocols, characterized by the direct differentiation of undifferentiated hESCs into SMCs; (ii) two-step protocols, characterized by the isolation of vascular progenitor cells and then the differentiation of the progenitor cells into SMCs; and (iii) induction of an intermediate state population, characterized by the formation of neuroectoderm, lateral plate mesoderm or paraxial mesoderme an further differentiation to SMCs [61]. Relatively to the first type of protocols, it has been shown that retinoic acid [56], PDGF-BB [58] [12] and TGF-β1 [58] [12] signaling pathways are very important for the direct differentiation of hESCs into SMCs. Relatively to the second type of protocols, the inductive signals to enhance the generation of vascular progenitor cells are described in section 3.1, while the signals to induce the differentiation of vascular progenitor cells into SMCs include PDGF-BB [8] [42] and retinoic acid [59]. We have shown that vascular progenitor cells ($CD34^+$ cells) differentiate into vascular smooth muscle-like cells in culture medium supplemented with PDGF-BB [8] [59]. The cells exhibited spindle-shape morphology, expressed several SMC markers (such as α-SMA, SM-MHC, calponin, caldesmon and SMα-22), had the ability to contract and relax *in vitro* in response to carbachol and atropine, and when transplanted subcutaneously in an animal model contributed to the formation of microvessels. We have also demonstrated that TGF-β1 had low inductive effect in the differentiation of vascular progenitor cells into SMCs [59]. In line with these studies, others have demonstrated that hESC-derived vascular progenitor cells (presenting a $Tra^-VEGF\text{-}R2^+PDGF\text{-}R^+$ phenotype) required PDGF-BB to differentiate into vascular smooth muscle-like cells [42]. These cells could enhance blood flow after transplantation into a mouse hindlimb ischemia model.

2.2.2.3 - Maturation and functionality of hESC-derived SMCs

The development of mature contractile SMCs from stem cells occurs in multiple steps comprising (i) the commitment to the SMC lineage, (ii) the differentiation into early immature and (iii) the maturation into the mature contractile phenotype [62]. We and others have reported that vascular progenitor cells ($CD34^+$ cells [8], $KDR^+/TRA1\text{-}61^-$ cells [42]) could give rise to SMLCs when cultured in medium supplemented with $PDGF_{BB}$;

however, the differentiation of SMLCs was not complete since the assembly of α-SMA or SM- MHC proteins into filaments was not observed [8], and the presence of some SMC markers was not detected [42]. Recently we have shown that the co-culture of SMLCs with fully differentiated hVSMCs induces the assembly of α-SMA and calponin proteins into individualized filaments [59]. This indicates that the cells are able to maturate into a fully contractile phenotype. We have further shown that the maturation of SMLCs can be induced by endothelin-1, an agonist of RhoA pathway (**Figure 3**).

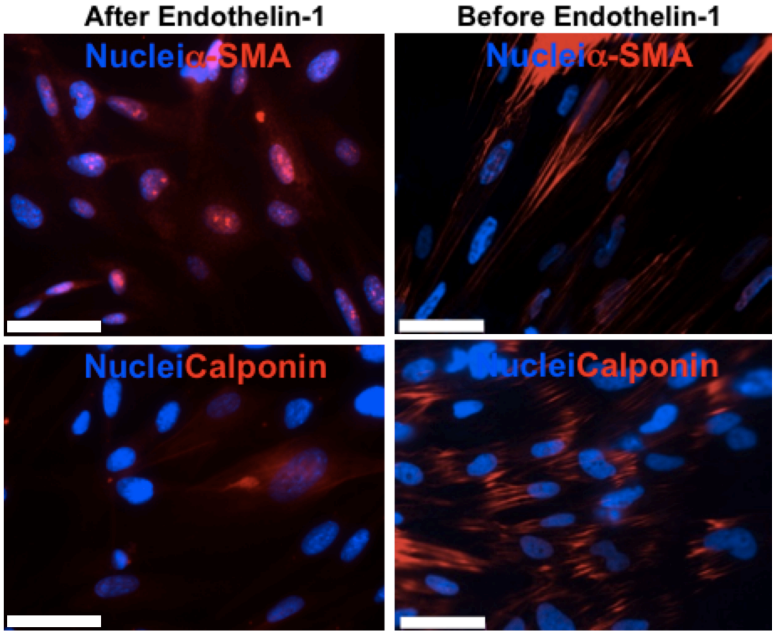

Figure 3: Expression and organization of SMC proteins in hESC-derived smooth muscle progenitor cells before and after treatment with endothelin-1 for 3 days. Bar corresponds to 50 μm. Figure adapted from Ref. [59] with permission from PLoS One.

2.2.2.4 - Therapeutic potential of SMCs

Very few studies have evaluated the therapeutic potential and functionality of SMCs transplanted *in vivo*. It has been shown that SMLCs can contribute for the formation of functional blood microvessels *in vivo* [8] [42] and improve blood flow after transplantation in an ischemic hind limb mouse model [42]. In this case, further studies are needed to understand whether the regenerative potential of SMCs is mediated by their ability to contribute structurally for the formation of blood vessels or their ability to secrete paracrine factors. It is also unclear the regenerative potential of mature hESC-derived SMCs [59].

Table 1- Derivation of vascular cells from hESCs and hiPSCs.

Human Pluripotent SC source	*Models of differentiation*	*Pathways/molecules*	*Differentiation in Vascular cells*	*Characterization and In vivo studies*	*Reference*
hESC	Collagen IV/ $Flk1^{+}$/$E\text{-cadherin}^{-}$	VEGF; PDGF-BB	EC / MC	EC and SMC markers; Tube formation; Contribution to the development of vasculature in chick embryos	[63]
hESC	VEGF-R2-positive but tumor rejection antigen 1-60 (TRA1-60)-negative cell isolation		EC / SMC	New blood vessels and improved blood flow	[64]
hESC	12 days of EB formation and 1.5 mg/ml of collagen I gel/EGM-2 medium with 5% knockout serum replacement	Wnt2	EC	Functional vessel formation, improved cardiac function	[10]
hESC	10 days of EB formation; $CD34^{+}$ cell isolation	VEGF; PDGF-BB	EC / SMC	Formation of a functional microvasculature	[8]
hESC	PECAM-1+ cell isolation		EC	Tube formation; in vivo new vessels formation	[9]
hESC	$VEGFR2^{+}TRA1^{-}$VE-cadherin+ cells isolation	PDGF-BB	EC / MC	Blood flow recovery of ischemic limbs, long term vascular integrity	[65]
hESC / hIPS	TRA1–60-Flk1+ cells; VE-cadherin–positive and –negative populations	VEGF, PDGF-BB	EC / SMC	EC and SMC markers	[54]
hESC	vWF^{+} cells isolation		EC	Improves blood perfusion and limb salvage by facilitating postnatal neovascularization in a mouse model of hindlimb ischemia	[66]
hESC / hIPS	$Flk1^{+}$/$VE\text{-cadherin}^{+}$ cells isolation; Sirt1	VEGF	EC	EC markers	[55]
hESC / hIPS	$CD34^{+}$ cells isolation	Inactivation of MEK/ERK signaling and activation of BMP4;	EC	blood perfusion and limb salvage through the neovasculogenesis in hind limb ischemic mice	[45]
hESC	M2-10B4 stromal cells or Wnt1 expressing M2-10B4 for 13–15 days; CD34+ cells isolation	Wnt1	EC / SMC	EC and SMC markers; tube formation	[43]

hESC / hIPS	EB formation; $CD31^+$ cell isolation	VEGF	EC	EC markers	[67]
hESC	$CD31^+CD34^+$ cell isolation Smad1/5/8	BMPs; TGFβ; VEGF	EC	EC markers	[47]
hESC	$CD34^+$	VEGF; RA	SMC	SMC markers and functionality	[59]
hESC	2D culture	PDGF-BB; TGFβ	SMC	SMC markers	[58]
hESC	CD144 promoter screen/Inhibition of TGFβ	Id1	EC	$hCD144p^-GFP^+$ cells	[37]
hIPS	EB formation; SMCM medium		SMC		[68]

hESC: human embryonic stem cells; hIPS: human induced pluripotent stem cells; EC: endothelial cells; MC: Mural cells, SMC: smooth muscle cells; VEGF: vascular endothelial growth factor; PDGF-BB: platelet derived growth factor BB; BMPs: bone morphogenetic proteins; TGFβ: transforming growth factor beta; RA: retinoic acid.

2.3. VASCULAR DIFFERENTIATION OF hiPSCs

2.3.1 - EC differentiation

2.3.1.1 - Differentiation methodologies: yields and kinetics

Several methodologies have been reported to induce the vascular differentiation of hiPSCs, including co-culture with OP9 cells [54], and EBs. In general, the vascular differentiation protocols of hESCs have been successfully implemented in hiPSCs. However, studies indicate that the vascular potential of hiPSCs is, in some aspects, different to hESCs. For example, TRA1-60$^-$/KDR$^+$/VE-cadherin$^+$ give rise to ECs while TRA1-60$^-$/KDR$^+$/VE-cadherin$^-$ give rise to SMCs [54]. Importantly, the differentiation efficiency was comparable to hESCs [54]. However, according to some studies, hiPSC-derived ECs had limited expansion capacity *in vitro*, and exhibited a gradual loss of CD31 marker expression over a period of 2 weeks [69] [44]. This contrasts with the capacity of hESC-derived endothelial cells to proliferate robustly *in vitro* with minimal loss of CD31 marker (85% for hESC-derived ECs vs 28% for hiPSC-derived ECs, at day 21) [69]. The variation in gene expression between hiPSCs and hESCs might account for the differences observed. Comparison between single hESCs and single hiPSCs revealed more heterogeneity in gene expression levels in the hiPSCs [69]. In addition, the variation in gene expression between hiPSC-derived ECs and hESC-derived ECs might contribute significantly for the biological differences among cells [44]. Several studies have revealed that somatic memory does exist [70,71,72]. That may explain the slower growth and fast loss of endothelial phenotype, depending on the donor somatic cells.

2.3.1.2 - Therapeutic potential of hiPSC-derived ECs

Few studies have documented the differentiation of hiPSCs into ECs [54] [55] [45] [44] and thus it is unclear the therapeutic potential of hiPSC-derived ECs for the treatment of ischemic diseases and how different is that potential from the one observed for hESC-derived ECs. So far, studies have shown that hiPSC-derived ECs have similar functional activity as normal ECs, including the ability to produce endothelial nitric oxide synthase [54] and the ability to form capillary-like structures when seeded in Matrigel [54] [73]. Furthermore, the transplantation of hiPSC-derived cells in ischemic hind-limb mice improved blood perfusion and limb salvage [45]. Further research is needed to investigate the therapeutic potential of these cells in other disease settings.

2.3.2- SMC differentiation

2.3.2.1 - Differentiation methodologies: yields and kinetics

The generation of hiPS cells from human aortic vascular smooth muscle cells (hAVSMCs) or human dermal fibroblasts and their differentiation into SMCs was recently reported [68] [61] . hiPSCs from hAVSMCs were obtained using lentiviral transduction of defined transcription factors and differentiated back into SMCs. hiPS cell-derived SMCs were very similar to parental hAVSMCs in gene expression patterns, epigenetic modifications of pluripotency related genes, and *in vitro* functional properties.

2.3.2.2 - Therapeutic potential of hiPSC-derived SMCs

Currently there are no studies documenting the *in vivo* functionality of hiPSC-derived SMCs. So far, the *in vitro* results have shown that hiPSC- derived SMCs were very similar to somatic SMCs in gene expression and *in vitro* functional properties [68] [54] [61]. The hiPSC-derived SMCs exhibited increased intracellular calcium influx in response to vasoconstrictive carbachol and KCl-induced membrane depolarization, and contract after treatment with carbachol or angiotensin II [68] [61].

2.4 Tissue engineering applications of vascular cells derived from hPSCs

hPSC are promising for the revascularization of ischemic tissues such as ischemic leg, chronic wounds, and infarcted heart [10] [7] [6]. Yet, there is a demand for scaffolds to allow efficient cellular transplantation *in vivo*, retaining them at the site they are needed, while improving their engraftment. The scaffold can be engineered to support migration, proliferation, and differentiation of vascular progenitor cells or differentiated cells and to help in the organization of these cells at three-dimensional level [74,75,76]. Examples of scaffolds that can support EC migration and their 3D organization include MMP-sensitive hydrogels incorporating RGD epitopes to promote cell adhesion [77] [6], fibrin gels [78], collagen gels [38], PLGA matrices [9], poly(hydroxyethyl methacrylate) gels [38], among others.

Pro-survival factors can be used to increase the survival of vascular cells after transplantation. Recently, we used a pro-angiogenic and pro-survival factor (thymosin $\beta 4$) along with hESC-derived vascular cells encapsulated in a MMP-sensitive gel for the treatment of myocardial infarction [6]. The gel, acting as scaffold, substituted the

degrading extracellular matrix in the infarcted myocardium of rats and promoted structural organization of native ECs, while some of the delivered hESC-derived vascular cells formed de novo capillaries in the infarct zone (**Figure 4**). Another approach to induce the three-dimensional organization of the vascular cells is by the use of prefabricate scaffolds that include channels that later may be coated with vascular cells. Nanofabrication techniques can be used to engineer network structures that might mimic the capillary network [79,80]. Also, ink-jet printing can be used to pattern cells into tubular structures [81] and be used in the future for the assembly of complex vascularized tissues obtained from hPSC.

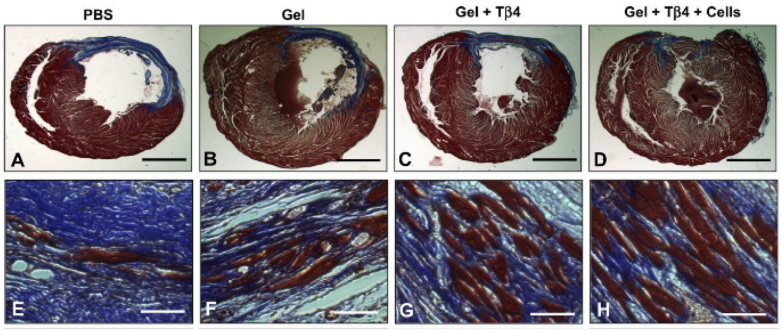

Figure 4: Preservation and alignment of cardiomyocytes in infarcted myocardium treated with hESC-derived vascular cells encapsulated in a metalloprotease-sensitive gel with a pro-survival peptide. (A-D) Representative trichrome stains of transverse heart sections. Collagen in the infarct areas is shown in blue, whereas myocytes are in red. Animals were treated with (A) PBS, (B) gel, (C) gel + thymosin β4 (Tβ4) and (D) gel + Tβ4 + cells. The cardiomyocytes appeared to be better preserved and aligned in bundles in hearts treated with the combined Tβ4 and cell delivery, as compared to the rats treated with PBS, gel alone or Tβ4 delivery alone. Low (A-D) and high (E-H) magnification. Bar corresponds to 2.5 mm (A-D) and 100 mm (E-H). Figure adapted from Ref. [6].

2.5. Future of pluripotent stem cells

Both hESCs and hiPSCs are promising sources of vascular cells for the treatment of ischemic diseases [82]. Similarities exist between hESCs and hiPSCs regarding their potential to differentiate into vascular cells, but whether the regulatory pathways that govern their differentiation are similar remains to be determined. Studies in both hESCs and hiPSCs suggest that factors implicated in EC differentiation are expressed in both cell systems but in slightly different temporal pattern [45]. Although vascular tissue engineering is promising for therapeutic applications, additional studies are needed to gain further insights about the long-term functionality of engrafted hPSC-derived vascular cells. **Figure 5** summarizes the important implementations needed to facilitate clinical translation of cell therapy. Human pluripotent stem cells have the advantage of generating higher number of

vascular cells than other stem cells, with a phenotype not affected by a disease state or an ageing process. Currently, there are several clinical trials using stem cells for the treatment of ischemic diseases. Most of them use mesenchymal stem cells, progenitor cells and adult autologous hematopoietic stem cells [83]. Human pluripotent stem cells, specifically human embryonic stem cells, have been recently used in clinical trials to treat spinal cord injury, Stargardt´s Macular Dystrophy and Dry Age-Related Macular Degeneration. The demonstration of the safety and efficacy of hESC-derived cells in these clinical trials might open new horizons for their clinical application in other diseases settings.

Human pluripotent stem cells have a huge potential for the development of cellular kits for toxicology and drug screening applications that should be further explored in the near future. Of particular interest is the development of cellular kits to assess cardiotoxicity and hepatotoxicity. Robust protocols to differentiate hPSC into functional cardiomyocytes and hepatocytes have already been described [84,85][90]. The electrophysiological response of hiPSCs-derived cardiomyocytes to several cardiac and non-cardiac drugs have been reported [86,87,88,89]**.** Cellular Dynamics International, a company located in USA, has started to commercialize hiPSCs-derived cardiomyocytes for pharmaceutical cardiotoxicity testing [63]. Cell kits formed by hPSC-derived neuronal cells are also important to assess neurotoxicity. The possibility of generating functional neurons from hPSCs provides a cellular platform for analyzing certain aspects of drug metabolism and adverse effects [91,92] (see **Table 2** for examples of studies in hPSC).

Cell kits formed by vascular cells are also important for drug screening/toxicological assessment of new drugs. Toxicological studies on mouse ES-derived vascular cells have been done to test inhibitors of vasculogenesis [93], but so far no study has documented the use of hPSC-derived vascular cells for drug screening/toxicology analyses. Some studies have used human umbilical vein cells for high-throughput screening of vascular disruption agents [94] and angiogenesis inhibitors [95]. Also a co-culture system of endothelial cells with smooth muscle cells has been used to identify anti-angiogenic and other therapeutic molecules [96]. Yet, hPSC-derived vascular cells compares favorably to adult vascular cells for the development of cellular kits since they allow the creation of personalized drug screening/toxicology kits.

One of the most exciting applications of hPSC technology is related to the use of disease cells for drug screening. Disease-specific hPSC can recapitulate known physio-pathological mechanisms and can open new perspectives for identifying new ones. Nonetheless, in many cases, these disease models have not yet been adapted for drug screening. Despite the already developed disease models for Parkinson [97], spinal

muscular atrophy [98], beta-thalassemia [99], among others, further disease models are needed particularly in the vascular area. Therefore, we anticipate that significant progresses will be done in the near future in the area of drug-screening using disease-specific hPSC. It remains to be determined whether hPSC-based systems can predict drug toxicity as observed on in vivo settings.

Table 2 – Drug screening in hPSC-derived cells

Cell type	Agent	Mode of action	hPSC line	Concentration	Detection	Effect on derived cells	Ref.
Cardiomyocytes	Acetylcholine	Muscarinic receptor agonist	SA002, SA121	10^{-6} - 10^{-3} M	Microscopy	Decreased Beat rate	[101]
Cardiomyocytes	Adrenaline	β1-Adenoreceptor agonist	SA002, SA121	10^{-8} - 10^{-6} M	Microscopy	Increased Beat rate	[101]
Cardiomyocytes	Adrenaline	β1-Adenoreceptor agonist	iPSC201 B7	10^{-7} - 10^{-5} M	Microelectode arrays	Increased Beat rate	[89]
Cardiomyocytes	Atropine	Competitive inhibitor of acetylcholine	SA002, SA121	10^{-4} M	Microscopy	Blocked effect of acetylcholine	[101]
Cardiomyocytes	Cisapride	Serotonin (5-hydroxytryptamine) agonist	H3	10^{-9} - 10^{-6} M	Microelectode arrays	Increased Field Potential duration	[102]
Cardiomyocytes	Domperidone	Blocks multiple channels	HES3	10^{-9} - 10^{-4} M	Microelectode arrays	Increased Field Potential duration	[102]
Cardiomyocytes	Isoprelanine	β1/β1-Adenoreceptor agonist	iPSC201 B7	10^{-7} - 10^{-5} M	Microelectode arrays	Increased Beat rate	[89]
Cardiomyocytes	Forskolin	Stimulator of adenylate cyclase leading to cAMP formation	SA002, SA121	10^{-11}- 10^{-6} M	Microscopy	Increased Beat rate	[101]
Cardiomyocytes	Lidocaine	Voltage-gated sodium channel inhibitor	HES3	10^{-4} M	Microelectode arrays	Decreased conduction rate	[102]
Cardiomyocytes	Mixileteine	Sodium channel blocker	iPSC201 B7	10^{-7} - 10^{-5} M	Microelectode arrays	No effect	[89]
Hepatocytes	Bufuralol Phenacetin Diclorofenac Midazolam	Metabolization	H9	50 - 100 μM	UPLC/MS/MS	Metabolism is similar to primary human hepatocytes	[103]
Neurons (BFCN)	Nicotin antagonists	Blok spontaneous g-aminobutynic acidergics	H9	10 nM - 1 mM	Electrophysiology	Blocked synaptic transmission	[92]

UPLC/MS/MS – ultraperformance liquid chromatography tandem mass spectometry; BFCN – basal forebrain cholinergic neurons.

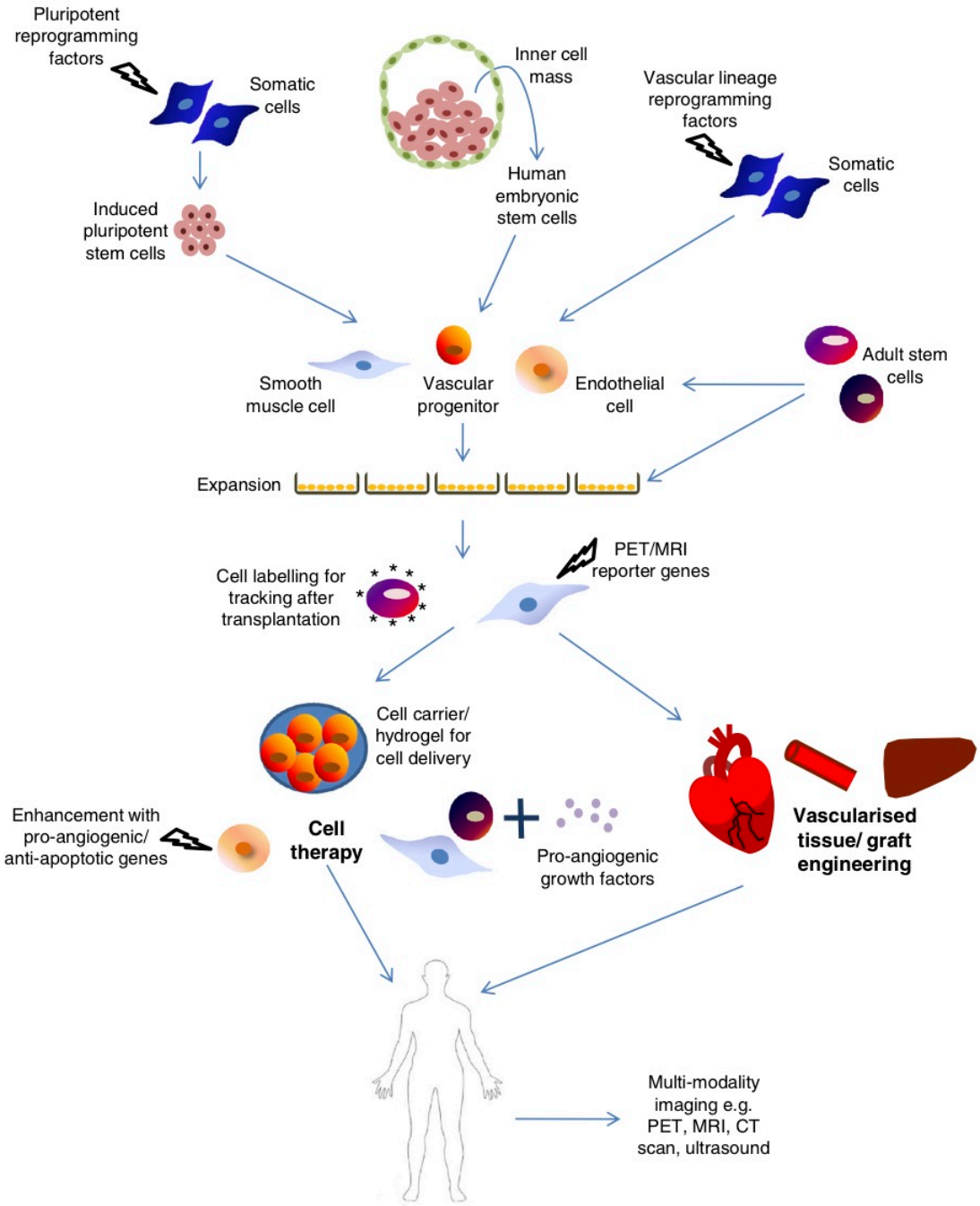

Figure 5: Schematic diagram of the pathways to clinical translation of ischemic and cardiovascular cell therapy. This figure outlines some of the key steps and methods being used or under consideration for implementing vascular cell therapy. Vascular progenitors or differentiated vascular cells may be derived from human pluripotent stem cells, adult stem cells or by direct conversion from somatic cells. Cells may then be expanded in vitro and labeled with reporters for subsequent tracking. Survival, homing and differentiation of injected cells in vivo may be augmented by a variety of approaches or alternatively cells may be used to generate intact tissues and organs in vitro before implantation in the patient. Non-invasive imaging techniques are likely to be essential for understanding the regenerative process in man and optimizing the procedure. Figure and legend adapted from [23].

3. Vascular modulation /applications

3.1 Vascular specification plasticity

Mature endothelial cells have different sub-phenotypes: arterial, venous, lymphatic or brain-like. Although the initial molecular identity of ECs is genetically predetermined, there is significant plasticity in later arterio-venous differentiation. Physiological requirements and hemodynamic influences may reverse the phenotype of an apparently committed cell. ECs in transplanted arterial and venous vessel grafts can alter identity, completely switching their expression profile to match the host vessel [104,105]. Forced overexpression or loss-of-function of critical molecular determinants of specification can also reprogram a differentiated EC. One example is Notch overexpression in the venous compartment that results in the up-regulation of arterial EC markers. Concomitantly, the inhibition of Notch signaling in the arterial compartment results in loss of arterial fate and up-regulation of venous markers [106]. Ablation of EC COUP-TFII permits veins to gain arterial characteristics and express arterial markers [107]. An unusual feedback regulatory equilibrium exists among the 3 major EC fate regulators (Notch, COUP-TFII, and Prox1) that direct the plasticity in arteriovenous-lymphatic cell fate [108].

The results of the previous studies also propose that additional components of the vascular wall are required to maintain and/or sufficient to redirect the arterial-venous identity of adjacent ECs. SMCs may be important piece for this function of the vessel wall. It may also be that the vessel wall serves simply to isolate ECs from other extrinsic inputs that influence arterial-venous identity and thus in a relatively passive way help to stabilize endothelial fate choice. Experimental reports have also shown that hemodynamic forces can alter ECs identity following the onset of the circulation [109]. Also, altered oxygen tension levels can change artery and vein specification in the developing mouse retina vasculature [110]. Additional studies will be needed to determine whether SMCs or other constituents of the vessel wall, hemodynamics, and oxygen tension actually play an instructive role in endothelial arterial-venous fate. A proposed system in which genetic predetermination controls initial arterial-venous specification and environmental inputs regulate subsequent vascular remodeling may resolve the debate between genetic versus epigenetic regulation of EC differentiation (reviewed elsewhere [111]).

Beyond the specification to arterial, venous, or lymphatic fate, it is currently recognized that ECs undergo further differentiation specific to the vascular bed or organ in which they reside. This phenotypic heterogeneity is the primary mechanism by which the endothelium carries out numerous vital functions, including control of microvascular permeability, vessel wall tone, coagulation and anticoagulation, inflammation, and

angiogenesis [112,113,114]. Endothelial heterogeneity is also responsible for the varied and diverse responses across differing vascular beds to pathological stimuli and disease states [115,116,117].

3.2 Vascular mechanobiology

3.2.1 Endothelial cell response to fluid shear stress

The homeostasis of the circulatory system has a principal player that additionally has a variety of functions: endothelial cells that coat blood vessels. As blood flows, the vascular wall is continuously exposed to physical forces, which regulate important physiological blood vessel responses, as well as being implicated in the development of arterial wall pathologies. It has become clear that biomechanical forces generated by blood flow regulate EC functions. ECs are in direct contact with blood flow and exposed to shear stress, a frictional force generated by flowing blood. A number of recent studies have revealed that ECs recognize changes in shear stress and transmit signals to the interior of the cell, which leads to cell responses that involve changes in cell morphology, cell function, and gene expression (reviewed elsewhere [118]). These EC responses to shear stress are thought to play important roles in blood flow dependent phenomena such as vascular tone control, angiogenesis, vascular remodeling, and atherogenesis. Much research has been done on shear stress sensing and signal transduction, and their molecular mechanisms are gradually becoming understood. However, much remains uncertain, and many candidates have been proposed for shear stress sensors. A noticeable feature of shear stress mechanotransduction is that the shear stress activates a variety of membrane molecules and microdomains almost simultaneously, leading to signal transduction through multiple pathways (**Figure 6**). Currently, it remains unclear which pathways are primary and which are secondary, because the initial sensing mechanism or sensors that recognize shear stress have not been identified. Thus far, various membrane molecules and cellular microdomains, including ion channels, growth factor receptors, G proteins, caveolae, adhesion proteins, the cytoskeleton, the glycocalyx, and primary cilia, have been shown to play important roles in the shear stress sensing mechanism. The molecular candidates able to act as shear stress sensors are briefly described in **Figure 6**.

The surface of ECs is covered with a layer of membrane-bound macromolecules that constitute the glycocalyx. G**lycocalyx** is expressed in endothelial cells cultured under flow shear stress (like in vivo [119]) but absent in cells cultured in static conditions. The

glycocalyx has been considered a possible shear stress sensor because it is located between the flowing blood and the cell membrane [120]. Involvement of the glycocalyx in EC responses to shear stress has been demonstrated by the finding that degradation of hyaluronic acid glycosaminoglycans (component of glycocalyx) with hyaluronidase significantly decreases flow-induced NO (nitric oxide) production in isolated canine femoral arteries [121] and by the finding that enzymatic removal of heparan sulfate with heparinase completely inhibits NO production in response to shear stress [122]. Two possible mechanisms have been proposed to explain how the EC glycocalyx mediates shear stress mechanotransduction. One is that heparan sulfate proteoglycan is present as a random coil under no flow conditions, but with increasing flow becomes unfolded into a filament structure [123]. This conformational change is accompanied by an increase in binding sites for Na^+ ions, and Na^+ binding may trigger the signal transduction. In addition to glycocalyx-mediated regulation of the local concentration gradient and transport of ions, amino acids, and growth factors, it is also possible that shear stress is transmitted to the cell interior through the actin cytoskeleton or intracellular signaling molecules that directly associate with the core protein of the glycocalyx [124].

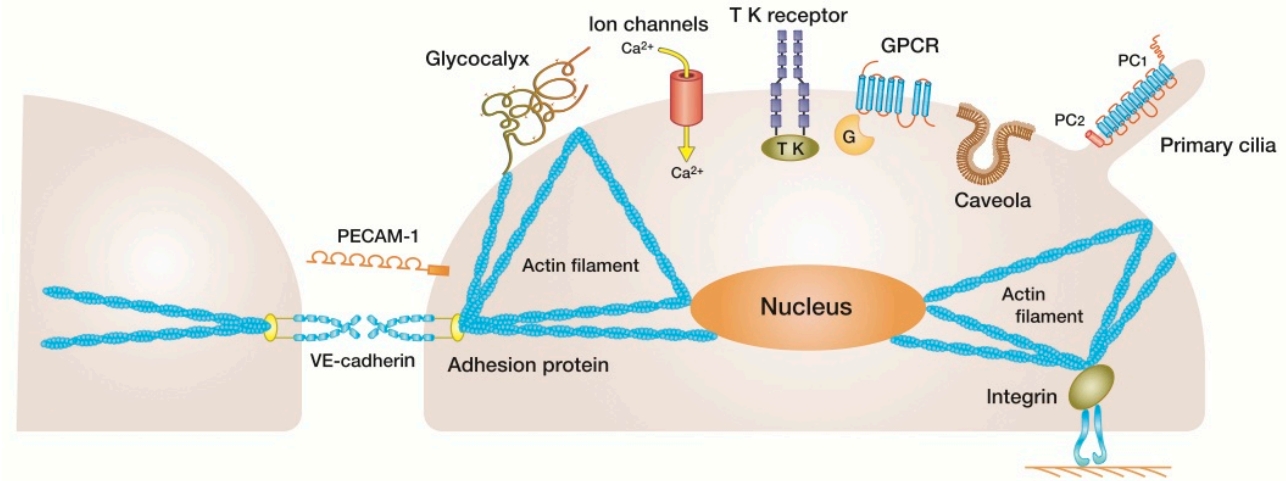

Figure 6: Candidates for shear stress sensors. **Ion channels**: various types of ion channels including K^+ channels, Cl^- channels, and Ca^{2+} channels have been shown to be shear stress-responsive. P2X4, a subtype of ATP-operated cation channel P2X purinoceptor, is one such ion channel and in the form of a trimer functions as Ca^{2+}-permeable channel. **Tyrosine kinase receptor**: rapid phosphorylation of vascular endothelial growth factor receptor 2 (VEGFR2) occurs in response to shear stress in a ligand-independent manner. **GPCRs**: G protein-coupled receptors and G protein itself have been shown to be activated by shear stress. **Caveolae**: caveolae, membrane microdomains containing a variety of receptors, ion channels, and signaling molecules, and their component protein caveolin-1 have been demonstrated to be involved in shear stress sensing and response mechanisms. **Adhesion proteins**: various adhesion proteins located at sites of cell-cell and cell-matrix attachment are subjected to tension under shear stress and respond to it, resulting in the activation of downstream signal transduction pathways. Integrins are one class of such adhesion proteins. **Tensegrity**: tensegrity is a form of architecture that self-stabilizes its structure through the use of isolated compression- resistant elements and tensile elements. When this model is applied to cells, microtubules and actin filaments are regarded as the struts and cables, respectively. It seems possible that these cytoskeleton components directly sense mechanical forces that deform cells. **Glycocalyx**: the random-

coiled glycocalyx unfolds into a filament structure under flow conditions, and this conformational change affects the local concentrations and transport of ions, amino acids, and growth factors or triggers signal transduction via the intracellular core protein of the glycocalyx. **Primary cilia**: the bending of primary cilia induced by flow activates polycystin-2 (PC2), which leads to an influx of extracellular Ca^{2+} via polycystin-1 (PC1), a member of the transient receptor potential (trp) ion channel family. Figure and legend adapted from [125].

3.2.2 Shear stress in endothelial differentiation

Several studies have shown that ECs alter their morphology, function, and gene expression in response to shear stress. Shear stress affects immature cells, as well as mature ECs, and promotes differentiation of bone-marrow-derived endothelial progenitor cells and embryonic stem cells into ECs. Bone-marrow-derived EPCs circulating in peripheral blood migrate toward their target tissue where they differentiate and contribute to the formation of new vessels [126]. During this process, they are exposed to shear stress generated by interstitial fluid flow and blood flow, and when cultured EPCs are subjected to shear stress in a flow-loading device, their differentiation into mature ECs accelerates significantly [127]. ES cells are exposed to fluid mechanical forces, including shear stress, and the cyclic strain generated by the beating heart during the process of embryonic development [128]. Interestingly, the differentiation of ES cells into ECs is mediated by ligand-independent phosphorylation of VEGFR2 receptor, respectively, by shear stress [129]. Moreover, it has been shown that shear stress increases expression of an arterial EC marker, ephrinB2, in EPCs, suggesting that shear stress can affect the arterial-venous differentiation of ECs [130]. It seems likely that fluid-mechanical forces act as regulators of EPC mediated neovascularization and of ES-cell-mediated early embryonic vascular development.

Fluid shear stress has been used as a tool to achieve differentiation of pluripotent cells into ECs [129,131] and, more recently, also into hematopoietic cell precursors [132]. In most of the cases, shear stress has been applied on ES cells differentiated at some extent into precursor cells but not in undifferentiated cells. More specifically, the majority of the data has been gathered on murine ES cells differentiated to generate cells positive for Flk1, considered the earliest marker of both hematopoietic and endothelial precursor lineages [48]. There are no reports of driving hESC to EC by shear stress or even modulation of EC derived from hESC. Nevertheless, shear stress has also been used as a tool to differentiate ‘‘naive’’ ES cells and in the context of other ES applications, which are discussed by others [133].

3.2.3 Shear stress in arterial and in venous endothelial phenotype

The magnitude of the shear stress can be estimated in most of the vasculature by Poiseuille's law [134] (**Figure 7**), which states that shear stress is proportional to blood flow viscosity, and inversely proportional to the third power of the internal radius [135,136,137,138]. Measurements using different modalities show that shear stress ranges from 1 to 6 dyne/cm^2 in the venous system (average is 4 dyne/cm^2) and between 10 and 70 dyne/cm^2 (average is 20 dyne/cm^2) in the arterial vascular network [136]**.** Figure 7 illustrates the range of wall shear stress magnitude in arteries and veins in healthy and disease states.

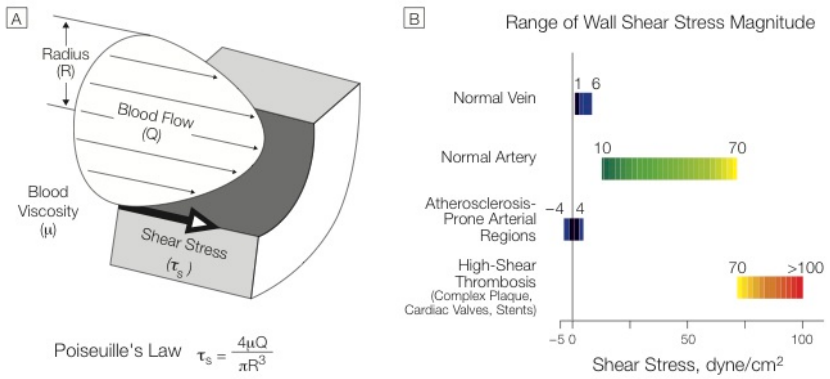

Figure 7: A) Cross-sectional schematic diagram of a blood vessel illustrating hemodynamic shear stress, τ_s, the frictional force per unit area acting on the inner vessel wall and on the luminal surface of the endothelium as a result of the flow of viscous blood. B) Tabular diagram illustrating the range of shear stress magnitudes encountered in veins, arteries, and in low-shear and high-shear pathologic states. Figure and legend adapted from [139].

3.2.4 Microfluidic technology in vascular research

Microfluidic systems have been recently adopted by the vascular biology community to recreate the dynamic and three-dimensional microenvironment found *in vivo* by vascular cells. Usually, the set-up consists of two parallel plates seeded with cells in which culture medium is pumped to simulate blood flow and exert shear stress. By scaling these set-ups down to micrometer-size, they become easier to handle and the flow rates that are needed to exert a physiologically relevant shear stress are several orders of magnitude lower. Moreover, small number of cells and tiny amounts of reagents are needed to perform the same experiments. The manipulation of fluid in these micrometer-sized channels is a topic of great interest in the field of microfluidics. Microfluidic technology allows for increasing scale and parallelization of current research, leading to more comprehensive insights into cell and tissue physiology. The advantages of microfluidic technology for cell culture in general have been reviewed elsewhere [140,141]. There are many recent applications of

microfluidic technology in the field of vascular biology. Microfluidics can be used for shear stress [142,143,144], growth factor gradient [145], co-cultures [146], migration [147] and flow cytometry studies [148].

In most cases, the microchannels in the microfluidic systems are rectangular or semi-circulars [149] [150] and therefore they not mimic the circular cross-section of the blood vessels. So far, only 3 studies replicated the circular cross-section of blood vessels in microfluidic devices. Eugenia Kumacheva and co-workers have recently reported the fabrication of microchannels in poly(dimethylsiloxane) with 40-100 mm of diameter using soft lithography [151]. In this case, the microchannels were firstly fabricated with a rectangular cross-section by a soft lithography method followed by its subsequent transformation to a circular one using a gas stream. The authors showed the capability to grow endothelial cells on the inner surface of the microchannels; however, it is unclear for how long and this is a major issue for the use of these 3D constructs. Kahp Suh and co-workers have created circular microchannels with tunable diameters in poly(methyl methacrylate). The authors have demonstrated that endothelial cells could adhere and proliferate in the microchannels forming a confluent monolayer of cells. The cells remained viable at least for 6 days [152]. Finally, Wilbur Lam and co-workers have created circular microchannels with diameters below 50 μm in PDMS using a single-mask microfabrication process [153]. The microfluidic system could reproduce specific pathophysiological characteristics related to the interactions between blood cells and endothelial cells, and the cells could be maintained viable in the microfluidic system for at least 3 days.

At present there is no report of the application of vascular cells derived from hESCs or iPSCs, using this type of technology. Integrating those promising cells in an *in vitro* model of the microvasculature would be ideal for studying hematologic diseases with pathologies that span the fields of both biology and biophysics, such as sepsis/inflammatory disorders, sudden cardiac death, thrombotic microangiopathies; besides other applications.

4. Stem cells-derived vascular cells as building blocks for regenerative medicine

Ischemic diseases such as coronary heart disease, wound healing or stroke are the primary cause of death in the world. In the last years, several cell-based therapies have been proposed to solve this issue, in particular those based in vascular cells derived from stem cells. It has been shown that the transplantation of endothelial progenitor cells

(EPCs) or vascular cells derived from different stem cells sources can increase significantly the vascularization of ischemic tissues. The integrated use with vascular cells, for example smooth muscle cells [154] and endothelial cells [78] is essential for the development of functional vessels [155,156]. This was demonstrated in animal models of hindlimb ischemia [157,158,159,160], myocardial ischemia [161,162,163] and diabetic chronic wounds [78]. Unfortunately, the survival of these cells is relatively low in the first days of post-transplantation [161,162,163]. A three-dimensional scaffold able to modulate cell activity and their survival will be of utmost importance in regenerative medicine. Although recent studies have reported the incorporation of pro-survival factors with vascular cells in the same matrix [77], it is difficult to decouple the growth factor delivery component from the cell-matrix component. In chapter 5 we propose a new platform to address this issue, based on vascular endothelial growth factor (VEGF). VEGF is very important in the context of pro-survival and pro-angiogenic therapies and in the control of endothelial cell migration [154,164].

4.1 Role of VEGF in vascular tissues

Research around VEGF has been intense over the last 20 years [165]. VEGF is a heparin-binding growth factor specific for vascular ECs that is able to induce angiogenesis *in vivo*, described for the first time in 1983 [166] and fully characterized and sequenced in 1989 [167]. VEGF has been tested in clinical trials for pro-angiogenic processes; however, the results obtained did not full address the expectations [168,169] (**Table 3**). One of the reasons for that failure was related to the inefficient delivery of the drug [164,168,169,170]. VEGF has a half-life below 30 min [171]. Therefore, significant efforts have been made in the last years to deliver efficiently VEGF with spatio-temporal control. For example, VEGF has been incorporated in polymeric matrices [172,173], immobilized covalently in matrices or surfaces [174,175], incorporated in composites, such as chitosan or chitosan/polylactic acid scaffolds [176], or calcium phosphate and heparin [177]; incorporated in matrices with other growth factors and biomolecules such as PDGF [156] or hyaluronic acid and keratinocyte growth factor [178]. Despite these advances, alternative therapeutic solutions are needed to potentiate the effect of VEGF in ischemic tissues and rapidly form blood vessels. Furthermore, new platforms are needed to potentiate the role of VEGF when used with transplanted cells.

Table 3 – Examples of low therapeutic efficacy in clinical trials using VEGF

Drug	Disease	N	Follow-up	Population studied	Conclusions	Ref
Telbermin (rhVEGF)	Chronic diabetic neuropathic foot ulcers	29	Up t 6 weeks	Diabetes type I & II	No adverse effects. Low ulcer healing compared with placebo group	[168]
rhVEGF	VIVA (VEGF in ischemia for vascular angiogenesis)	178	120 days	Stable exertional angina	No improve beyond placebo by day 60. Requires higher doses.	[169]
rhVEGF	VIVA (VEGF in ischemia for vascular angiogenesis)	178	9 days	Coronary artery disease	Short half-live of VEGF. Hypotension after administration.	[171]
Bevacizumab	Cancers	1850	Weeks	Different cancers (7 trials)	Significant increase risk of proteinuria and hypertension	[179]

4.2 VEGF signaling activation pathways

VEGF plays a main role on the homeostasis of blood vessels in non-pathological conditions [180]. VEGF is an important survival factor of endothelial cells [181], a process mediated by the activation of phosphatidylinositol 3-kinase (PI3K)/Akt signalling pathway [181]. Furthermore, VEGF has neuroprotective activity, by increasing the VEGFR2 (VEGF receptor 2) expression, and stimulating the activation of the PI3K/Akt and ERK-1/2 pathway [182]. The VEGF binding to VEGFR2 leads to receptor dimerization, internalization through endocytosis and subsequent signal transduction. The VEGF matrix immobilization impairs the event, but leads to prolonged activation kinetics of VEGFR2 that recurs to β1- integrin dimerization for signal transduction. This phenomena leads to different VEGFR2 phosphorylation patterns and enhancement of the p38/MAPK (Mitogen-activated protein kinase) cascade [183], leading to actin reorganization and inducing cell migration.

Bibliography:

1. Thomson JA, Itskovitz-Eldor J, Shapiro SS, Waknitz MA, Swiergiel JJ, et al. (1998) Embryonic stem cell lines derived from human blastocysts. Science 282: 1145-1147.
2. Takahashi K, Tanabe K, Ohnuki M, Narita M, Ichisaka T, et al. (2007) Induction of pluripotent stem cells from adult human fibroblasts by defined factors. Cell 131: 861-872.
3. Yu J, Vodyanik MA, Smuga-Otto K, Antosiewicz-Bourget J, Frane JL, et al. (2007) Induced pluripotent stem cell lines derived from human somatic cells. Science 318: 1917-1920.
4. Takahashi K, Yamanaka S (2006) Induction of pluripotent stem cells from mouse embryonic and adult fibroblast cultures by defined factors. Cell 126: 663-676.
5. Schmidt A, Brixius K, Bloch W (2007) Endothelial precursor cell migration during vasculogenesis. Circulation Research 101: 125-136.
6. Kraehenbuehl TP, Ferreira LS, Hayward AM, Nahrendorf M, van der Vlies AJ, et al. (2011) Human embryonic stem cell-derived microvascular grafts for cardiac tissue preservation after myocardial infarction. Biomaterials 32: 1102-1109.
7. Cho S-W, Moon S-H, Lee S-H, Kang S-W, Kim J, et al. (2007) Improvement of postnatal neovascularization by human embryonic stem cell derived endothelial-like cell transplantation in a mouse model of hindlimb ischemia. Circulation 116: 2409-2419.
8. Ferreira LS, Gerecht S, Shieh HF, Watson N, Rupnick MA, et al. (2007) Vascular progenitor cells isolated from human embryonic stem cells give rise to endothelial and smooth muscle like cells and form vascular networks in vivo. Circulation Research 101: 286-294.
9. Levenberg S, Golub JS, Amit M, Itskovitz-Eldor J, Langer R (2002) Endothelial cells derived from human embryonic stem cells. Proc Natl Acad Sci USA 99: 4391-4396.
10. Li Z, Wilson KD, Smith B, Kraft DL, Jia F, et al. (2009) Functional and transcriptional characterization of human embryonic stem cell-derived endothelial cells for treatment of myocardial infarction. PLoS ONE 4: e8443.
11. Kane NM, Xiao Q, Baker AH, Luo Z, Xu Q, et al. (2011) Pluripotent stem cell differentiation into vascular cells: a novel technology with promises for vascular re(generation). Pharmacol Ther 129: 29-49.
12. Gerecht-Nir S, Ziskind A, Cohen S, Itskovitz-Eldor J (2003) Human embryonic stem cells as an in vitro model for human vascular development and the induction of vascular differentiation. Lab Invest 83: 1811-1820.
13. Bai H, Wang ZZ (2008) Directing human embryonic stem cells to generate vascular progenitor cells. Gene Ther 15: 89-95.
14. Levenberg S, Zoldan J, Basevitch Y, Langer R (2007) Endothelial potential of human embryonic stem cells. Blood 110: 806-814.
15. Iacobas I, Vats A, Hirschi KK (2010) Vascular potential of human pluripotent stem cells. Arteriosclerosis, Thrombosis, and Vascular Biology 30: 1110-1117.
16. Ferguson JE, Kelley RW, Patterson C (2005) Mechanisms of endothelial differentiation in embryonic vasculogenesis. Arteriosclerosis, Thrombosis, and Vascular Biology 25: 2246-2254.
17. Drake CJ, Fleming PA (2000) Vasculogenesis in the day 6.5 to 9.5 mouse embryo. Blood 95: 1671-1679.
18. Kennedy M, D'Souza S, Lynch-Kattman M, Schwantz S, Keller G (2007) Development of the hemangioblast defines the onset of hematopoiesis in human ES cell differentiation cultures. Blood 109: 2679-2687.
19. Jakobsson L, Kreuger J, Claesson-Welsh L (2007) Building blood vessels--stem cell models in vascular biology. The Journal of Cell Biology 177: 751-755.
20. Flamme I, Risau W (1992) Induction of vasculogenesis and hematopoiesis in vitro. Development 116: 435-439.

21. Motoike T, Markham DW, Rossant J, Sato TN (2003) Evidence for novel fate of Flk1+ progenitor: contribution to muscle lineage. Genesis 35: 153-159.
22. Suri C, Jones PF, Patan S, Bartunkova S, Maisonpierre PC, et al. (1996) Requisite role of angiopoietin-1, a ligand for the TIE2 receptor, during embryonic angiogenesis. Cell 87: 1171-1180.
23. Cheung C, Sinha S (2011) Human embryonic stem cell-derived vascular smooth muscle cells in therapeutic neovascularisation. Journal of Molecular and Cellular Cardiology 51: 651-664.
24. Peppel K, Zhang L, Orman ES, Hagen P-O, Amalfitano A, et al. (2005) Activation of vascular smooth muscle cells by TNF and PDGF: overlapping and complementary signal transduction mechanisms. Cardiovasc Res 65: 674-682.
25. Rzucidlo EM, Martin KA, Powell RJ (2007) Regulation of vascular smooth muscle cell differentiation. J Vasc Surg 45 Suppl A: A25-32.
26. Lee SH, Hungerford JE, Little CD, Iruela-Arispe ML (1997) Proliferation and differentiation of smooth muscle cell precursors occurs simultaneously during the development of the vessel wall. Dev Dyn 209: 342-352.
27. Hungerford JE, Little CD (1999) Developmental biology of the vascular smooth muscle cell: building a multilayered vessel wall. J Vasc Res 36: 2-27.
28. Rensen SSM, Doevendans PAFM, van Eys GJJM (2007) Regulation and characteristics of vascular smooth muscle cell phenotypic diversity. Netherlands heart journal : monthly journal of the Netherlands Society of Cardiology and the Netherlands Heart Foundation 15: 100-108.
29. Frid M, Shekhonin B, Koteliansky V, Glukhova M (1992) Phenotypic changes of human smooth muscle cells during development: late expression of heavy caldesmon and calponin. Developmental biology(Print) 153: 185-193.
30. Yoshida T, Owens GK (2005) Molecular determinants of vascular smooth muscle cell diversity. Circ Res 96: 280-291.
31. Wang L, Li L, Shojaei F, Levac K, Cerdan C, et al. (2004) Endothelial and Hematopoietic Cell Fate of Human Embryonic Stem Cells Originates from Primitive Endothelium with Hemangioblastic Properties. Immunity 21: 31-41.
32. Lu S-J, Feng Q, Caballero S, Chen Y, Moore MAS, et al. (2007) Generation of functional hemangioblasts from human embryonic stem cells. Nat Methods 4: 501-509.
33. Sone M, Itoh H, Yamahara K, Yamashita JK, Yurugi-Kobayashi T, et al. (2007) Pathway for Differentiation of Human Embryonic Stem Cells to Vascular Cell Components and Their Potential for Vascular Regeneration. Arteriosclerosis, Thrombosis, and Vascular Biology 27: 2127-2134.
34. Woll PS, Morris JK, Painschab MS, Marcus RK, Kohn AD, et al. (2008) Wnt signaling promotes hematoendothelial cell development from human embryonic stem cells. Blood 111: 122-131.
35. Wang ZZ, Au P, Chen T, Shao Y, Daheron LM, et al. (2007) Endothelial cells derived from human embryonic stem cells form durable blood vessels in vivo. Nat Biotechnol 25: 317-318.
36. Vodyanik MA, Thomson JA, Slukvin II (2006) Leukosialin (CD43) defines hematopoietic progenitors in human embryonic stem cell differentiation cultures. Blood 108: 2095-2105.
37. James D, Nam H-s, Seandel M, Nolan D, Janovitz T, et al. (2010) Expansion and maintenance of human embryonic stem cell-derived endothelial cells by TGFbeta inhibition is Id1 dependent. Nat Biotechnol 28: 161-166.
38. Nourse MB, Halpin DE, Scatena M, Mortisen DJ, Tulloch NL, et al. (2010) VEGF Induces Differentiation of Functional Endothelium From Human Embryonic Stem Cells: Implications for Tissue Engineering. Arterioscler Thromb Vasc Biol 30: 80-89.

39. Ferreira LS, Gerecht S, Fuller J, Shieh HF, Vunjak-Novakovic G, et al. (2007) Bioactive hydrogel scaffolds for controllable vascular differentiation of human embryonic stem cells. Biomaterials 28: 2706-2717.
40. Ferreira L, Squier T, Park H, Choe H, Kohane DS, et al. (2008) Human Embryoid Bodies Containing Nano- and Microparticulate Delivery Vehicles. Adv Mater 20: 2285-2291.
41. Prado-Lopez S, Conesa A, Armiñán A, Martínez-Losa M, Escobedo-Lucea C, et al. (2010) Hypoxia promotes efficient differentiation of human embryonic stem cells to functional endothelium. Stem Cells 28: 407-418.
42. Yamahara K, Sone M, Itoh H, Yamashita JK, Yurugi-Kobayashi T, et al. (2008) Augmentation of neovascularization [corrected] in hindlimb ischemia by combined transplantation of human embryonic stem cells-derived endothelial and mural cells. PLoS ONE 3: e1666.
43. Hill KL, Obrtlikova P, Alvarez DF, King JA, Keirstead SA, et al. (2010) Human embryonic stem cell-derived vascular progenitor cells capable of endothelial and smooth muscle cell function. Experimental Hematology 38: 246-257.e241.
44. Li Z, Hu S, Ghosh Z, Han Z, Wu JC (2011) Functional Characterization and Expression Profiling of Human Induced Pluripotent Stem Cell- and Embryonic Stem Cell-Derived Endothelial Cells. Stem Cells and Development 20: 1701-1710.
45. Park S-W, Jun Koh Y, Jeon J, Cho Y-H, Jang M-J, et al. (2010) Efficient differentiation of human pluripotent stem cells into functional CD34+ progenitor cells by combined modulation of the MEK/ERK and BMP4 signaling pathways. Blood 116: 5762-5772.
46. Kane NM, Meloni M, Spencer HL, Craig MA, Strehl R, et al. (2010) Derivation of endothelial cells from human embryonic stem cells by directed differentiation: analysis of microRNA and angiogenesis in vitro and in vivo. Arterioscler Thromb Vasc Biol 30: 1389-1397.
47. Bai H, Gao Y, Arzigian M, Wojchowski DM, Wu W-S, et al. (2010) BMP4 regulates vascular progenitor development in human embryonic stem cells through a smad-dependent pathway. J Cell Biochem 109: 363-374.
48. Yamashita J, Itoh H, Hirashima M, Ogawa M, Nishikawa S, et al. (2000) Flk1-positive cells derived from embryonic stem cells serve as vascular progenitors. Nature 408: 92-96.
49. Glaser DE, Gower RM, Lauer NE, Tam K, Blancas AA, et al. (2011) Functional Characterization of Embryonic Stem Cell-Derived Endothelial Cells. J Vasc Res 48: 415-428.
50. Red-Horse K, Ueno H, Weissman IL, Krasnow MA (2010) Coronary arteries form by developmental reprogramming of venous cells. Nature 464: 549-553.
51. Kume T (2010) Specification of arterial, venous, and lymphatic endothelial cells during embryonic development. Histol Histopathol 25: 637-646.
52. Swift MR, Weinstein BM (2009) Arterial-venous specification during development. Circulation Research 104: 576-588.
53. Wang H, Chen Z, Anderson D (1998) Molecular distinction and angiogenic interaction between embryonic arteries and veins revealed by ephrin-B2 and its receptor Eph-B4. Cell 93: 741-753.
54. Taura D, Sone M, Homma K, Oyamada N, Takahashi K, et al. (2009) Induction and isolation of vascular cells from human induced pluripotent stem cells--brief report. Arteriosclerosis, Thrombosis, and Vascular Biology 29: 1100-1103.
55. Homma K, Sone M, Taura D, Yamahara K, Suzuki Y, et al. (2010) Sirt1 plays an important role in mediating greater functionality of human ES/iPS-derived vascular endothelial cells. Atherosclerosis 212: 42-47.

56. Huang H, Zhao X, Chen L, Xu C, Yao X, et al. (2006) Differentiation of human embryonic stem cells into smooth muscle cells in adherent monolayer culture. Biochemical and Biophysical Research Communications 351: 321-327.
57. Xie C-Q, Zhang J, Villacorta L, Cui T, Huang H, et al. (2007) A highly efficient method to differentiate smooth muscle cells from human embryonic stem cells. Arteriosclerosis, Thrombosis, and Vascular Biology 27: e311-312.
58. Vo E, Hanjaya-Putra D, Zha Y, Kusuma S, Gerecht S (2010) Smooth-Muscle-Like Cells Derived from Human Embryonic Stem Cells Support and Augment Cord-Like Structures In Vitro. Stem Cell Rev and Rep.
59. Vazão H, das Neves RP, Grãos M, Ferreira L (2011) Towards the maturation and characterization of smooth muscle cells derived from human embryonic stem cells. PLOS one 6: e17771.
60. Yamaguchi S, Yamahara K, Homma K, Suzuki S, Fujii S, et al. (2011) The role of microRNA-145 in human embryonic stem cell differentiation into vascular cells. Atherosclerosis 219: 468-474.
61. Cheung C, Bernardo AS, Trotter MWB, Pedersen RA, Sinha S (2012) Generation of human vascular smooth muscle subtypes provides insight into embryological origin-dependent disease susceptibility. Nature Biotechnology 30: 165-173.
62. Owens GK (1995) Regulation of differentiation of vascular smooth muscle cells. Physiol Rev 75: 487-517.
63. Anson B, Nuwaysir E, Wang WB, Swanson B (2011) Industrialized production of human iPSC-derived cardiomyocytes for use in drug discovery and toxicity testing. Biopharm Int 24: 58-67.
64. Sone M, Itoh H, Yamahara K, Yamashita JK, Yurugi-Kobayashi T, et al. (2007) Pathway for differentiation of human embryonic stem cells to vascular cell components and their potential for vascular regeneration. Arterioscler Thromb Vasc Biol 27: 2127-2134.
65. Yamahara K, Sone M, Itoh H, Yamashita J, Yurugi-Kobayashi T, et al. (2008) Augmentation of neovascularizaiton in hindlimb ischemia by combined transplantation of human embryonic stem cells-derived endothelial and mural cells. PLOS one.
66. Cho S-W, Moon S-H, Lee S-H, Kang S-W, Kim J, et al. (2007) Improvement of postnatal neovascularization by human embryonic stem cell-derived endothelial-like cell transplantation in a mouse model of hindlimb ischemia. Circulation.
67. Li Z, Hu S, Ghosh Z, Han Z, Wu JC (2011) Functional Characterization and Expression Profiling of Human Induced Pluripotent Stem Cell- and Embryonic Stem Cell-Derived Endothelial Cells. Stem Cells and Development.
68. Lee T-H, Song S-H, Kim KL, Yi J-Y, Shin G-H, et al. (2010) Functional recapitulation of smooth muscle cells via induced pluripotent stem cells from human aortic smooth muscle cells. Circulation Research 106: 120-128.
69. Narsinh KH, Sun N, Sanchez-Freire V, Lee AS, Almeida P, et al. (2011) Single cell transcriptional profiling reveals heterogeneity of human induced pluripotent stem cells. J Clin Invest 121: 1217-1221.
70. Doi A, Park I-H, Wen B, Murakami P, Aryee MJ, et al. (2009) Differential methylation of tissue- and cancer-specific CpG island shores distinguishes human induced pluripotent stem cells, embryonic stem cells and fibroblasts. Nat Genet 41: 1350-1353.
71. Stadtfeld M, Apostolou E, Akutsu H, Fukuda A, Follett P, et al. (2010) Aberrant silencing of imprinted genes on chromosome 12qF1 in mouse induced pluripotent stem cells. Nature 465: 175-181.

72. Urbach A, Bar-Nur O, Daley GQ, Benvenisty N (2010) Differential modeling of fragile X syndrome by human embryonic stem cells and induced pluripotent stem cells. Cell Stem Cell 6: 407-411.
73. Choi K, Yu J, Smuga-Otto K, Salvagiotto G, Rehrauer W, et al. (2009) Hematopoietic and endothelial differentiation of human induced pluripotent stem cells. Stem Cells 27: 559.
74. Kraehenbuehl TP, Aday S, Ferreira LS (2010) Biological and Medical Physics, Biomedical Engineering. 49-67.
75. Ferreira L, Pedroso DCS, Vazão H, Gomes RSM (2010) Stem cell-based therapies for heart regeneration: what did the bench teach us? Cardiovasc Hematol Disord Drug Targets 10: 173-185.
76. Gerecht S, Ferreira LS, Langer R (2010) Vascular differentiation of human embryonic stem cells in bioactive hydrogel-based scaffolds. Methods Mol Biol 584: 333-354.
77. Kraehenbuehl TP, Ferreira LS, Zammaretti P, Hubbell JA, Langer R (2009) Cell-responsive hydrogel for encapsulation of vascular cells. Biomaterials 30: 4318-4324.
78. Pedroso DCS, Tellechea A, Moura L, Fidalgo-Carvalho I, Duarte J, et al. (2011) Improved Survival, Vascular Differentiation and Wound Healing Potential of Stem Cells Co-Cultured with Endothelial Cells. PLOS one 6: e16114.
79. Fidkowski C, Kaazempur-Mofrad MR, Borenstein J, Vacanti JP, Langer R, et al. (2005) Endothelialized microvasculature based on a biodegradable elastomer. Tissue Eng 11: 302-309.
80. Kaihara S, Borenstein J, Koka R, Lalan S, Ochoa ER, et al. (2000) Silicon micromachining to tissue engineer branched vascular channels for liver fabrication. Tissue Eng 6: 105-117.
81. Xu T, Jin J, Gregory C, Hickman JJJJ, Boland T (2005) Inkjet printing of viable mammalian cells. Biomaterials 26: 93-99.
82. Narazaki G, Uosaki H, Teranishi M, Okita K, Kim B, et al. (2008) Directed and systematic differentiation of cardiovascular cells from mouse induced pluripotent stem cells. Circulation 118: 498-506.
83. Lasala GP, Minguell JJ (2011) Vascular disease and stem cell therapies. Br Med Bull 98: 187-197.
84. Greenbaum LE (2010) From skin cells to hepatocytes: advances in application of iPS cell technology. J Clin Invest 120: 3102-3105.
85. Dambrot C, Passier R, Atsma D, Mummery CL (2011) Cardiomyocyte differentiation of pluripotent stem cells and their use as cardiac disease models. Biochem J 434: 25-35.
86. Inoue H, Yamanaka S (2011) The use of induced pluripotent stem cells in drug development. Clin Pharmacol Ther 89: 655-661.
87. Tanaka T, Tohyama S, Murata M, Nomura F, Kaneko T, et al. (2009) In vitro pharmacologic testing using human induced pluripotent stem cell-derived cardiomyocytes. Biochemical and Biophysical Research Communications 385: 497-502.
88. Asai Y, Tada M, Otsuji TG, Nakatsuji N (2010) Combination of functional cardiomyocytes derived from human stem cells and a highly-efficient microelectrode array system: an ideal hybrid model assay for drug development. Curr Stem Cell Res Ther 5: 227-232.
89. Yokoo N, Baba S, Kaichi S, Niwa A, Mima T, et al. (2009) The effects of cardioactive drugs on cardiomyocytes derived from human induced pluripotent stem cells. Biochemical and Biophysical Research Communications 387: 482-488.
90. Behbahan IS, Duan Y, Lam A, Khoobyari S, Ma X, et al. (2011) New approaches in the differentiation of human embryonic stem cells and induced pluripotent stem cells toward hepatocytes. Stem Cell Rev 7: 748-759.

91. Hester ME, Murtha MJ, Song S, Rao M, Miranda CJ, et al. (2011) Rapid and efficient generation of functional motor neurons from human pluripotent stem cells using gene delivered transcription factor codes. Mol Ther 19: 1905-1912.
92. Bissonnette CJ, Lyass L, Bhattacharyya BJ, Belmadani A, Miller RJ, et al. (2011) The controlled generation of functional basal forebrain cholinergic neurons from human embryonic stem cells. Stem Cells 29: 802-811.
93. Kim GD, Kim GJ, Seok JH, Chung H-M, Chee K-M, et al. (2008) Differentiation of endothelial cells derived from mouse embryoid bodies: a possible in vitro vasculogenesis model. Toxicol Lett 180: 166-173.
94. Zhu X, Fu A, Luo KQ (2012) A high-throughput fluorescence resonance energy transfer (FRET)-based endothelial cell apoptosis assay and its application for screening vascular disrupting agents. Biochemical and Biophysical Research Communications 418: 641-646.
95. Hada K, Suda A, Asoh K, Tsukuda T, Hasegawa M, et al. (2012) Angiogenesis inhibitors identified by cell-based high-throughput screening: synthesis, structure-activity relationships and biological evaluation of 3-[(E)-styryl]benzamides that specifically inhibit endothelial cell proliferation. Bioorganic & Medicinal Chemistry 20: 1442-1460.
96. Truskey GA (2010) Endothelial Cell Vascular Smooth Muscle Cell Co-Culture Assay For High Throughput Screening Assays For Discovery of Anti-Angiogenesis Agents and Other Therapeutic Molecules. IJHTS 2010: 171-181.
97. Seibler P, Graziotto J, Jeong H, Simunovic F, Klein C, et al. (2011) Mitochondrial Parkin recruitment is impaired in neurons derived from mutant PINK1 induced pluripotent stem cells. J Neurosci 31: 5970-5976.
98. Ebert AD, Yu J, Rose FF, Mattis VB, Lorson CL, et al. (2009) Induced pluripotent stem cells from a spinal muscular atrophy patient. Nature 457: 277-280.
99. Wang Y, Jiang Y, Liu S, Sun X, Gao S (2009) Generation of induced pluripotent stem cells from human beta-thalassemia fibroblast cells. Cell Res 19: 1120-1123.
100. Desbordes SC, Placantonakis DG, Ciro A, Socci ND, Lee G, et al. (2008) High-throughput screening assay for the identification of compounds regulating self-renewal and differentiation in human embryonic stem cells. Cell Stem Cell 2: 602-612.
101. Norström A, Akesson K, Hardarson T, Hamberger L, Björquist P, et al. (2006) Molecular and pharmacological properties of human embryonic stem cell-derived cardiomyocytes. Exp Biol Med (Maywood) 231: 1753-1762.
102. Braam SR, Tertoolen L, van de Stolpe A, Meyer T, Passier R, et al. (2010) Prediction of drug-induced cardiotoxicity using human embryonic stem cell-derived cardiomyocytes. Stem Cell Res 4: 107-116.
103. Duan Y, Ma X, Ma X, Zou W, Wang C, et al. (2010) Differentiation and characterization of metabolically functioning hepatocytes from human embryonic stem cells. Stem Cells 28: 674-686.
104. Moyon D, Pardanaud L, Yuan L, Bréant C, Eichmann A (2001) Plasticity of endothelial cells during arterial-venous differentiation in the avian embryo. Development 128: 3359-3370.
105. Othman-Hassan K, Patel K, Papoutsi M, Rodriguez-Niedenführ M, Christ B, et al. (2001) Arterial identity of endothelial cells is controlled by local cues. Developmental Biology 237: 398-409.
106. Roca C, Adams RH (2007) Regulation of vascular morphogenesis by Notch signaling. Genes Dev 21: 2511-2524.
107. You L-R, Lin F-J, Lee CT, DeMayo FJ, Tsai M-J, et al. (2005) Suppression of Notch signalling by the COUP-TFII transcription factor regulates vein identity. Nature 435: 98-104.

108. Kang J, Yoo J, Lee S, Tang W, Aguilar B, et al. (2010) An exquisite cross-control mechanism among endothelial cell fate regulators directs the plasticity and heterogeneity of lymphatic endothelial cells. Blood 116: 140-150.
109. le Noble F, Moyon D, Pardanaud L, Yuan L, Djonov V, et al. (2004) Flow regulates arterial-venous differentiation in the chick embryo yolk sac. Development 131: 361-375.
110. Claxton S, Fruttiger M (2005) Oxygen modifies artery differentiation and network morphogenesis in the retinal vasculature. Dev Dyn 233: 822-828.
111. Jones EAV, le Noble F, Eichmann A (2006) What determines blood vessel structure? Genetic prespecification vs. hemodynamics. Physiology (Bethesda) 21: 388-395.
112. Aitsebaomo J, Portbury AL, Schisler JC, Patterson C (2008) Brothers and sisters: molecular insights into arterial-venous heterogeneity. Circulation Research 103: 929-939.
113. Aird WC (2007) Phenotypic heterogeneity of the endothelium: II. Representative vascular beds. Circulation Research 100: 174-190.
114. Aird WC (2007) Phenotypic heterogeneity of the endothelium: I. Structure, function, and mechanisms. Circulation Research 100: 158-173.
115. Molema G (2010) Heterogeneity in endothelial responsiveness to cytokines, molecular causes, and pharmacological consequences. Semin Thromb Hemost 36: 246-264.
116. Davies PF, Civelek M, Fang Y, Guerraty MA, Passerini AG (2010) Endothelial heterogeneity associated with regional athero-susceptibility and adaptation to disturbed blood flow in vivo. Semin Thromb Hemost 36: 265-275.
117. Kwaan HC, Samama MM (2010) The significance of endothelial heterogeneity in thrombosis and hemostasis. Semin Thromb Hemost 36: 286-300.
118. Li Y-SJ, Haga JH, Chien S (2005) Molecular basis of the effects of shear stress on vascular endothelial cells. Journal of Biomechanics 38: 1949-1971.
119. Potter DR, Damiano ER (2008) The hydrodynamically relevant endothelial cell glycocalyx observed in vivo is absent in vitro. Circulation Research 102: 770-776.
120. Tarbell JM, Pahakis MY (2006) Mechanotransduction and the glycocalyx. J Intern Med 259: 339-350.
121. Mochizuki S, Vink H, Hiramatsu O, Kajita T, Shigeto F, et al. (2003) Role of hyaluronic acid glycosaminoglycans in shear-induced endothelium-derived nitric oxide release. Am J Physiol Heart Circ Physiol 285: H722-726.
122. Florian JA, Kosky JR, Ainslie K, Pang Z, Dull RO, et al. (2003) Heparan sulfate proteoglycan is a mechanosensor on endothelial cells. Circulation Research 93: e136-142.
123. Siegel G, Walter A, Kauschmann A, Malmsten M, Buddecke E (1996) Anionic biopolymers as blood flow sensors. Biosens Bioelectron 11: 281-294.
124. Thi MM, Tarbell JM, Weinbaum S, Spray DC (2004) The role of the glycocalyx in reorganization of the actin cytoskeleton under fluid shear stress: a "bumper-car" model. Proc Natl Acad Sci USA 101: 16483-16488.
125. Yamamoto K, Ando J (2011) New molecular mechanisms for cardiovascular disease:blood flow sensing mechanism in vascular endothelial cells. J Pharmacol Sci 116: 323-331.
126. Asahara T, Murohara T, Sullivan A, Silver M, van der Zee R, et al. (1997) Isolation of putative progenitor endothelial cells for angiogenesis. Science 275: 964-967.
127. Yamamoto K, Takahashi T, Asahara T, Ohura N, Sokabe T, et al. (2003) Proliferation, differentiation, and tube formation by endothelial progenitor cells in response to shear stress. J Appl Physiol 95: 2081-2088.

128. Jones EAV, Baron MH, Fraser SE, Dickinson ME (2004) Measuring hemodynamic changes during mammalian development. Am J Physiol Heart Circ Physiol 287: H1561-1569.
129. Yamamoto K, Sokabe T, Watabe T, Miyazono K, Yamashita JK, et al. (2005) Fluid shear stress induces differentiation of Flk-1-positive embryonic stem cells into vascular endothelial cells in vitro. Am J Physiol Heart Circ Physiol 288: H1915-1924.
130. Obi S, Yamamoto K, Shimizu N, Kumagaya S, Masumura T, et al. (2009) Fluid shear stress induces arterial differentiation of endothelial progenitor cells. J Appl Physiol 106: 203-211.
131. Masumura T, Yamamoto K, Shimizu N, Obi S, Ando J (2009) Shear stress increases expression of the arterial endothelial marker ephrinB2 in murine ES cells via the VEGF-Notch signaling pathways. Arterioscler Thromb Vasc Biol 29: 2125-2131.
132. Adamo L, Naveiras O, Wenzel PL, McKinney-Freeman S, Mack PJ, et al. (2009) Biomechanical forces promote embryonic haematopoiesis. Nature 459: 1131-1135.
133. Adamo L, García-Cardeña G (2011) Directed stem cell differentiation by fluid mechanical forces. Antioxidants & Redox Signaling 15: 1463-1473.
134. Fung YC (1997) Biomechanics: Circulation. New York, NY: Springer.
135. LaBarbera M (1990) Principles of design of fluid transport systems in zoology. Science 249: 992-1000.
136. Kamiya A, Bukhari R, Togawa T (1984) Adaptive regulation of wall shear stress optimizing vascular tree function. Bull Math Biol 46: 127-137.
137. Hishikawa K, Nakaki T, Marumo T, Suzuki H, Kato R, et al. (1995) Pressure enhances endothelin-1 release from cultured human endothelial cells. Hypertension 25: 449-452.
138. Zamir M (1976) The role of shear forces in arterial branching. J Gen Physiol 67: 213-222.
139. Malek AM, Alper SL, Izumo S (1999) Hemodynamic shear stress and its role in atherosclerosis. JAMA 282: 2035-2042.
140. El-Ali J, Sorger PK, Jensen KF (2006) Cells on chips. Nature 442: 403-411.
141. Meyvantsson I, Beebe DJ (2008) Cell culture models in microfluidic systems. Annu Rev Anal Chem (Palo Alto Calif) 1: 423-449.
142. van der Meer AD, Kamphuis MMJ, Poot AA, Feijen J, Vermes I (2009) Lowering caveolin-1 expression in human vascular endothelial cells inhibits signal transduction in response to shear stress. International Journal of Cell Biology 2009: 532432.
143. van der Meer AD, Poot AA, Feijen J, Vermes I (2010) Analyzing shear stress-induced alignment of actin filaments in endothelial cells with a microfluidic assay. Biomicrofluidics 4: 11103.
144. Song JW, Gu W, Futai N, Warner KA, Nor JE, et al. (2005) Computer-controlled microcirculatory support system for endothelial cell culture and shearing. Anal Chem 77: 3993-3999.
145. van der Meer AD, Li Y, Duits MHG, Poot AA, Feijen J, et al. (2010) Shear stress induces a transient and VEGFR-2-dependent decrease in the motion of injected particles in endothelial cells. Biorheology 47: 179-192.
146. Vickerman V, Blundo J, Chung S, Kamm R (2008) Design, fabrication and implementation of a novel multi-parameter control microfluidic platform for three-dimensional cell culture and real-time imaging. Lab Chip 8: 1468-1477.
147. van der Meer AD, Vermeul K, Poot AA, Feijen J, Vermes I (2010) A microfluidic wound-healing assay for quantifying endothelial cell migration. Am J Physiol Heart Circ Physiol 298: H719-725.

148. van der Meer AD, Vermeul K, Poot AA, Feijen J, Vermes I (2010) Flow cytometric analysis of the uptake of low-density lipoprotein by endothelial cells in microfluidic channels. Cytometry A 77: 971-975.
149. Prabhakarpandian B, Pant K, Scott RC, Patillo CB, Irimia D, et al. (2008) Synthetic microvascular networks for quantitative analysis of particle adhesion. Biomed Microdevices 10: 585-595.
150. Shin M, Matsuda K, Ishii O, Terai H, Kaazempur-Mofrad M, et al. (2004) Endothelialized networks with a vascular geometry in microfabricated poly(dimethyl siloxane). Biomed Microdevices 6: 269-278.
151. Fiddes LK, Raz N, Srigunapalan S, Tumarkan E, Simmons CA, et al. (2010) A circular cross-section PDMS microfluidics system for replication of cardiovascular flow conditions. Biomaterials 31: 3459-3464.
152. Lee SH, Kang DH, Kim HN, Suh KY (2010) Use of directly molded poly(methyl methacrylate) channels for microfluidic applications. Lab Chip 10: 3300-3306.
153. Tsai M, Kita A, Leach J, Rounsevell R, Huang JN, et al. (2012) In vitro modeling of the microvascular occlusion and thrombosis that occur in hematologic diseases using microfluidic technology. J Clin Invest 122: 408-418.
154. Carmeliet P (2000) Mechanisms of angiogenesis and arteriogenesis. Nature Medicine 6: 389-395.
155. Jay SM, Shepherd BR, Andrejecsk JW, Kyriakides TR, Pober JS, et al. (2010) Dual delivery of VEGF and MCP-1 to support endothelial cell transplantation for therapeutic vascularization. Biomaterials 31: 3054-3062.
156. Richardson TP, Peters MC, Ennett AB, Mooney DJ (2001) Polymeric system for dual growth factor delivery. Nature Biotechnology 19: 1029-1034.
157. Silva EA, Kim E-S, Kong HJ, Mooney DJ (2008) Material-based deployment enhances efficacy of endothelial progenitor cells. Proc Natl Acad Sci USA 105: 14347-14352.
158. Ziebart T, Yoon C-H, Trepels T, Wietelmann A, Braun T, et al. (2008) Sustained Persistence of Transplanted Proangiogenic Cells Contributes to Neovascularization and Cardiac Function After Ischemia. Circulation Research 103: 1327-U1275.
159. Kalka C, Masuda H, Takahashi T, Kalka-Moll WM, Silver M, et al. (2000) Transplantation of ex vivo expanded endothelial progenitor cells for therapeutic neovascularization. Proceedings of the National Academy of Sciences of the United States of America 97: 3422-3427.
160. Kupatt C, Horstkotte J, Vlastos G, Pfosser A, Lebherz C, et al. (2005) Embryonic endothelial progenitor cells expressing a broad range of proangiogenic and remodeling factors enhance vascularization and tissue recovery in acute and chronic ischemia. The FASEB journal : official publication of the Federation of American Societies for Experimental Biology 19: 1576-1578.
161. Taguchi A, Soma T, Tanaka H, Kanda T, Nishimura H, et al. (2004) Administration of CD34+ cells after stroke enhances neurogenesis via angiogenesis in a mouse model. Journal Of Clinical Investigation 114: 330-338.
162. Kawamoto A, Asahara T, Losordo DW (2002) Transplantation of endothelial progenitor cells for therapeutic neovascularization. Cardiovascular Radiation Medicine 3: 221-225.
163. Kocher AA, Schuster MD, Szabolcs MJ, Takuma S, Burkhoff D, et al. (2001) Neovascularization of ischemic myocardium by human bone-marrow-derived angioblasts prevents cardiomyocyte apoptosis, reduces remodeling and improves cardiac function. Nat Med 7: 430-436.
164. Phelps EA, Garcia AJ (2009) Update on therapeutic vascularization strategies. Regenerative Medicine 4: 65-80.

165. Ferrara N (2002) VEGF and the quest for tumour angiogenesis factors. Nat Rev Cancer 2: 795-803.
166. Senger DR, Galli SJ, Dvorak AM, Perruzzi CA, Harvey VS, et al. (1983) Tumor cells secrete a vascular permeability factor that promotes accumulation of ascites fluid. Science 219: 983-985.
167. Leung DW, Cachianes G, Kuang WJ, Goeddel DV, Ferrara N (1989) Vascular endothelial growth factor is a secreted angiogenic mitogen. Science 246: 1306-1309.
168. Hanft JR, Pollak RA, Barbul A, van Gils C, Kwon PS, et al. (2008) Phase I trial on the safety of topical rhVEGF on chronic neuropathic diabetic foot ulcers. J Wound Care 17: 30-37.
169. Henry TD, Annex BH, McKendall GR, Azrin MA, Lopez JJ, et al. (2003) The VIVA trial: Vascular endothelial growth factor in Ischemia for Vascular Angiogenesis. Circulation 107: 1359-1365.
170. Henry TD, Rocha-Singh K, Isner JM, Kereiakes DJ, Giordano FJ, et al. (2001) Intracoronary administration of recombinant human vascular endothelial growth factor to patients with coronary artery disease. American Heart Journal 142: 872-880.
171. Eppler SM, Combs DL, Henry TD, Lopez JJ, Ellis SG, et al. (2002) A target-mediated model to describe the pharmacokinetics and hemodynamic effects of recombinant human vascular endothelial growth factor in humans. Clin Pharmacol Ther 72: 20-32.
172. Ji JA, Liu J, Shire SJ, Kamerzell TJ, Hong S, et al. (2010) Characteristics of rhVEGF release from topical hydrogel formulations. Pharmaceutical research 27: 644-654.
173. Sun G, Shen Y-I, Ho CC, Kusuma S, Gerecht S (2010) Functional groups affect physical and biological properties of dextran-based hydrogels. J Biomed Mater Res A 93: 1080-1090.
174. Sharon JL, Puleo DA (2008) Immobilization of glycoproteins, such as VEGF, on biodegradable substrates. Acta Biomat 4: 1016-1023.
175. Shen YH, Shoichet MS, Radisic M (2008) Vascular endothelial growth factor immobilized in collagen scaffold promotes penetration and proliferation of endothelial cells. Acta Biomat 4: 477-489.
176. De la Riva B, Nowak C, Sánchez E, Hernández A, Schulz-Siegmund M, et al. (2009) VEGF-controlled release within a bone defect from alginate/chitosan/PLA-H scaffolds. Eur J Pharm Biopharm 73: 50-58.
177. Lode A, Reinstorf A, Bernhardt A, Wolf-Brandstetter C, König U, et al. (2008) Heparin modification of calcium phosphate bone cements for VEGF functionalization. J Biomed Mater Res A 86: 749-759.
178. Peattie RA, Rieke ER, Hewett EM, Fisher RJ, Shu XZ, et al. (2006) Dual growth factor-induced angiogenesis in vivo using hyaluronan hydrogel implants. Biomaterials 27: 1868-1875.
179. Zhu X, Wu S, Dahut WL, Parikh CR (2007) Risks of proteinuria and hypertension with bevacizumab, an antibody against vascular endothelial growth factor: systematic review and meta-analysis. Am J Kidney Dis 49: 186-193.
180. Lee S, Chen TT, Barber CL, Jordan MC, Murdock J, et al. (2007) Autocrine VEGF signaling is required for vascular homeostasis. Cell 130: 691-703.
181. Gerber H, McMurtrey A, Kowalski J, Yan M, Keyt B, et al. (1998) Vascular endothelial growth factor regulates endothelial cell survival through the phosphatidylinositol 3 '-kinase Akt signal transduction pathway - Requirement for Flk-1/KDR activation. J Biol Chem 273: 30336-30343.
182. Kilic E, Kilic U, Wang Y, Bassetti CL, Marti HH, et al. (2006) The phosphatidylinositol-3 kinase/Akt pathway mediates VEGF's neuroprotective activity and induces

blood brain barrier permeability after focal cerebral ischemia. The FASEB journal : official publication of the Federation of American Societies for Experimental Biology 20: 1185-1187.
183. Chen TT, Luque A, Lee S, Anderson SM, Segura T, et al. (2010) Anchorage of VEGF to the extracellular matrix conveys differential signaling responses to endothelial cells. J Cell Biol 188: 595-609.

CHAPTER 3 - TOWARDS THE MATURATION AND CHARACTERIZATION OF SMOOTH MUSCLE CELLS DERIVED FROM HUMAN EMBRYONIC STEM CELLS

Helena Vazão[1,2], Ricardo Pires das Neves[1,2], Mário Grãos[2], Lino Ferreira[1,2]

[1] CNC - Center of Neurosciences and Cell Biology, University of Coimbra, Coimbra, Portugal, [2] Biocant - Center of Innovation in Biotechnology, Cantanhede, Portugal

Published on PLoS ONE (Research article, published 10 March 2011, doi:10.1371/journal.pone.0017771)

Abstract

In this study we demonstrate that $CD34^+$ cells derived from human embryonic stem cells (hESCs) have higher smooth muscle cell (SMC) potential than $CD34^-$ cells. We report that from all inductive signals tested, retinoic acid (RA) and platelet derived growth factor ($PDGF_{BB}$) are the most effective agents in guiding the differentiation of $CD34^+$ cells into smooth muscle progenitor cells (SMPCs) characterized by the expression of SMC genes and proteins, secretion of SMC-related cytokines, contraction in response to depolarization agents and vasoactive peptides and expression of SMC-related genes in a 3D environment. These cells are also characterized by a low organization of the contractile proteins and the contractility response is mediated by Ca^{2+}, which involves the activation of Rho A/Rho kinase- and Ca^{2+}/calmodulin (CaM) /myosin light chain kinase (MLCK)-dependent pathways. We further show that SMPCs obtained from the differentiation of $CD34^+$ cells with RA, but not with $PDGF_{BB,}$ can be maturated in medium supplemented with endothelin-1 showing at the end individualized contractile filaments. Overall the hESC-derived SMCs presented in this work might be an unlimited source of SMCs for tissue engineering and regenerative medicine.

Introduction

Vascular smooth muscle cells (VSMCs) have enormous applications in regenerative medicine [1,2,3]. Studies have demonstrated that smooth muscle-like cells (SMLCs) can be derived from bone marrow- [4,5], adipose- [6,7] and umbilical cord blood-derived stem cells [8]. Due to the easy expansion, human embryonic stem cells (hESCs) represent an alternative source of VSMCs particularly for old patients having stem cells with impaired function. Recent studies reported different strategies to differentiate hESCs into SMLCs by exposing a monolayer of undifferentiated hESCs to retinoic acid [9] or a combination of cell culture medium and extracellular matrix environment [10,11,12] either in single-hESC- [13], embryoid bodies (EBs)- [12] or stromal cell- [14] culture conditions. In one case, SMLCs transplanted subcutaneously in an animal model were able to contribute for the formation of functional blood microvessels [12]. Despite these advances, several issues remain poorly understood: (i) what hESC-derived population has the most SMC potential, (ii) the bioactive molecules involved in the differentiation process, (iii) the modulatory effect of 3D environments in SMLCs, (iv) the functionality of the differentiated SMLCs, and (v) the level of organization of the contractile protein filaments.

Here we evaluate the smooth muscle cell (SMC) differentiation of different cell populations isolated from human embryoid bodies grown in suspension for 10 days. The isolated cells were cultured in media supplemented with several inductive signals, including platelet-derived growth factor ($PDGF_{BB}$), retinoic acid (RA), transforming growth factor beta 1 ($TGF_{\beta 1}$) or a combination of $PDGF_{BB}$ with $TGF_{\beta 1}$. We show that $CD34^+$ cells have higher SMC potential than $CD34^-$ cells and $PDGF_{BB}$ and RA are the most effective agents to drive the differentiation of hESCs into smooth muscle progenitor cells (SMPCs). We further demonstrate that these cells contract and relax in response to SMC agonists or inhibitors, respectively, and the effect is mediated by Rho A/Rho kinase- and Ca^{2+}/ CaM / MLCK-dependent pathways. In addition, cells encapsulated in 3D gel scaffolds further differentiate towards SMC lineage as confirmed by gene analysis. Finally, we show that Endothelin-1 induces the organization of the contractile protein filaments.

Materials and Methods

hESC culture and embryoid body (EB) formation

Undifferentiated hESCs (passages 27-62; H9, WiCell, Wisconsin, http://www.wicell.org/) were grown on an inactivated mouse embryonic fibroblast (MEF) feeder layer, as previously described [12]. To induce the formation of EBs, the undifferentiated hESCs were treated with 2 mg/mL type IV collagenase (Invitrogen, http://www.invitrogen.com) for 2 h and then transferred (2:1) to low attachment plates (Corning, http://www.corning.com) containing 10 mL of differentiation medium [80% KO-DMEM, 20% fetal bovine serum (FBS, Invitrogen), 0.5% L-glutamine, 0.2% β-mercaptoethanol, 1% nonessential amino acids and 50 U/ml:50 μg/ml penicillin-streptomycin solution]. EBs were cultured for 10 days at 37ºC, 5% CO_2 in a humidified atmosphere, with media changes every 3-4 days.

Isolation and differentiation of $CD34^+$, $CD34^-$ and $CD34^+KDR^-$ cells

$CD34^+$ cells were isolated from EBs at day 10 according to a protocol previously reported by us [12]. For some experiments, the $CD34^+$ cells were further separated in $CD34^+KDR^-$ cells. In this case, cells were labeled with anti-VEGF R2/KDR-PE antibody (R&D, http://www.rndsystems.com/), then conjugated with anti-PE antibody coupled with magnetic beads, and finally the magnetically labeled cells were separated into $CD34^+KDR^+$ and $CD34^+KDR^-$ using a MS-MACS column (Miltenyi Biotec, http://www.miltenyibiotec.com). Isolated cells were grown on 24-well plates (1.5×10^4 cells/cm^2) coated with 0.1% gelatin and containing one of the following media: smooth muscle growth medium-2 (SMGM-2), endothelial growth medium-2 (EGM-2) or EGM-2 supplemented with $PDGF_{BB}$ (50 ng/mL, Prepotech, http://www.peprotech.com/) or RA (1 μM, Sigma, http://www.sigmaaldrich.com) or $TGF_{\beta 1}$ (10 ng/mL, Prepotech) or a mixture of $PDGF_{BB}$ with $TGF_{\beta 1}$ (50 ng/mL; 10 ng/mL). Human vascular smooth muscle cells (hVSMCs, isolated from the arteries of human umbilical cord, Lonza, http://www.lonza.com) were used as controls for the differentiation studies. Cells were cultured in SMGM-2 media (Lonza; until passage 6) being the medium changed every 2 days.

Immunofluorescence analysis

Cells were transferred to gelatin-coated slides containing differentiation medium, allowed to attach overnight, and then fixed with 4% paraformaldehyde (Electron Microscopy Sciences, http://www.emsdiasum.com/microscopy) for 15 min at room temperature. Cells were blocked with 1% (w/v) BSA and stained for 1 h with anti-human primary antibodies specific for smooth muscle α-actin (α-SMA, 1A4, Dako, http://www.dako.com/), smooth muscle myosin heavy chain (SM-MHC, SMMS-1, Dako) and calponin (CALP, Calponin1, Santa Cruz Biotec, http://www.scbt.com/). In each immunofluorescence experiment, an isotype-matched IgG control was used. Binding of primary antibodies to specific cells was detected with anti-mouse IgG Cy3 conjugate or anti-mouse IgG FITC (both form Sigma). Cell nuclei were stained with 4', 6'-diamidino-2-phenylindole (DAPI) (Sigma) and the slides examined with either a Zeiss fluorescence microscope or Zeiss LSM 50 confocal microscope.

Flow cytometry analysis

Cells were tripsinized, aliquoted (1.25-2.5 × 10^5 cells per condition) and fixed for 10 minutes in cold 4% (v/v, in PBS) paraformaldehyde (Electron Microscopy Sciences). Afterwards, the cells were washed in PBS, centrifuged at 1200 g and ressuspended in permeabilization buffer (PBS containing 0.5% Triton X-100) for 7 minutes. Cells were incubated in permeabilization buffer containing human smooth muscle α-actin monoclonal antibody (R&D) or isotype control IgG2a antibody (R&D). Cells were characterized by using a FACS Calibur (BD) and the data analysed by Cell Quest software. Twenty thousand events were collected in each run.

Reverse transcription-polymerase chain reaction (RT-PCR) analysis

Total RNA from experimental groups was isolated using a protocol with TRIzol (Invitrogen) and RNeasy Minikit (Qiagen, Valencia, http://www1.qiagen.com/). cDNA was prepared from 1 mg total RNA using Taqman Reverse transcription reagents (Applied Biosystems, CA). Quantitative PCR (qPCR) was performed using Power SYBR Green PCR Master Mix and the detection using an ABI PRISM 7500 System (Applied Biosystems, http://www3.appliedbiosystems.com). Quantification of target genes was performed relative to the reference GAPDH gene: relative expression= $2^{[-(Ct_{sample}-Ct_{GADPH})]}$. The mean minimal cycle threshold values (Ct) were calculated from quadruplicate reactions. Then,

the relative gene expression in each experimental group was normalized to the relative gene expression found in hVSMCs. Primer sequences used are in **Table 1**. For the RT^2 Profiler™ PCR Array, cDNA was prepared from 1 mg total RNA using the RT^2 PCR Array first strand kit (SABiosciences, http://www.sabiosciences.com/). RT-PCR assays were performed using the human extracellular matrix and adhesion molecules RT^2 Profiler™ PCR Array (SABiosciences) on an ABI PRISM 7500 System. Data analysis was performed using analysis software provided by the kit manufacturer.

Table 1 Primers used for Real Time PCR

	Sense	Antisense
GAPDH [12]	AGCCACATCGCTCAGACACC	GTACTCAGCGCCAGCATCG
α-SMA [12]	CCAGCTATGTGAAGAAGAAGAGG	GTGATCTCCTTCTGCATTCGGT
SM-MHC [5]	CAGGAGTTCCGCCAACGCTA	TCCCGTCCATGAAGCCTTTGG
SMα22 [5]	TCCCCGTCCATGAAGCCTTTGG	CGAAAGCCGGCCTTACAGA
Calponin [5]	TTTTGAGGCCAACGACCTGT	TCCTTTCGTCTTCGCCATG
Oct-4 [15]	GTGGAGGAAGCTGACAACAA	CTCCAGGTTGCCTCTCACTC
α-actinin	CTGCTGCTTTGGTGTCAGAG	TTCCTATGGGGTCATCCTTG

PCR conditions: initial denaturation step at 94ºC for 5 min; 40 cycles of denaturation at 94ºC for 30 sec, annealing at 60ºC for 33 sec and extension at 72ºC for 30 sec. At the end was performed a final 7 minutes extension at 72ºC. After amplification, the melting curve profile or agarose gel electrophoresis was used to determine the specificity of PCR products.

Intracellular Ca^{2+} variation measurements

SMCs, HUVEC or hESC-derived SMPCs were loaded with Fura-2 calcium fluorescent indicator by incubation with 10 μM of the membrane permeable acetoxymethyl (AM) derivative FURA-2/AM (1 mM in DMSO, Molecular Probes) and 0.06% (w/v) Pluronic F-127 (Sigma), using basal medium (M199, Sigma) as vehicle (35 μl/well, not supplemented with serum or antibiotics), for 1 h at 37ºC in 5% CO_2 and 90% humidity. The medium was then replaced by the respective basal medium and cells were incubated in the same conditions for 30 min to allow hydrolysis of the acetoxymethyl (AM) esters by cellular esterases, resulting in intracellular capture of the membrane impermeant Fura-2. Cells were then washed twice with 100 μL sodium salt solution (140 mM NaCl, 5 mM KCl, 1 mM

$CaCl_2$, 1 mM $MgCl_2$, 10 mM Glucose, 10 mM HEPES-Na^+ pH 7.4). The buffer was then replaced again (100 µl/well) immediately prior to incubating or not with test compounds.

Cells located in wells on a plate row were incubated at 25ºC (inside the microplate reader, during basal reading). Cells were then stimulated with 100 µM Histamine (Sigma) [16,17], 10^{-7} M Bradykinin (Calbiochem) [18], 10^{-5} M Angiotensin II (Calbiochem) [18] or 50 mM KCl (Merck) [16,17] by adding 1 µl of a stock solution.

Fluorescence was measured at emission 510 nm using two alternating excitation wavelengths (340nm and 380nm) [19] using a microplate fluorescence reader (Spectramax Gemini EM, Molecular Devices, with SoftMax® Pro software). The microplate reader was set to "top-read kinetics"; PMT was "high"; temperature was 25ºC; each fluorescence time point was an average of 18 reads; and during basal/inhibitors incubation periods and KCl/Histamine stimulation, each well was read every 3 sec. Fluorescence intensity values (in relative fluorescence units - RFU) measured at 340 nm and 380 nm were taken from the stabilized signal obtained at basal conditions and after incubation or not with the inhibitors. Following stimulation with Histamine/Bradykinin/Angiotensin II/KCl, the fluorescence values were taken from the time point at the peak of the response. Typically, each experiment consisted of three or four wells plus three or four wells containing cells incubated with inhibitors and all cells were stimulated and read simultaneously. The dose-response curves for the effect of stimuli on the intracellular Ca^{2+} variation were determined using the software GraphPad Prism™.

Contractility assays

Agonist-induced contractile activity of the differentiated cells was evaluated as previously described [6,12]. hECS-derived cells cultured for 3 passages were washed with DMEM and contraction was induced by incubating these cells with 10^{-5}M carbachol in DMEM (Sigma) medium for 30 min. Contraction was calculated as the difference in cell area between time zero and 30 minutes. The same microscopic fields were imaged before and after treatment for contraction analysis. In a distinct experiment, cell relaxation was induced by incubation with 10^{-4} M atropine (AlfaAesar) in DMEM for 1 h followed by contraction with 10^{-5} M carbachol. Contraction was calculated as before. hVSMCs (3rd passage) were used as controls.

Effect of RhoA/Rho kinase- and CaM/MLCK- agonists in cell contraction and maturation

hVSMCs or hESC-derived SMPCs were treated with the inhibitor W-7 (12 mg/mL, Sigma) for 30 min and the agonist U46619 (1 mM, a CAM kinase-agonist) (Cayman Chemicals, http://www.caymanchem.com) in serum-free M199 medium for 3 days. At the end, cells were characterized for the expression of SMC markers by immunostaining. Finally, the contraction of U46619-treated cells was evaluated by embedding the cells in fibrin gels (3.5×10^4 cells/50 μL) and measuring gel size at time 0 and 14 h by microscopy. This methodology was repeated to evaluate the effect of Rho kinase-agonist in cell contraction and maturation. In this case, the cells were exposed to the inhibitor Y27632 (13 mM) (Cayman Chemicals) and the agonist endothelin-1 (End-1, 10 nM, Sigma).

Cytokine measurements

Cell culture supernatants were assayed for cytokines using a Bio-plex human 17-plex panel immunoassay kit (Bio-Rad), according to manufacturer's instructions. The 17-Plex panel consisted of the following analytes: interleukin-1 (IL-1β), IL-2, IL-4, IL-5, IL-6, IL-7, IL-8; IL-10, IL-12(p70), IL-13, IL-17, granulocyte colony-stimulating factor (G-CSF), granulocyte/macrophage colony-stimulating factor (GM-CSF), interferon (IFN-γ), monocyte chemotactic protein (MCP-1 (MCAF)), macrophage inflammatory protein (MIP-1b), and tumor necrosis factor (TNF-α). A standard range of 0.2 to 3,200 pg/mL was used. Supernatants media samples were collected, centrifuged and frozen. Samples and controls were run in triplicate, standards and blanks in duplicate. Cell culture supernatants were assayed for cytokines using a Bio-plex human 17-plex panel immunoassay kit (Bio-Rad, http://www.bio-rad.com) and cytokines concentrations were determined using Bio-Plex Manager 5, according to manufacturer's instructions.

Co-culture of hESC-derived SMPCs with hVSMCs

To evaluate the effect of both soluble and insoluble factors, fluorescently-labeled hESC-derived SMPCs (stained with PKH67 dye, Sigma) were plated on top of mytomycin-inactivated hVSMC cultured on a 24 well plate for 2 days before use. This co-culture system was maintained for 5 days after which the overall cells were tripsinized, and fluorescent ($PKH67^+$ cells) cells sorted by a FACS Aria (BD). The sorted cells were

characterized by immunohistochemistry to evaluate the expression and organization of α-SMA, SM-MHC and calponin filaments.

Culture of SMPCs in three-dimensional gels

Fibrin gels were obtained by the crosslinking of 20 mg/mL fibrinogen/TBS pH 7.4 in the presence of 50 U/mL thrombin/TBS pH 7.4 (both from Sigma-Aldrich). Fibrin gels (50 μL) were prepared by mixing the following components: 10 mg/mL fibrinogen, 2.5 mM $CaCl_2$, 2 U/mL thrombin and 0.01 mg/mL aprotinin (Sigma-Aldrich). This solution was allowed to gel at 37ºC in 100% relative humidity. hVSMC or hESC-derived SMPCs (3×10^5 cells) were encapsulated in fibrin gels (50 μl). Cells were centrifuged and resuspended in the fibrin gel precursor solution and included in 1 mL sterile syringes with cut tips. Polymerization was initiated at 37ºC and allowed to proceed over 30 min. After polymerization, the cell constructs were removed from the syringe and placed in 24-well plates, containing specific medium, for up to 96 h.

Statistical analysis

An unpaired *t* test or one-way ANOVA analysis of variance with Bonferroni post test was performed for statistical tests using SigmaStat. Results were considered significant when $P < 0.05$. Data are shown as mean ± SEM.

Results and Conclusions

Effect of initial cell population and inductive signals on cell proliferation

We evaluated the SMC differentiation potential of three cell populations isolated from EBs at day 10: $CD34^+$ cells, $CD34^-$ cells and $CD34^+KDR^-$ cells (mesenchymal origin [20]) (**Fig. 1A**). The percentages of $CD34^+$ and $CD34^+KDR^-$ cells in EBs were approximately 2% and 1.7%, respectively, after MACS isolation. As evaluated by flow cytometry, the purity of the cell populations $CD34^+$, $CD34^-$, and $CD34^+KDR^-$ was > 80%, > 98% and > 98%, respectively (**Fig. 1B**). These cells were plated on gelatin coated dishes, at low density ($1.5\times10^4/cm^2$), and cultured on basal media (EGM-2 or SMGM-2) supplemented or not with different inductive signals to guide their SMC differentiation: $PDGF_{BB}$ (50 ng/mL) [5,12,21], RA (1 μM) [9,18,22], $TGF_{\beta1}$ (10 ng/mL) [5,23,24] or a combination of $TGF_{\beta1}$ (10 ng/mL) with $PDGF_{BB}$ (50 ng/mL) (**Fig. 1A**). These concentrations have been used previously in the differentiation of stem cells from different origins into vascular cells [5,9,23]. $CD34^+$ cells cultured on EGM-2 medium supplemented with $PDGF_{BB}$ presented the highest proliferation (more than 8 population doublings over 20 days), followed by the ones cultured in EGM-2 medium supplemented with RA (**Fig. 1C.1**). $CD34^+$ cells grown in EGM-2 medium without $PDGF_{BB}$ or RA proliferated poorly over 40 days (**Fig. 1C.1**). Interestingly, $CD34^+$ cells cultured in medium supplemented with $TGF_{\beta1}$ and $PDGF_{BB}$ had low proliferation suggesting that $TGF_{\beta1}$ inhibited the effect of $PDGF_{BB}$. $CD34^+KDR^-$ cells cultured on EGM-2 medium without any supplements proliferated extensively, showing more than 8 population doublings over 20 days (**Fig. 1C.2**). Similar proliferation potential was observed for $CD34^+KDR^-$ cells grown in EGM-2 medium supplemented with RA, but not on medium supplemented with $PDGF_{BB}$.

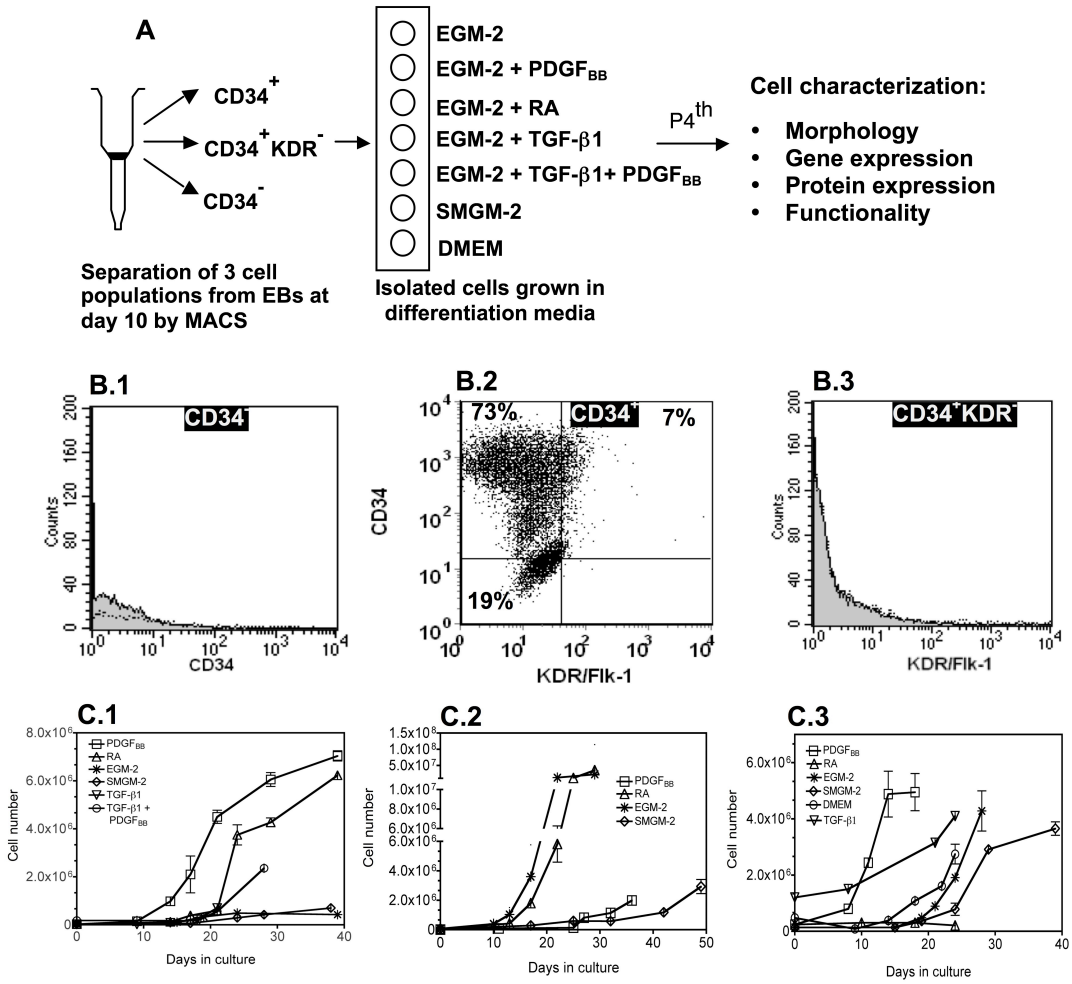

Figure 1 - The effect of initial cell population and inductive signals on cell proliferation. (A) Protocols adopted to drive the differentiation of $CD34^+$, $CD34^+KDR^-$ and $CD34^-$ cells isolated from EBs at day 10 into the SMC lineage. (B) Flow cytometric analysis of hES-derived cells: $CD34^-$ (B.1), $CD34^+$ (B.2) and $CD34^+KDR^-$ (B.3) cells (in this last case isolated from the $CD34^+$ cell population). The results show that $CD34^-$ cells do not express $CD34^+$ marker (B.1), $CD34^+$ cells are formed by $CD34^+KDR^-$ and $CD34^+KDR^+$ cells (B.2), and $CD34^+KDR^-$ do not express the KDR marker (B.3). Percent of positive cells (dash plot) were calculated based in the isotype controls (grey plot). (C) Time-course proliferation of $CD34^+$ (C.1), $CD34^+KDR^-$ (C.2) and $CD34^-$ cells (C.3).

The proliferation rate of $CD34^-$ cells was also assessed in the media formulations tested for $CD34^+$ and $CD34^+KDR^-$ cells. $CD34^-$ cells cultured on EGM-2 medium supplemented with $PDGF_{BB}$ showed the highest proliferation, having more than 8 population doublings over an 18 days period (**Fig. 1C.3**). In contrast, cells grown in EGM-2 medium supplemented with RA did show a poor proliferation over more than 20 days.

All taken together, the proliferation potential of the cells was dependent on the initial cell population and the supplements added to the basal media.

Effect of initial cell population and inductive signals on SMC differentiation

Next we evaluated the expression of SMC-specific genes in the hESC-derived cells (passage 4) by quantitative RT-PCR (**Fig. 2**). The genes analyzed included: α-smooth muscle actin (α-SMA), an early marker of SMC differentiation and highly specific marker for SMCs in adult animals [25]; smooth muscle myosin heavy chain (SM-MHC), a later marker in SMC differentiation that seems to be highly restricted to SMCs [26]; calponin and smooth muscle α-22, definitive SMC markers [27]. The gene expression in the hESC-derived cells was normalized by the corresponding gene expression in hVSMCs.

Undifferentiated $CD34^+$ cells expressed low levels of SM-MHC (~2.0%), SMα-22 (< 1%) and calponin (~2.0%), in most cases comparable to the levels found in undifferentiated hESCs, and moderate levels of a-SMA (~10%) (**Fig. 2**). Culture of these cells in the presence of EGM-2 medium supplemented with $PDGF_{BB}$ or RA contributed for the up-regulation of SMC genes, as confirmed by the significant increase in the expression of α-SMA (>400-fold) and SM-MHC (>1,600-fold) when compared with undifferentiated $CD34^+$ cells ($p<0,05$), and hVSMCS (α-SMA: >39-fold; SM-MHC: >27-fold) (**Fig. 2**). Addition of $TGF_{\beta1}$, or $TGF_{\beta1}$ plus $PDGF_{BB}$ increased the cellular expression of α-SMA, SM-MHC, SMα-22 and calponin when compared to undifferentiated $CD34^+$ cells; however, the expression was one order of magnitude lower than the one in hVSMCS, suggesting that the $CD34^+$-derived cells were not fully differentiated into SMCs.

$CD34^+KDR^-$ cells cultured in SMGM-2 medium or EGM-2 medium in the presence or absence of $PDGF_{BB}$ expressed higher levels of α-SMA (>42-fold), SM-MHC (>150-fold), SMα-22 (>18-fold) and calponin (>2-fold) than undifferentiated $CD34^+$ cells (**Fig. 2**). In addition, these cells showed similar levels of expression of α-SMA and SM-MHC to the one found in hVSMCs, suggesting that these cells shared features with SMCs.

In contrast to the $CD34^+$ and $CD34^+KDR^-$ cells, $CD34^-$ cells cultured in several media formulations had lower expression of SMC markers, indicating low efficiency of differentiation into SMCs (**Fig. 2**). Of note, all the hESC-derived cells previously described had low expression of Oct-4 confirming their loss of pluripotency. In addition, hESC-derived cells expressing high levels of SMC markers had no expression of PECAM-1 (endothelial cell marker) and a-actinin (a marker of cardiomyocytes) (data not shown) confirming again their SMC differentiation.

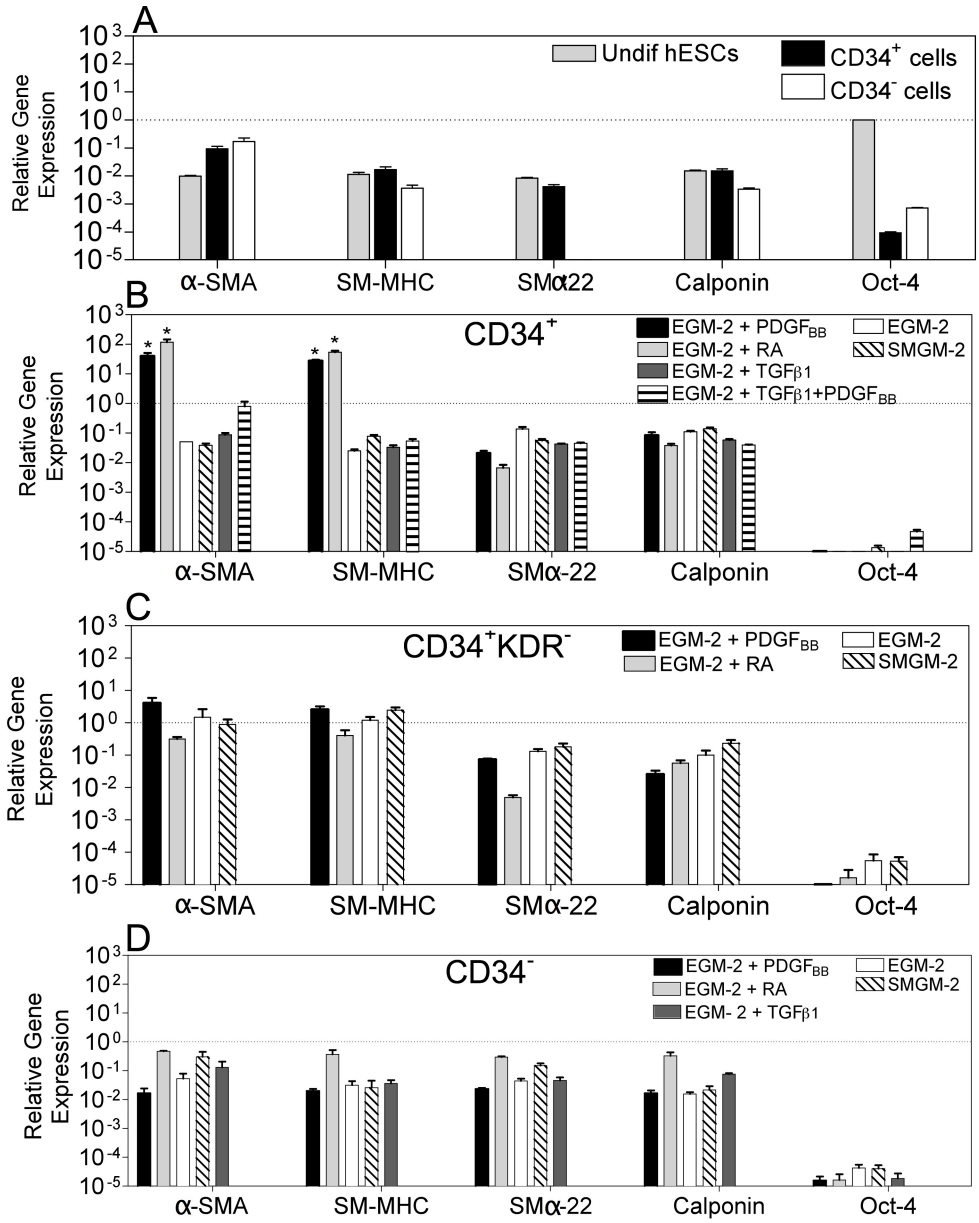

Figure 2 - **Gene expression in hESC-derived cells evaluated by qRT-PCR.** Gene expression in each experimental group was normalized by the corresponding gene expression observed in hVSMCs. Oct-4 was normalized by the expression in undifferentiated hESCs. (A) Gene expression of hESCs, $CD34^+$ and $CD34^-$ cells before differentiation. SM_α-22 expression in $CD34^-$ cells is very low ($<8.5 \times 10^{-6}$) and not visible in the graph. $CD34^+$ (B), $CD34^+KDR^-$ (C), and $CD34^-$ (D) cells were cultured in SMGM-2 medium, EGM-2 medium, and EGM-2 medium supplemented with $PDGF_{BB}$ or $TGF_{\beta-1}$ or RA or $TGB_{\beta-1}$ plus $PDGF_{BB}$. Cells were characterized at passage 4 (≈20 days). Results are Mean ± SEM (n=4); * denotes statistical significance (P< 0.05).

Next, the expression and filament organization of contractile proteins was evaluated in cell populations having similar or higher a-SMA and SM-MHC gene expression than hVSMCs, i.e., $CD34^+$RA, $CD34^+PDGF_{BB}$, $CD34^+KDR^-PDGF_{BB}$ and $CD34^+KDR^-$EGM-2. All hESC-derived cells stained positive for a-SMA, SM-MHC and calponin (**Fig. 3 and Fig. 4**). More

than 70% of the cells expressed a-SMA as evaluated by FACS analyses (**Fig. 5**). Individualized calponin filaments were observed in 16 to 60% of the overall cells; however, organized a-SMA protein filaments were only observed in $CD34^+PDGF_{BB}$ (6.0%) and $CD34^+KDR^-$EGM-2 (6.1%) cells, and no organized SM-MHC filaments were observed in the hESC-derived populations (**Fig. 5**). In contrast, hVSMCs expressed high levels of organized a-SMA (84.6%), SM-MHC (94.6%) and calponin (80.1%) filaments.

Collectively, gene and protein analyses indicate that several inductive signals ($PDGF_{BB}$, or RA or EGM-2 basal medium) are able to drive the SMC differentiation of $CD34^+$ or $CD34^+KDR^-$ cells, characterized by variable expression of SMC proteins and minimal assembly of the a-SMA protein into filaments.

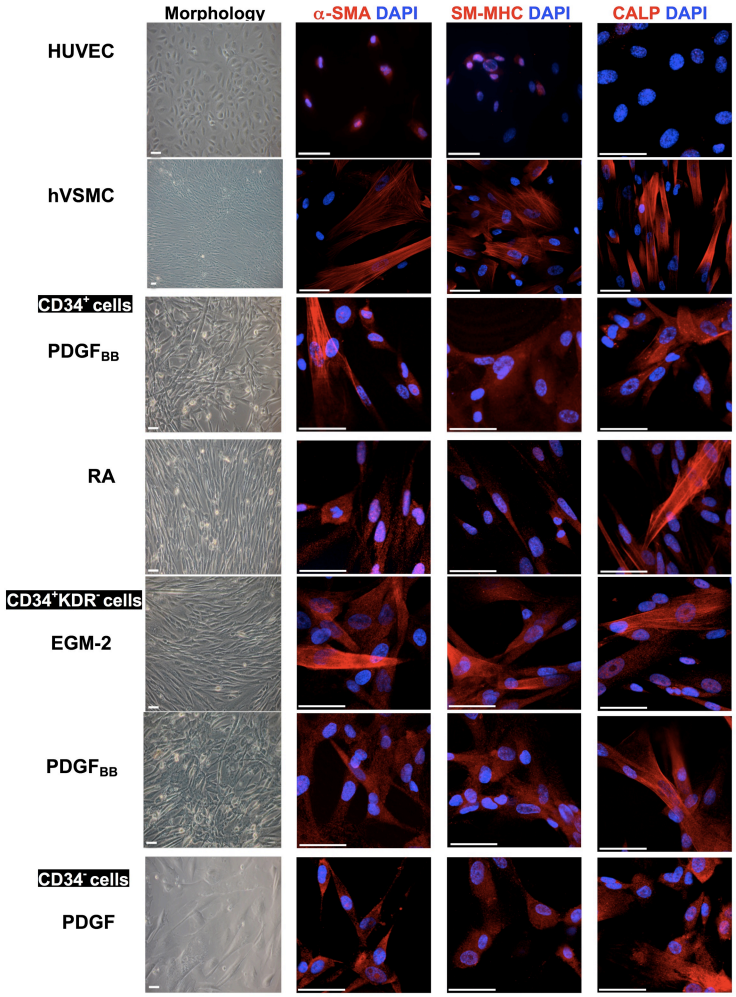

Figure 3 - **SMC proteins are expressed on hESC-derived SMPCs.** $CD34^+$, $CD34^+KDR^-$ and $CD34^-$ cells differentiated under different media conditions express α-SMA, calponin and SM-MHC, as evaluated by immunofluorescence. hVSMCs were used as a positive control and HUVECs as a negative control for the SMC markers. In all figures, bar corresponds to 50 μm.

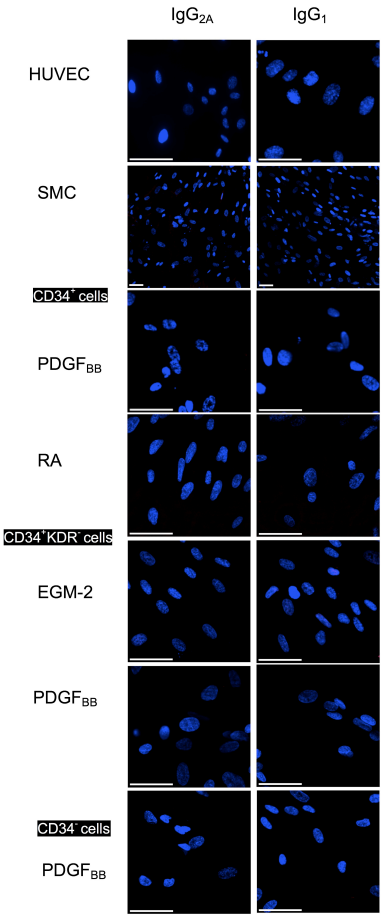

Figure 4 - Isotype controls for SMPC immunostainning. stained the isotype controls IgG_{2A} and IgG_1 for the SMC markers: α-SMA, SM-MHC and Calponin. Cell nuclei were stained with 4', 6'-diamidino-2-phenylindole (DAPI). Cells were labeled with mouse anti–human IgG_{2A} and IgG_1 antibodies. Bar corresponds to 50 μm.

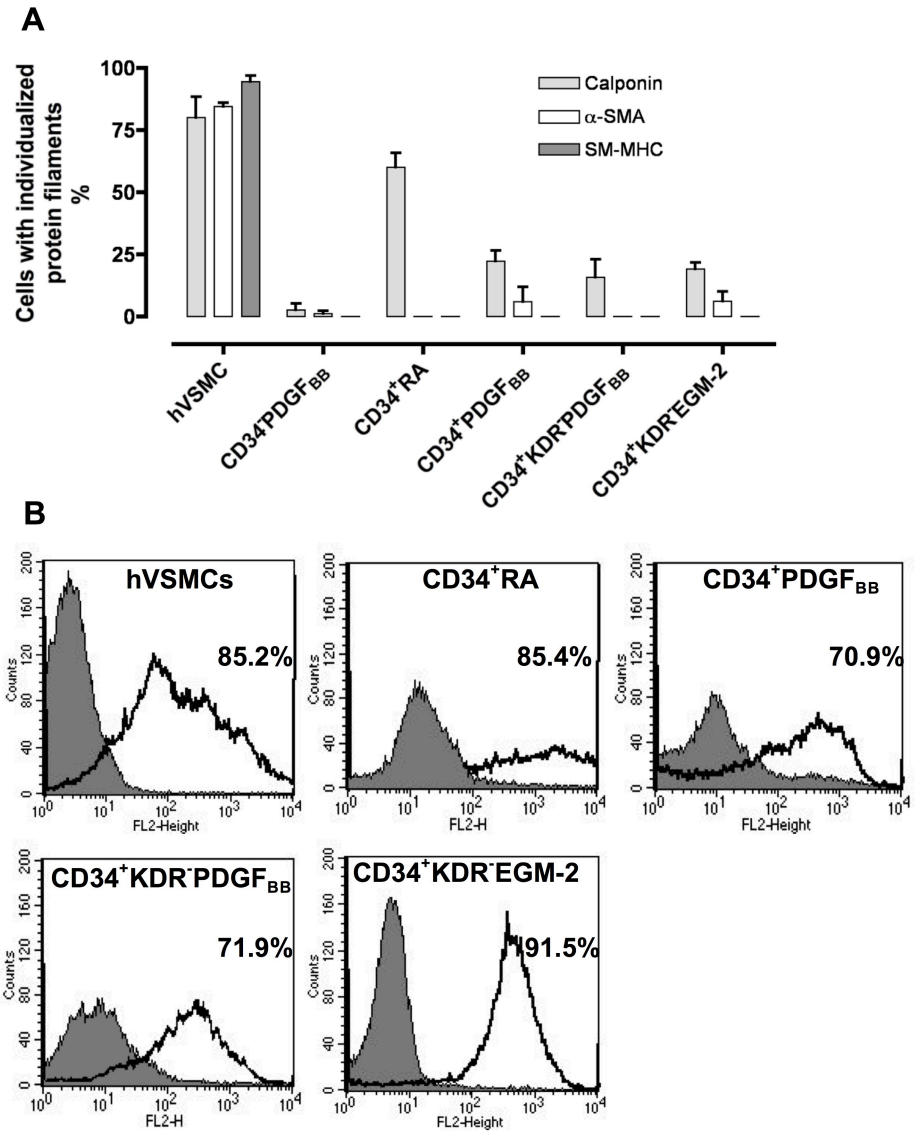

Figure 5 - Organization and expression of contractile proteins. (**A**) Quantification of organized α-SMA, SM-MHC and calponin filaments. (B) Expression of α-SMA in differentiated $CD34^+$, $CD34^+KDR^-$ and $CD34^-$ cells. Cells were differentiated for 3 passages (approximately 18 days after cell seeding). hVSMCs and HUVECs were used as positive and negative controls, respectively. In all graphs, the percentages of positive cells were calculated based in the isotype controls (gray plot) and are shown in each histogram plot.

Some hESC-derived cells present a secretion profile similar to hVSMCs

Using the multiplex cytometric bead array method we investigated the secretion of 17 analytes by hVSMC, $CD34^+PDGF_{BB}$, $CD34^+$RA, $CD34^+KDR^-PDGF_{BB}$, $CD34^+KDR^-$EGM-2 and $CD34^-PDGF_{BB}$ cells. Out of the 17 analytes analyzed, hVSMCs secreted IL-6, IL-7, IL-8, G-CSF, IFN-γ, MCP-1 (MCAF) and TNF-α, above the detection limit (>0.2 pg/mL) (**Fig. 6**). Cytokines IL-6 and IL-8 were the most secreted cytokines. $CD34^+PDGF_{BB}$ and $CD34^+KDR^-$EGM-2 cells secreted the same analytes as hVSMCs. $CD34^+KDR^-PDGF_{BB}$

and CD34$^-$PDGF$_{BB}$ cells did not secrete IL-7, while CD34$^+$RA cells secreted all seven cytokines mentioned and 4 cytokines more (IL-1β, IL-2, IL-4 and GM-CSF) (**Fig. 7**).

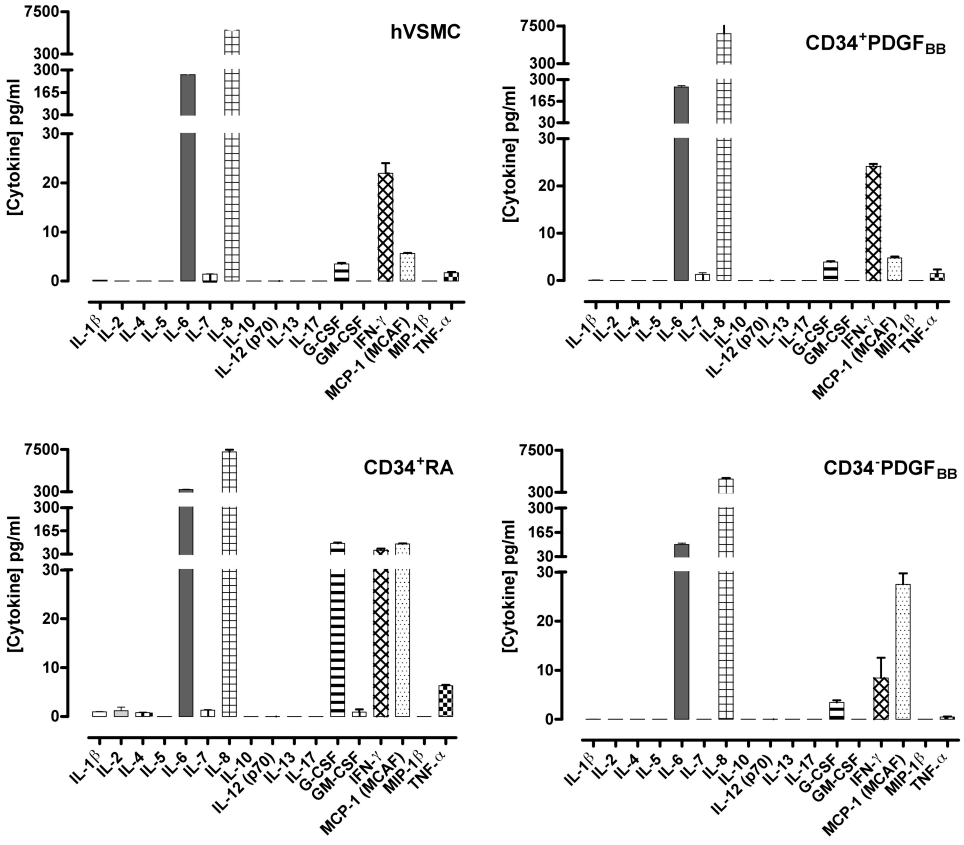

Figure 6 - **Secretomic profile of hVSMC and hECS-derived cells.** Seventeen cytokines were measured simultaneously in medium collected from hVSMC, CD34$^+$PDGF$_{BB}$, CD34$^+$RA, and CD34$^-$PDGF$_{BB}$ cells at passage 4. Results are Mean ± SEM (*n*=3).

Interestingly, the secretion profile of CD34$^+$PDGF$_{BB}$ cells is very similar to the one observed for hVSMCS, either in the type and concentration of the analytes secreted (**Fig. 6**). In contrast, CD34$^-$PDGF$_{BB}$ cells secreted analytes at different concentration than hVSMCs, and the other cell populations seemed to be in an intermediate stage in terms of secretion profile (**Fig.6 and Fig. 7**). CD34$^+$RA cells secreted higher levels of cytokines than all the remaining cell populations, including hVSMCs.

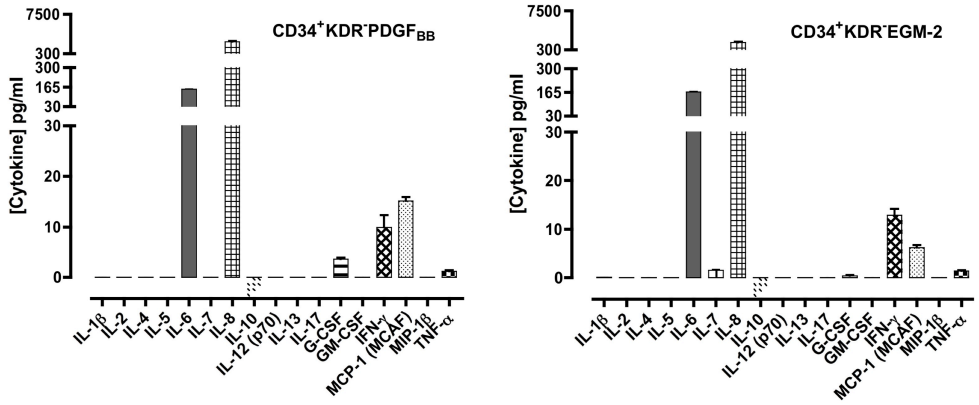

Figure 7 - Secretomic profile of hESC-derived cells. 17 cytokines were measured simultaneously in the medium collected from $CD34^+KDR^-PDGF_{BB}$ and $CD34^+KDR^-$EGM-2 cells. A standard range of 0.2 to 3,200 pg/mL was used. Samples and controls were run in triplicate, standards and blanks in duplicate.

Some hESC-derived cells like hVSMCs have the ability to contract when treated with vasoactive agonists and the process is mediated by Ca^{2+}

The ability of SMCs to contract in response to vasoactive agonists is mediated by an increase of intracellular Ca^{2+} levels which triggers the SMC contractile apparatus [28]. To evaluate whether hESC-derived cells had contractility mediated by Ca^{2+}, the cells were loaded with FURA-2, a Ca^{2+} sensitive dye, and their response to vasoactive agonists (bradykinin, angiotensin II, carbachol and histamine) and depolarization agents (KCl) was monitored by fluorescence (**Fig. 8A**). The response profile was compared to the one observed for hVSMCs and human umbilical vein endothelial cells (HUVECs), as positive and negative controls, respectively. Intracellular free Ca^{2+} $[Ca^{2+}]_i$ levels increase when hVSMCs are exposed to bradykinin, angiotensin II and carbachol, while no measurable effect is observed in HUVECs. KCl induces a higher increase in the $[Ca^{2+}]_i$ levels in HUVECs than in hVSMCs, while histamine induces similar levels of $[Ca^{2+}]_i$ in both cell types but following different profiles. These response patterns are typical for HUVECs and hVSMCs [29,30,31,32,33].

$CD34^+$RA and $CD34^+PDGF_{BB}$ cells exposed to histamine, bradykinin, angiotensin II, carbachol or KCl had similar response profiles as observed for hVSMCs (**Fig. 8A and Fig. 9**). For bradykinin and KCl the response intensity was lower than in hVSMCs, however similar intensity was observed for angiotensin II, carbachol and histamine. On the other

hand, although $CD34^+KDR^-RA$, $CD34^+KDR^-PDGF_{BB}$ and $CD34^+KDR^-EGM\text{-}2$ cells had similar response profiles as hVSMCs, in general the intensity of response was lower (**Fig. 10**). In contrast to the previous hESC-derived populations, $CD34^-PDGF_{BB}$ cells showed a very low variation in the intracellular levels of Ca^{2+} when exposed to depolarization and vasoactive peptides.

To examine whether hESC-derived cells were able to contract, they were subjected to the effects of carbachol and atropine (**Fig. 8B**). With the exception of $CD34^-PDGF_{BB}$ cells, all cells were able to contract after exposure to carbachol (13 to 38% contraction after 30 min, depending on the cell population). In most cases, cell contraction was not significantly different (P>0.05) from the one observed for hVSMCs. Moreover, with the exception of $CD34^-PDGF_{BB}$ cells, the muscarinic inhibitor atropin significantly blocked or reduced the carbachol-mediated effect (P<0.05) (**Fig. 8B**).

Based on the expression of SMC proteins and genes, secretion of cytokines and cellular contraction, $CD34^+PDGF_{BB}$ and $CD34^+RA$ cells were selected for further characterization. These cells are likely at a smooth muscle progenitor cell stage (SMPCs), which can potentially be further induced into a more mature SMC phenotype.

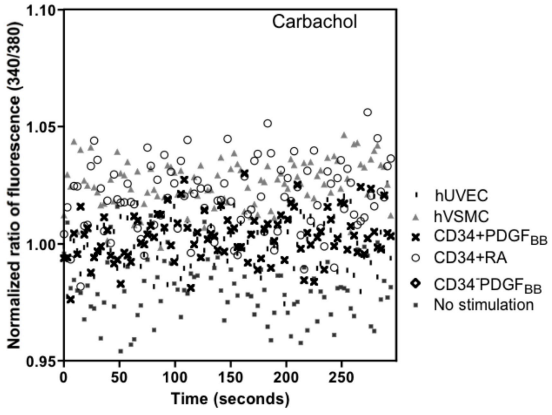

Figure 9 - Contractility of hESC-derived cells. Cells were loaded with FURA-2/AM and their response to carbachol (10^{-5}M) was monitored by fluorescence. The response profile was compared to the one observed for hVSMCs and HUVECs, as positive and negative controls, respectively.

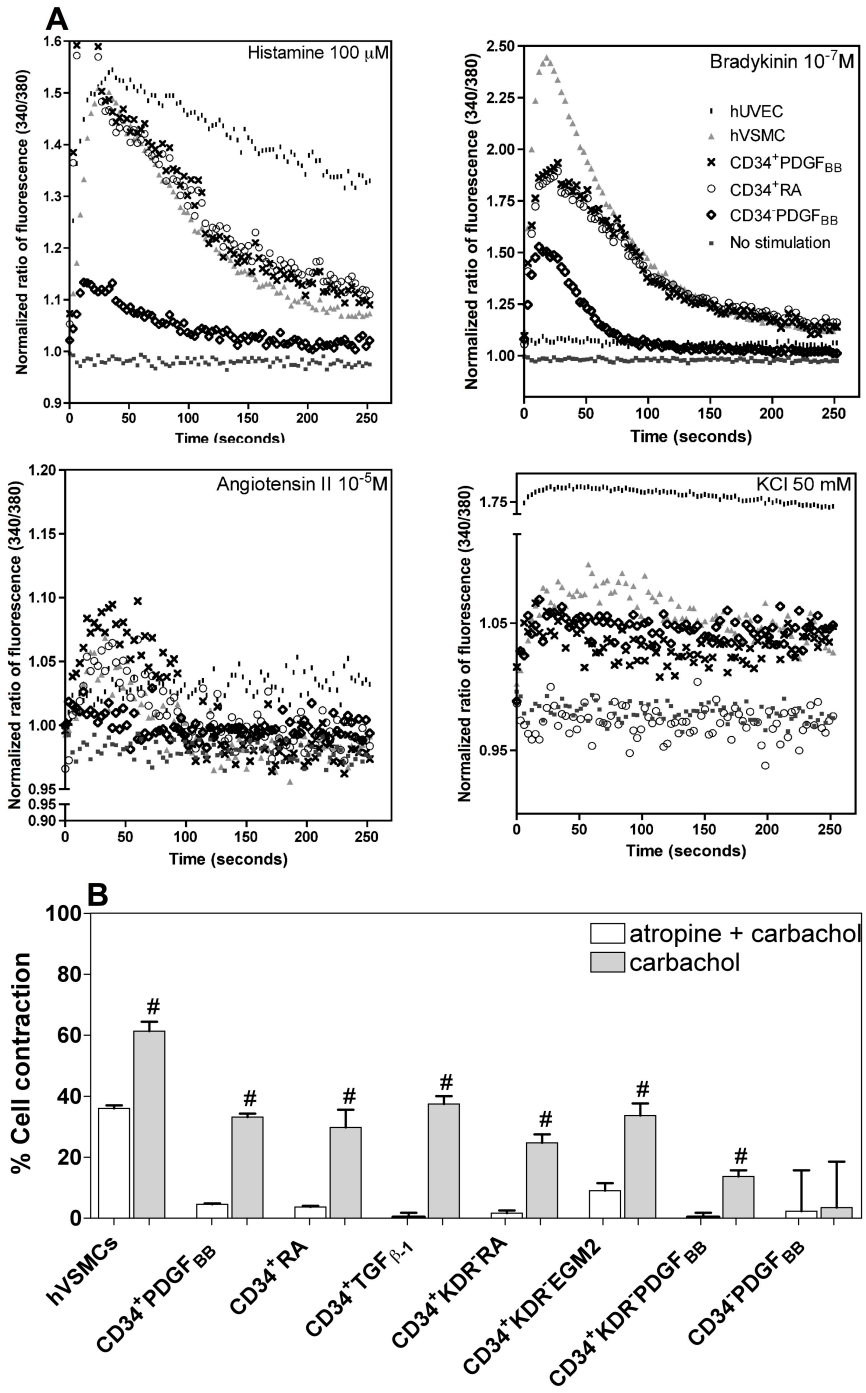

Figure 8 - **Contractility of hESC-derived cells.** (A) Concentration of intracellular Ca^{2+} in FURA-2-loaded cultured hESC-derived cells in response to several agonists (100 μM histamine, 10^{-7}M bradykinin , 10^{-5}M angiotensin II or 50mM KCl). hVSMCs and HUVECs were used as positive and negative controls, respectively. Traces are representative of 4 independent experiments for each condition. (B) Contractility of hESC-derived cells when exposed to the effects of carbachol (10^{-5} M in DMEM medium, for 30 min) or atropine (10^{-4} M, 1 h) plus carbachol (10^{-5} M for 30 min). hVSMCs were used as controls. Results are Mean ± SEM (*n*=3); # denotes statistical significance (*P*< 0.05) in the same experimental group.

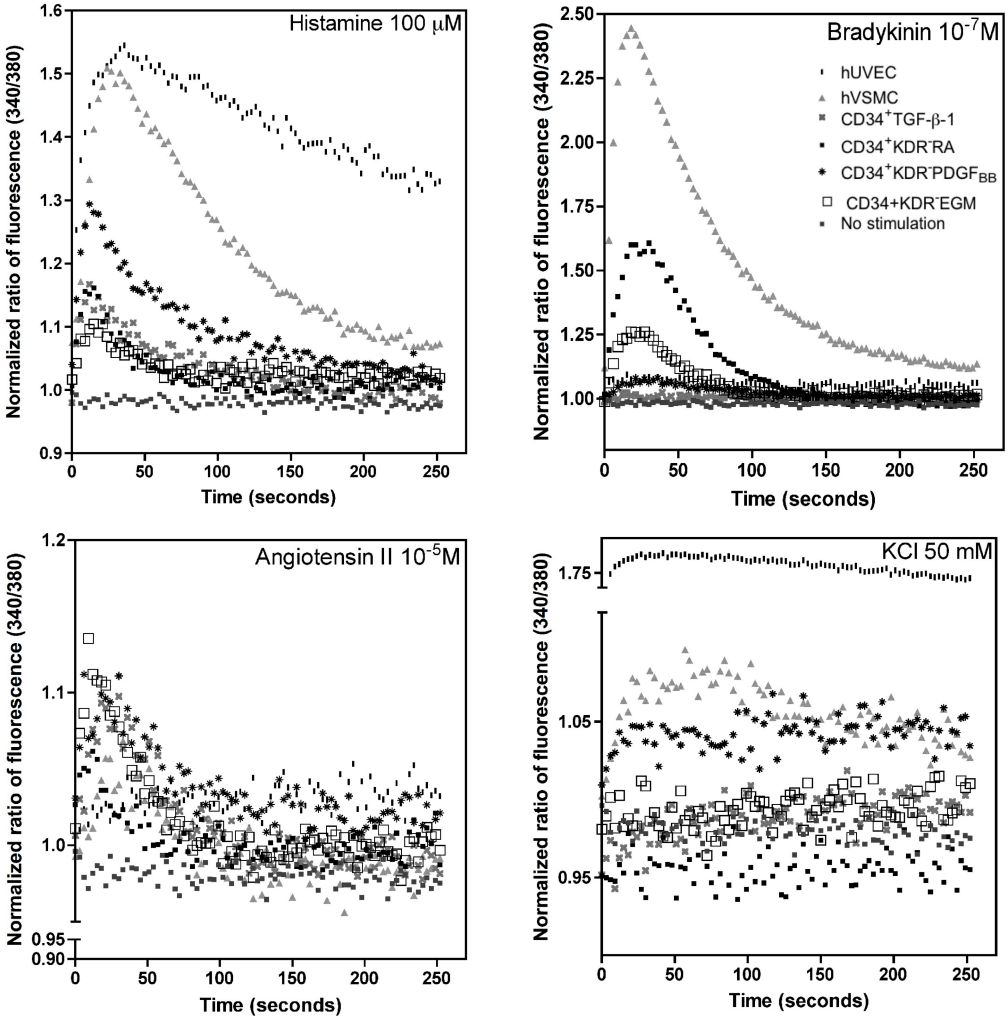

Figure 10- Contractility of hESC-derived cells. Cells were loaded with FURA-2/AM and their response to vasoactive agonists (bradykinin (10^{-7}M), angiotensin II (10^{-5}M) and histamine (100 μM)) and depolarization agents (KCl; 50 mM) was monitored by fluorescence. The response profile was compared to the one observed for hVSMCs and HUVECs, as positive and negative controls, respectively.

The contraction of both hESC-derived SMPCs and hVSMCs involves Rho A/Rho kinase- and Ca^{2+}/ CaM / MLCK-dependent pathways

CaM/MLCK- and RhoA/Rho kinase-dependent pathways play a pivotal role in SMC contraction [7,28]. The Ca^{2+}/CaM pathway plays a key role in SMC contraction through the stimulation of MLCK-mediated phosphorylation of myosin light chain 20,000 Da (MLC_{20}) [28]. To assess whether Ca^{2+}/CaM pathway was involved in the contraction of hESC-derived SMPCs, cells were exposed to the CaM-specific inhibitor W-7 [34], and then contraction was induced by exposing them to the CaM agonist U46619 [7]. To facilitate the evaluation of cell contraction, cells were encapsulated in fibrin gels, and gel diameter was determined after 14 h. Pre-incubation of hESC-derived SMPCs with W-7 significantly

inhibited U46619-induced contraction (**Figs. 11A and 11B**). Similar results were obtained for the control cells hVSMCs. Overall the results indicate the involvement of CaM/ MLCK-kinase pathway in cell contraction.

To examine whether Rho kinase was involved in the hESC-derived SMPC contraction, the cells were pre-treated with the Rho kinase-specific inhibitor Y27632 [7] and then contraction was induced by the agonist End-1 [35]. Cells treated with Y27632 and End-1 showed no significant contraction (**Figs. 11A and 11B**). In contrast, cells treated with End-1 but not Y27632 contracted significantly. Similar response profiles were obtained for hVSMCs and hESC-derived SMPCs. Collectively the results indicate the involvement of a Rho/Rho kinase-dependent pathway in SMC contraction.

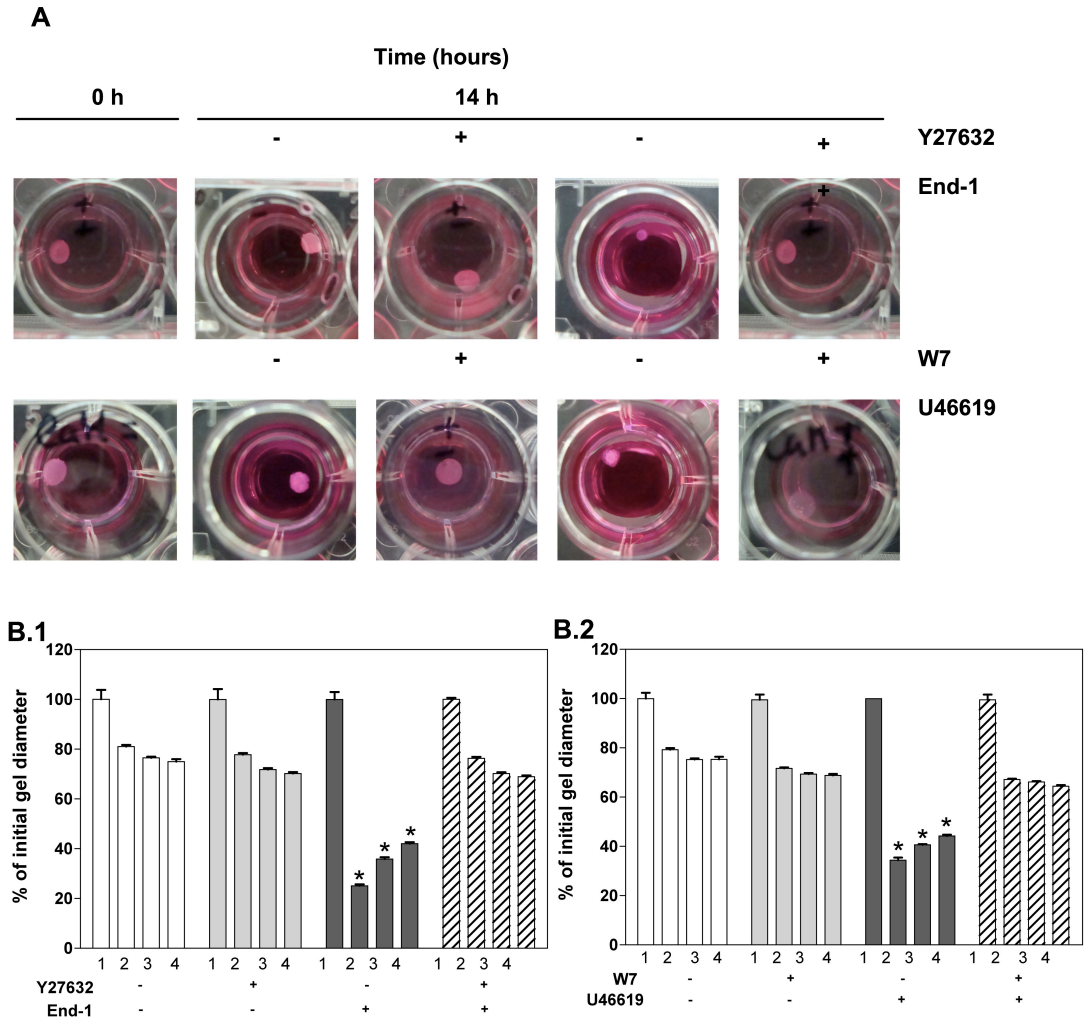

Figure 11 - Evaluation of the role of Rho A/Rho kinase- and Ca^{2+}/ CaM / MLCK-dependent pathways in the contraction of SMPCs and hVSMCs. $CD34^{+}$PDGF or $CD34^{+}$RA cells were initially treated for 3 days with serum-free medium containing the agonists endothelin-1 (End-1 (10 nM), A and B.1) or U46619 (1 μM) (A and B.2) in the presence or absence of the Rho-kinase inhibitor Y27632 (13 μM) or the calmodulin inhibitor W-7 (12 μg/mL). The cells were then encapsulated in fibrin gels and the diameter of the gel assessed at time 0 (1) and 14 h (2,3,4). Graph displays the variation in gel

diameter (percentage) encapsulating hVSMCs (2), $CD34^+PDGF_{BB}$ cells (3) or $CD34^+RA$ cells (4). Data are shown as mean ± SEM (*n*=6), * *P*<0.001 relatively to samples inhibited with Y27632 or W-7, by Student´s *t*-test.

3D culture of hESC-derived SMPCs modulates gene expression towards the expression observed in hVSMCs

We investigated the use of hESC-derived SMPCs for tissue engineering applications [2,3]. Fibrin gels previously used for the encapsulation of neonatal SMCs [36] were selected as scaffolds for the encapsulation of SMPCs. These gels allow cell attachment and can be remodeled by cellular metalloproteinases. SMPCs were encapsulated in fibrin gels for 3 days after which the cells were characterized at protein and gene levels.

Gene expression of SMPCs ($CD34^+RA$ and $CD34^+PDGF$) was compared to hVSMCs under the same culture conditions (**Figs. 12A and 12B**). The culture of SMPCs in 3D gels modulated the expression of SMC genes (α-SMA, SM-MHC or SMα-22) towards the one observed for hVSMCs cultured in 3D gels. We complemented these studies by evaluating the expression of extracellular matrix and adhesion molecules by a quantitative real-time PCR array. This array evaluated the expression of 84 genes involved in cell-cell and cell-matrix interactions. Again, the 3D culture of SMPCs modulated extracellular matrix and adhesion molecule genes towards the expression observed in hVSMCs (**Fig. 12B**). The number of genes with similar expression increased from 23 to 58 or 9 to 53 when $CD34^+PDGF_{BB}$ cells or $CD34^+RA$ cells are cultured in 2D or 3D, respectively. Finally, gene expression associated with SMCs including collagen I and thrombospondin 1 [37], integrins α2, α3, α5, αV and β1 [38], the enzyme metalloproteinase 2 [39], and the growth factor $TGF_{\beta 1}$ was similar in SMPCs and hVSMCs **(Fig. 12C and Fig. 13)**.

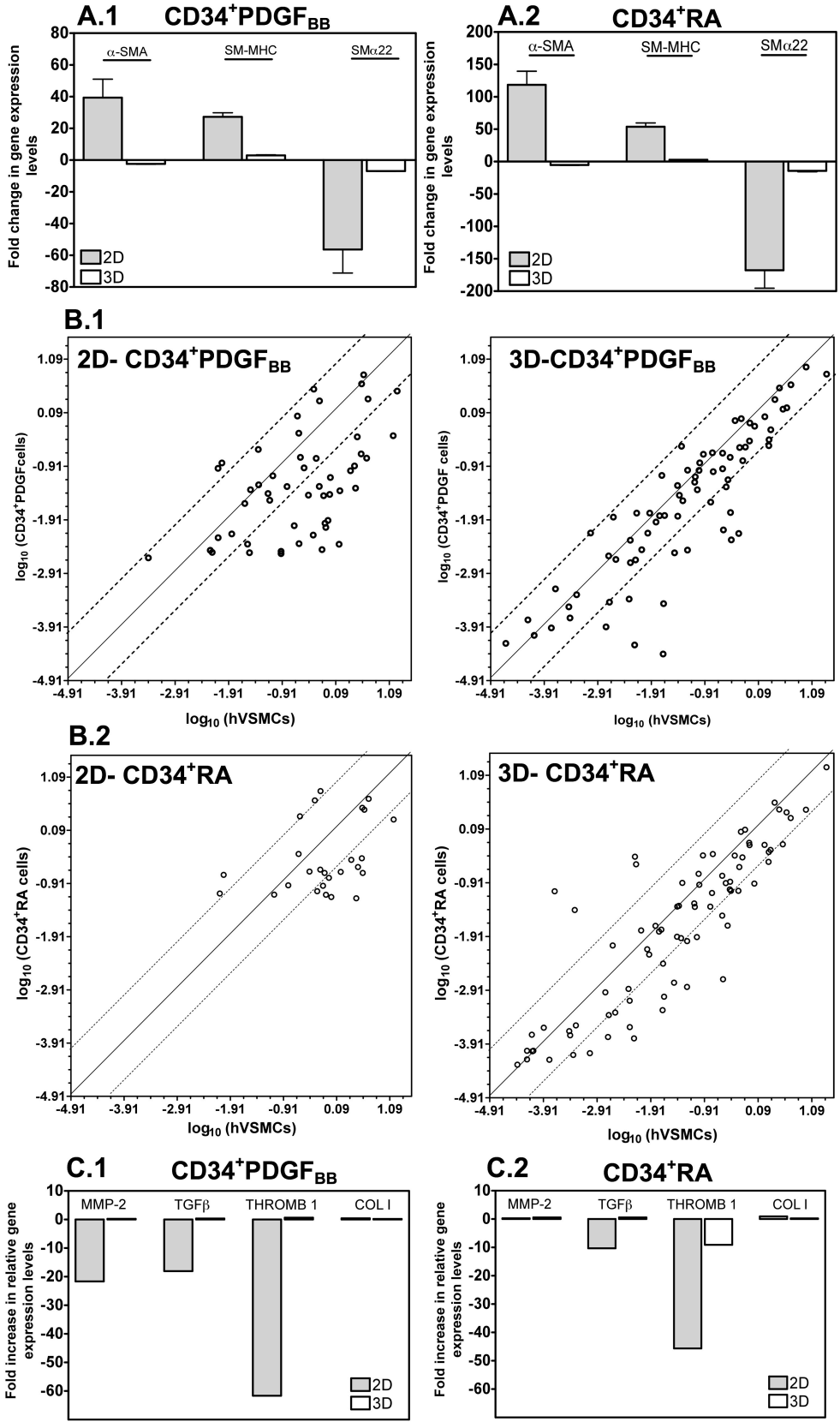

Figure 12 - Characterization of hESC-derived SMPCs encapsulated in 3D fibrin gel scaffolds. SMPCs were characterized after being encapsulated in fibrin gels for 3 days. (A) SMC gene expression on $CD34^+RA$ (A.1) and $CD34^+PDGF$ (A.2) cells, as assessed by qRT-PCR. Gene expression of hESC-derived SMPCs was normalized by gene expression of hVSMCs under the same culture conditions. Results are Mean ± SEM (*n*=4). (B)

Comparison of extracellular matrix and adhesion molecules-related gene expression in $CD34^+PDGF_{BB}$ (B.1) or $CD34^+RA$ cells (B.2) with hVSMCs cultured in 2D (tissue culture polystyrene) or cultured in 3D fibrin gels. Gene expression was evaluated using a RT^2 Profiler™ PCR array. (C) Normalized extracellular matrix and soluble factor gene expression of SMPCs relatively to hVSMCs, both cultured in 3D or 2D systems.

Co-culture of hESC-derived SMPCs with hVSMCs induces the assembly of α-SMA and calponin into filaments

Next we sought to investigate whether hESC-derived SMPCs could be further matured into a SMC phenotype with an organized contractile filament network. To accomplish this goal, hESC-derived SMPCs were initially labeled with PKH67 fluorescent dye and co-cultured on top of hVSMCs for 5 days. After this time, the cells were sorted and characterized by immunocytochemistry. Remarkably, hESC-derived SMPCs showed significant improvement in the organization of the fibers after contact with hVSMCs: 36.3% and 41.2% of $CD34^+PDGF_{BB}$ and $CD34^+RA$ cells, respectively, had organized α-SMA fibers, while 64.8% and 73.8% had organized calponin fibers (**Figs. 14A and 14B**). These results show that hESC-derived SMPCs are plastic cells and can be induced to differentiate into a more mature SMC phenotype displaying an organized contractile network.

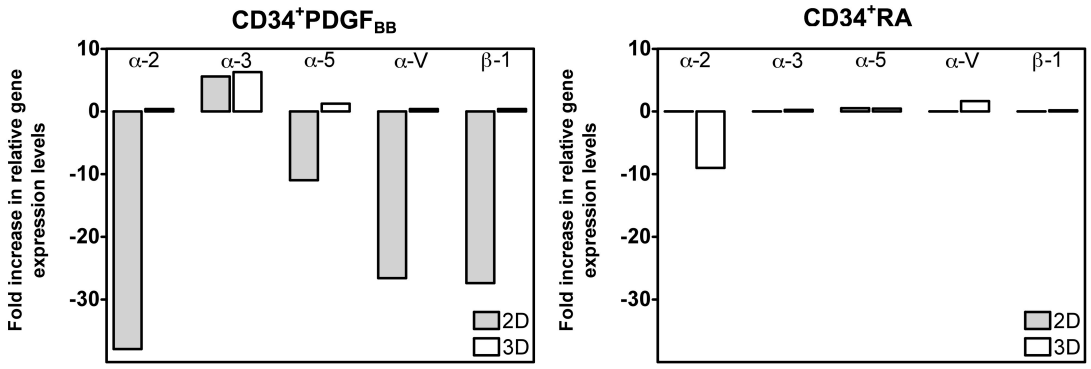

Figure 13- Integrin gene expression. Gene expression on $CD34^+PDGF_{BB}$ and $CD34^+RA$ cells was normalized by gene expression on hVSMCs, both cultured in 3D or 2D systems. Gene expression was obtained from the RT^2 Profiler™ PCR array.

Vasoactive agents U46619 and End-1 improve the organization of contractile protein fibers

Next, we identified molecules able to maturate the hESC-derived SMPCs into SMCs having an organized contractile network. We sought to evaluate the effect of the agonists

U46619 and End-1 involved in the CaM/MLCK- and RhoA/Rho kinase-contraction pathways, respectively. In $CD34^+RA$ cells, each agonist independently improved dramatically the organization of a-SMA and calponin fibers, being End-1 the most effective. The addition of both agonists did not significantly improve the effect of End-1 (**Fig. 14C and 14D)**. Importantly, the induction effect of the vasoactive agents was not observed on $CD34^+PDGF_{BB}$ (**Fig. 14D**) or $CD34^-PDGF_{BB}$ cells (**Fig. 15**) showing that the inductive effect is dependent on the differentiation history of the SMPCs. The mature SMCs (derived from $CD34^+RA$) express SMC markers including a-SMA, SM-MHC and calponin but not the cardiac marker a-actinin (**Fig. 16**). Furthermore, the cells show no expression of troponin T, a protein found in skeletal and cardiac muscle but not in smooth muscle and vascular endothelial-cadherin, a protein typically expressed in endothelial cells (**Fig. 17**).

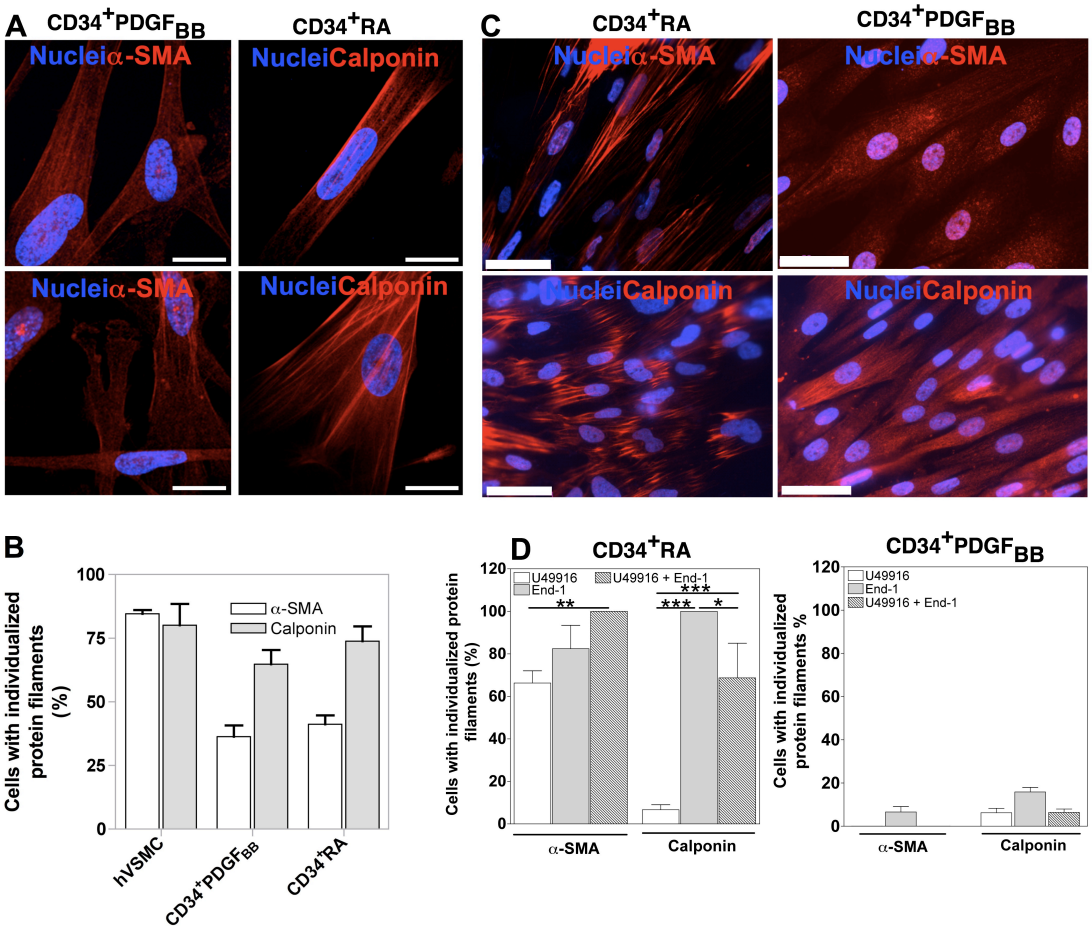

Figure 14 - Maturation of hESC-derived SMPCs. (A and B) Expression and organization of SMC proteins on hESC-derived SMPCs cultured on top of inactivated-hVSMCs for 5 days. hVSMCs were used as controls. Bar corresponds to 50 μm. Results are Mean ± SEM (*n*=10). (C and D) Expression and organization of SMC proteins on hESC-derived SMPCs treated with vasoactive agents for 3 days. Bar corresponds to 50 μm. Results are Mean ± SEM (*n*=8); *, **, *** denote statistical significance (*P*<0.05, *P*<0.01, *P*<0.001, respectively).

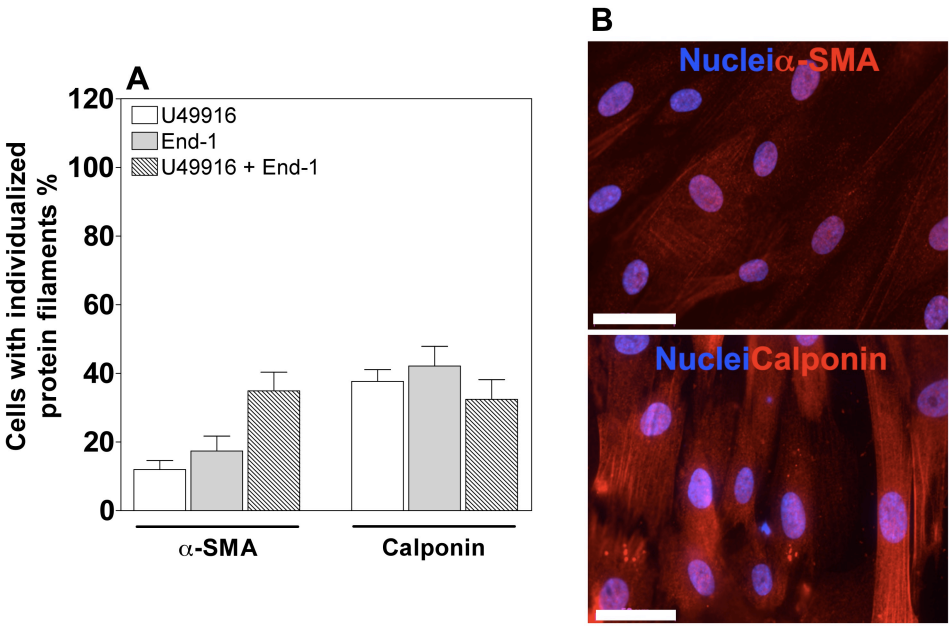

Figure 15- Expression and organization of SMC proteins on CD34$^-$PDGF$_{BB}$ cells treated with vasoactive agents for 3 days. A) Quantification by immunocytochemistry analysis. Results are Mean ± SEM (*n*=8). B) Expression of α-SMA and calponin in CD34$^-$ PDGF$_{BB}$ cells treated with End-1 (10nM) for 3 days. Bar corresponds to 50 μm.

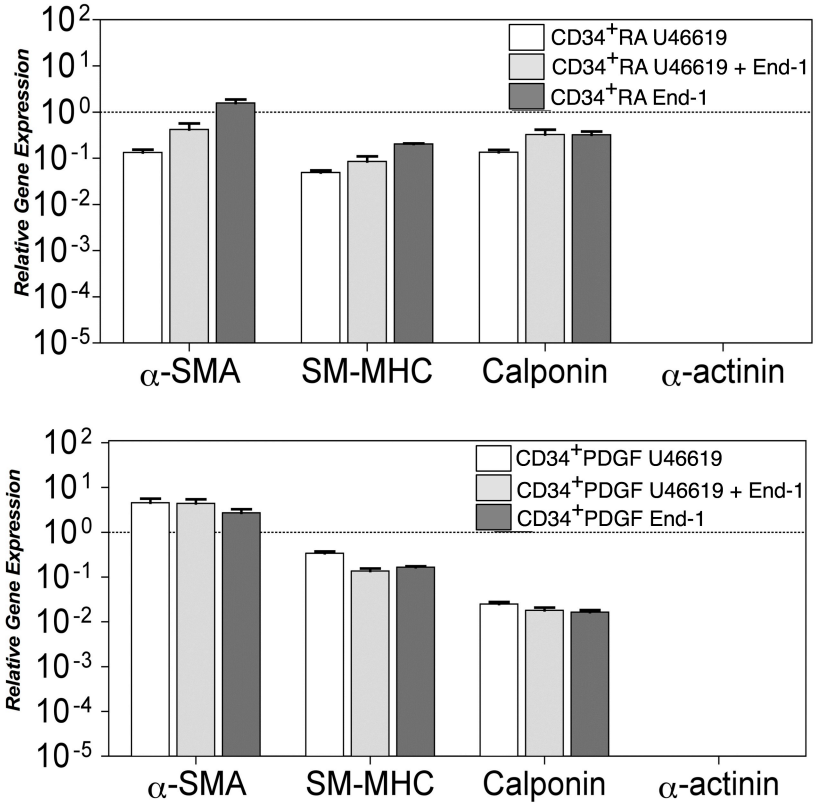

Figure 16- Gene expression in CD34$^+$PDGF$_{BB}$ and CD34$^+$RA cells after treatment with vasoactive agents for 3 days. Gene expression in CD34$^+$PDGF$_{BB}$ and CD34$^+$RA cells was normalized by gene expression in hVSMCs. Results are Mean ± SEM (*n*=4).

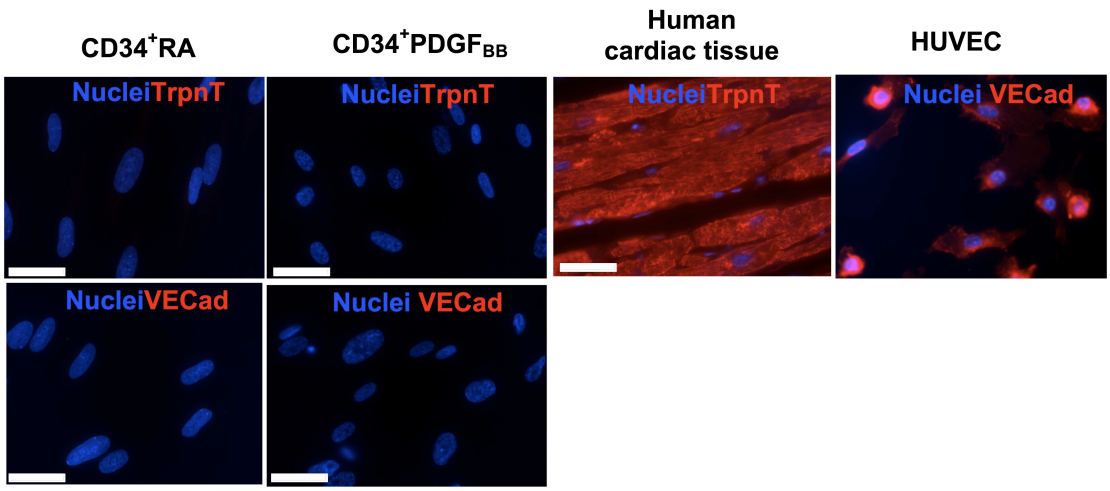

Figure 17- Expression and organization of troponin T (TrpnT) and vascular endothelial-cadherin (VECad) on $CD34^{+}RA$ (A) and $CD34^{+}PDGF_{BB}$ (B) cells treated with End-1 for 3 days. Human cardiac tissue (for TrpnT) and HUVECs (for VeCad) were used as positive controls. Bar corresponds to 50 μm.

Discussion

In this study, we demonstrate that $CD34^+$ cells have higher SMC potential than $CD34^-$ cells. We further show that RA or $PDGF_{BB}$ drive the differentiation of $CD34^+$ cells into SMPCs We have characterized the differentiated cells at gene and at protein level, their secretome, the ability to contract when incubated with several pharmacological agents, and contraction mechanism mediated by Ca^{2+}. Envisioning the use of these cells for vascular engineering, they were encapsulated on 3D fibrin scaffolds and characterized at gene and functional levels. Finally, we identified End-1 as a key molecule to induce the polymerization of contractile proteins in SMPCs ($CD34^+$RA cells).

We examined the capacity of three hESC populations ($CD34^+$, $CD34^+KDR^-$, $CD34^-$) isolated from EBs at day 10, and cultured as single cells on media supplemented with inductive signals including $PDGF_{BB,}$ RA, $TGF_{\beta1}$ and $TGF_{\beta1}$ plus $PDGF_{BB}$ to differentiate into SMCs. Notably, $TGF_{\beta1}$ [5,23,40], $PDGF_{BB}$ [5,12,21], and RA [9,18] have been reported to be very important inductive signals for SMC differentiation from different initial stem cell populations. We report that from all inductive signals tested in this study, RA and $PDGF_{BB}$ are the most effective in guiding the differentiation of hESC-derived $CD34^+$ cells into SMPCs, based on gene and protein analysis, response to the depolarization agents and vasoactive peptides, contraction profile, secretion of cytokines, and behavior in a 3D scaffold. Although SMPCs express most of the SMC markers, they exhibit disorganized contractile proteins.

We further show that $CD34^+$ cells have higher propensity to yield contractile SMPCs than $CD34^-$ cells, when exposed to the same inductive signals. Interestingly, $CD34^+KDR^-$ cells which have been reported to be of mesenchymal origin [20], can give rise to SMPCs but they respond less efficiently to vasoactive peptides and depolarization agents, have lower contractile properties than $CD34^+$PDGF cells, and have a different cytokine secretion profile as compared to hVSMCs. In line with previous results [41], our results suggest that cells expressing KDR receptor are needed for an efficient SMC differentiation.

The development of mature contractile SMCs from stem cells occurs in multiple steps comprising (i) the commitment to the SMC lineage, (ii) the differentiation into early immature and (iii) the maturation into the mature contractile phenotype [42]. Previously, we have reported that $CD34^+$ cells could give rise to SMLCs when cultured in medium supplemented with $PDGF_{BB}$; however, the differentiation of SMLCs was not complete since the assembly of a-SMA or SM-MHC proteins into filaments was not observed [12].

Curiously, similar results have been obtained in this work for the cell populations tested and exposed to different inductive signals including RA and $TGF_{\beta 1}$.

Our results indicate that the co-culture of SMPCs with fully differentiated hVSMCs induces the assembly of α-SMA and calponin proteins into individualized filaments. This indicates that the cells are able to maturate into a fully contractile phenotype. It is known that both assembly and disassembly of actin filaments is regulated by RhoA [43]. Consistent with this, our results show that End-1, an agonist of RhoA pathway, dramatically increases actin polymerization in $CD34^{+}RA$ cells and the cells exhibit individualized a-SMA and calponin filaments. However, such inductive effect was not observed in $CD34^{+}PDGF_{BB}$ cells, and this could be due to the inhibition of mature SMC marker expression by $PDGF_{BB}$ [44]. Strikingly, these cells are contractile (**Fig. 11**) despite presenting a small percentage of polymerized actin fibers (6%; **Fig. 5**). Nevertheless, it is known that the total amount of actin that undergoes polymerization after induction of contraction is relatively small [45]. Further research is needed to study the molecular processes that regulate the assembly of actin filaments in smooth muscle tissues and the nature of the actin filaments network that are formed during contractile activation [45].

Contractile and synthetic SMCs, which represent the two ends of a spectrum of SMCs with intermediate phenotypes, clearly show different morphologies [24]. The SMPCs derived in this work seem to have the contractile phenotype, as they are spindle-shaped [46], express proteins involved in SMC contraction including α-SMA, SM-MHC, calponin and SMα-22 [24,26], and contract when exposed to carbachol and vasoactive peptides being this effect reversed by the presence of the respective antagonists.

We show that SMPCs are able to contract to a plethora of vasoactive agents including carbachol, angiotensin II, histamine, thromboxane-mimetic U46619, endothelin-1, and bradykinin, as hVSMCs. Most of these agonists act through different receptors coupled to G-proteins activating membrane-bound phospholipase C, which leads to the formation of inositol-1,4,5-triphosphate (IP_3) and diacylglycerol (DAG) [28]. Through different mechanisms, both molecules induce the accumulation of Ca^{2+} in the cell cytoplasm [28]. The increase of intracellular Ca^{2+} activates the cell's contraction machinery. Our results agree with previous ones showing that hESC-derived SMCs respond to bradykinin, histamine and carbachol by increasing at different levels the intracellular concentration of Ca^{2+} [14]. The accumulation of intracellular Ca^{2+} in hESC-derived SMCs exposed to carbachol is minimal, indicating that the contraction of the cell may involve the activation of

other intracellular players (e.g. protein kinase C) than Ca^{2+}, as described in other studies [47].

Our results show that hESC-derived SMPC contraction is mediated by the activation of CaM/MLCK- and Rho/Rho kinase-dependent pathways [7,28]. A similar mechanism has been reported recently for SMLCs obtained from human adipose tissue-derived mesenchymal stem cells [7]. The results also indicate that the absence of fully organized protein filaments did not prevent the contraction of SMLCs. This is in line with results reported previously by us [12] and by others [13] despite the absence of maturity and organization in the contractile machinery of the cell.

SMCs have key biological functions in terms of contraction and secretion of soluble signaling molecules [48]. In the present study we report for the first time the secretion profile of hES-derived SMPCs. $CD34^+$ cells that differentiate in medium supplemented with $PDGF_{BB}$ have similar secretome profile as hVSMCs. They express high levels (>100 pg/mL) of IL-6 and IL-8, moderate levels (between 100 and 10 pg/mL) of IFN-γ, and small levels of (between 10 and 1 pg/mL) of IL-7, G-CSF, MCP-1 and TNF-α. IL-6 is a cytokine with potent inflammatory properties and metabolic effects in SMCs. It has been shown that IL-6 secretion is inversely correlated to glucose consumption [49]. IL-8 is a cytokine that induces the proliferation and chemotaxis of smooth muscle cells and increases the activity of mitogen-activated protein kinase (MAPK) [50]. IFN-γ acts on vascular smooth muscle cells to induce cellular proliferation [51].

Although several studies have reported the differentiation of different stem cells into SMCs, very few evaluated the impact of the 3D environment at the geno- and phenotype of the differentiated cells [5]. Gene studies have demonstrated that human aortic SMCs encapsulated in a 3D collagen matrix have significantly less focal adhesions, lower proliferation, and lower α-SMA expression than cells in 2D [52]. However, to our knowledge, no study has compared the gene expression of SMLCs from different origins with fully differentiated SMCs when cultured in 2D or 3D systems. Our results show that hESC-derived SMPCs encapsulated for 3 days in fibrin gels express similar gene levels of α-SMA, SM-MHC, and SMα22 as encapsulated hVSMCs. In addition, considering an array of 84 genes related to cell-cell and cell-matrix interactions, 3D-cultured-SMPCs had a more hVSMC-similar gene expression profile than 2D-cultured SMPCs. This shows that 3D scaffolds may induce further the differentiation of SMPCs into SMCs. Several factors might account for the differences found between 2D and 3D culture systems including (i) ECM stiffness and (ii) ECM 3D environment. It has been demonstrated that the stiffness of

the ECM has a high impact in the cytoskeletal and focal adhesion assembly of SMCs [53]. Furthermore, SMCs cultured within 3D polyethylene glycol-fibrinogen [54] or collagen [52] gels had less proliferation, stress fibers and focal adhesion than on 2D culture systems. Future studies should evaluate the effect of both factors in the modulation of geno- and phenotype of the differentiated cells over the time and study the underlining mechanism. In this study we assessed the effect of the 3D matrix after 3 days of cell encapsulation. During this time, previous studies have shown that SMCs are able to migrate and remodel the ECM [55]; however, it would be interesting to extend these studies in time.

Although very recent studies have identified and characterized hESC-derived populations with SMC potential [13,14], identified bioactive agents involved in their SMC differentiation, and evaluated their functionality, our study advance these results in several ways. First, it provides a detailed analysis of the phenotype, secretome and function (unraveling the mechanism of cell contraction) of hESC-derived SMCs at levels not documented before. In contrast to the previous studies that have used monolayer-based differentiation protocols, our methodology uses an EB-differentiation step to isolate progenitor cells, which might have advantages for the scale-up of the process through the use of bioreactors. Second, our study identifies a methodology to induce the organization of the contractile protein filaments. Third, it demonstrates the importance of a 3D environment to modulate the activity of hESC-derived SMLCs.

Recent studies reported the derivation of pluripotent stem cells from human somatic cells by retroviral transduction [56]. These reprogrammed cells share many features with hESCs in terms of morphology, gene expression and differentiation potential, and open a new avenue for the potential derivation of autologous cells for regenerative medicine and drug screening. Indeed, the differentiation of iPSCs into SMCs has been recently reported [57]. It remains to be determined whether the methodology described in this work can be applied on iPSCs and this is an issue that will be evaluated in future work.

Acknowledgments

This work was supported by a Marie Curie-Reintegration Grant, MIT-Portugal program, Crioestaminal, Associação Viver a Ciência and Fundação para a Ciência e a Tecnologia (PTDC/SA-BEB/098468/2008 and PTDC/CTM/099659/2008 to L.F.; SFRH/BD/40077/2007 to H.V.). The funders had no role in study design, data collection and analysis, decision to publish, or preparation of the manuscript.

Bibliography

1. Matsubayashi K, Fedak PWM, Mickle DAG, Weisel RD, Ozawa T, et al. (2003) Improved left ventricular aneurysm repair with bioengineered vascular smooth muscle grafts. Circulation 108 Suppl 1: II219-225.
2. Niklason LE, Gao J, Abbott WM, Hirschi KK, Houser S, et al. (1999) Functional arteries grown in vitro. Science 284: 489-493.
3. Oberpenning F, Meng J, Yoo JJ, Atala A (1999) De novo reconstitution of a functional mammalian urinary bladder by tissue engineering. Nat Biotechnol 17: 149-155.
4. Kashiwakura Y, Katoh Y, Tamayose K, Konishi H, Takaya N, et al. (2003) Isolation of bone marrow stromal cell-derived smooth muscle cells by a human SM22alpha promoter: in vitro differentiation of putative smooth muscle progenitor cells of bone marrow. Circulation 107: 2078-2081.
5. Ross JJ, Hong Z, Willenbring B, Zeng L, Isenberg B, et al. (2006) Cytokine-induced differentiation of multipotent adult progenitor cells into functional smooth muscle cells. J Clin Invest 116: 3139-3149.
6. Rodríguez LV, Alfonso Z, Zhang R, Leung J, Wu B, et al. (2006) Clonogenic multipotent stem cells in human adipose tissue differentiate into functional smooth muscle cells. Proc Natl Acad Sci USA 103: 12167-12172.
7. Kim M, Jeon E, Kim Y, Lee J, Kim J (2008) Thromboxane A2 Induces Differentiation of Human Mesenchymal Stem Cells to Smooth Muscle-Like Cells. Stem Cells.
8. Le Ricousse-Roussanne S, Barateau V, Contreres J-O, Boval B, Kraus-Berthier L, et al. (2004) Ex vivo differentiated endothelial and smooth muscle cells from human cord blood progenitors home to the angiogenic tumor vasculature. Cardiovascular Research 62: 176-184.
9. Huang H, Zhao X, Chen L, Xu C, Yao X, et al. (2006) Differentiation of human embryonic stem cells into smooth muscle cells in adherent monolayer culture. Biochemical and Biophysical Research Communications 351: 321-327.
10. Xie C-Q, Zhang J, Villacorta L, Cui T, Huang H, et al. (2007) A highly efficient method to differentiate smooth muscle cells from human embryonic stem cells. Arteriosclerosis, Thrombosis, and Vascular Biology 27: e311-312.
11. Gerecht-Nir S, Ziskind A, Cohen S, Itskovitz-Eldor J (2003) Human embryonic stem cells as an in vitro model for human vascular development and the induction of vascular differentiation. Lab Invest 83: 1811-1820.
12. Ferreira LS, Gerecht S, Shieh HF, Watson N, Rupnick MA, et al. (2007) Vascular progenitor cells isolated from human embryonic stem cells give rise to endothelial and smooth muscle like cells and form vascular networks in vivo. Circulation Research 101: 286-294.
13. Vo E, Hanjaya-Putra D, Zha Y, Kusuma S, Gerecht S (2010) Smooth-Muscle-Like Cells Derived from Human Embryonic Stem Cells Support and Augment Cord-Like Structures In Vitro. Stem Cell Rev and Rep.
14. Hill KL, Obrtlikova P, Alvarez DF, King JA, Keirstead SA, et al. (2010) Human embryonic stem cell-derived vascular progenitor cells capable of endothelial and smooth muscle cell function. Experimental Hematology 38: 246-257.e241.
15. O'connor MD, Kardel MD, Iosfina I, Youssef D, Lu M, et al. (2008) Alkaline phosphatase-positive colony formation is a sensitive, specific, and quantitative indicator of undifferentiated human embryonic stem cells. Stem Cells 26: 1109-1116.
16. Agasse F, Bernardino L, Kristiansen H, Christiansen SH, Ferreira R, et al. (2008) Neuropeptide Y promotes neurogenesis in murine subventricular zone. Stem Cells 26: 1636-1645.
17. Bernardino L, Agasse F, Silva B, Ferreira R, Grade S, et al. (2008) Tumor necrosis factor-alpha modulates survival, proliferation, and neuronal differentiation in neonatal subventricular zone cell cultures. Stem Cells 26: 2361-2371.
18. Drab M, Haller H, Bychkov R, Erdmann B, Lindschau C, et al. (1997) From totipotent embryonic stem cells to spontaneously contracting smooth muscle cells: a retinoic acid and db-cAMP in vitro differentiation model. FASEB J 11: 905-915.
19. Grynkiewicz G, Poenie M, Tsien RY (1985) A new generation of Ca2+ indicators with greatly improved fluorescence properties. J Biol Chem 260: 3440-3450.

20. Vodyanik MA, Thomson JA, Slukvin II (2006) Leukosialin (CD43) defines hematopoietic progenitors in human embryonic stem cell differentiation cultures. Blood 108: 2095-2105.
21. Simper D, Stalboerger PG, Panetta CJ, Wang S, Caplice NM (2002) Smooth muscle progenitor cells in human blood. Circulation 106: 1199-1204.
22. Sinha S, Hoofnagle MH, Owens GK (2009) Derivation of contractile smooth muscle cells from embryonic stem cells. Methods Mol Biol 482: 345-367.
23. Sinha S, Hoofnagle M, Kingston P, McCanna M, Owens G (2004) Transforming growth factor-β1 signaling contributes to development of smooth muscle cells from embryonic stem cells. American Journal of Physiology- Cell Physiology 287: 1560-1568.
24. Rensen SSM, Doevendans PAFM, van Eys GJJM (2007) Regulation and characteristics of vascular smooth muscle cell phenotypic diversity. Netherlands heart journal : monthly journal of the Netherlands Society of Cardiology and the Netherlands Heart Foundation 15: 100-108.
25. Frid M, Shekhonin B, Koteliansky V, Glukhova M (1992) Phenotypic changes of human smooth muscle cells during development: late expression of heavy caldesmon and calponin. Developmental biology(Print) 153: 185-193.
26. Owens GK, Kumar MS, Wamhoff BR (2004) Molecular regulation of vascular smooth muscle cell differentiation in development and disease. Physiol Rev 84: 767-801.
27. Duband J, Gimona M, Scatena M, Sartore S, Small J (1993) Calponin and SM22 as differentiation markers of smooth muscle: spatiotemporal distribution during avian embryonic development. Differentiation 55: 1-11.
28. Hathaway DR, March KL, Lash JA, Adam LP, Wilensky RL (1991) Vascular smooth muscle. A review of the molecular basis of contractility. Circulation 83: 382-390.
29. Dora KA, Xia J, Duling BR (2003) Endothelial cell signaling during conducted vasomotor responses. Am J Physiol Heart Circ Physiol 285: H119-126.
30. Takeda T, Yamashita Y, Shimazaki S, Mitsui Y (1992) Histamine decreases the permeability of an endothelial cell monolayer by stimulating cyclic AMP production through the H2-receptor. J Cell Sci 101 (Pt 4): 745-750.
31. Graier WF, Simecek S, Bowles DK, Sturek M (1994) Heterogeneity of caffeine- and bradykinin-sensitive Ca2+ stores in vascular endothelial cells. Biochem J 300 (Pt 3): 637-641.
32. Montiel M, Gámez MI, García-Vallejo JJ, Pérez De La Blanca E, Martín E, et al. (2003) Angiotensin II effect on calcium mobilization and mitogen-activated protein kinase activation in human umbilical vein endothelial cells. Signal Transduction 3: 201-208.
33. Kansui Y, Garland CJ, Dora KA (2008) Enhanced spontaneous Ca2+ events in endothelial cells reflect signalling through myoendothelial gap junctions in pressurized mesenteric arteries. Cell Calcium 44: 135-146.
34. Frampton JE, Orchard CH (1992) The effect of a calmodulin inhibitor on intracellular [Ca2+] and contraction in isolated rat ventricular myocytes. J Physiol 453: 385-400.
35. Bouallegue A, Daou GB, Srivastava AK (2007) Endothelin-1-induced signaling pathways in vascular smooth muscle cells. Curr Vasc Pharmacol 5: 45-52.
36. Ross JJ, Tranquillo RT (2003) ECM gene expression correlates with in vitro tissue growth and development in fibrin gel remodeled by neonatal smooth muscle cells. Matrix Biol 22: 477-490.
37. Majack RA, Cook SC, Bornstein P (1986) Control of smooth muscle cell growth by components of the extracellular matrix: autocrine role for thrombospondin. Proc Natl Acad Sci U S A 83: 9050-9054.
38. Deb A, Skelding KA, Wang S, Reeder M, Simper D, et al. (2004) Integrin profile and in vivo homing of human smooth muscle progenitor cells. Circulation 110: 2673-2677.
39. Wang H, Keiser JA (1998) Vascular endothelial growth factor upregulates the expression of matrix metalloproteinases in vascular smooth muscle cells: role of flt-1. Circ Res 83: 832-840.
40. Dickson M, Martin J, Cousins F, Kulkarni A, Karlsson S, et al. (1995) Defective haematopoiesis and vasculogenesis in transforming growth factor-beta 1 knock out mice. Development 121: 1845-1854.
41. Yamashita J, Itoh H, Hirashima M, Ogawa M, Nishikawa S, et al. (2000) Flk1-positive cells derived from embryonic stem cells serve as vascular progenitors. Nature 408: 92-96.

42. Owens GK (1995) Regulation of differentiation of vascular smooth muscle cells. Physiol Rev 75: 487-517.
43. Hellstrand P, Albinsson S (2005) Stretch-dependent growth and differentiation in vascular smooth muscle: role of the actin cytoskeleton. Can J Physiol Pharmacol 83: 869-875.
44. Dandré F, Owens GK (2004) Platelet-derived growth factor-BB and Ets-1 transcription factor negatively regulate transcription of multiple smooth muscle cell differentiation marker genes. Am J Physiol Heart Circ Physiol 286: H2042-2051.
45. Gunst SJ, Zhang W (2008) Actin cytoskeletal dynamics in smooth muscle: a new paradigm for the regulation of smooth muscle contraction. Am J Physiol, Cell Physiol 295: C576-587.
46. Hao H, Gabbiani G, Bochaton-Piallat ML (2003) Arterial smooth muscle cell heterogeneity: implications for atherosclerosis and restenosis development. Arterioscler Thromb Vasc Biol 23: 1510-1520.
47. Harnett KM, Biancani P (2003) Calcium-dependent and calcium-independent contractions in smooth muscles. Am J Med 115 Suppl 3A: 24S-30S.
48. Gerthoffer WT, Singer CA (2002) Secretory functions of smooth muscle: cytokines and growth factors. Mol Interv 2: 447-456.
49. Mayr M, Zampetaki A, Sidibe A, Mayr U, Yin X, et al. (2008) Proteomic and metabolomic analysis of smooth muscle cells derived from the arterial media and adventitial progenitors of apolipoprotein E-deficient mice. Circ Res 102: 1046-1056.
50. Yue TL, Wang X, Sung CP, Olson B, McKenna PJ, et al. (1994) Interleukin-8. A mitogen and chemoattractant for vascular smooth muscle cells. Circ Res 75: 1-7.
51. Wang Y, Bai Y, Qin L, Zhang P, Yi T, et al. (2007) Interferon-gamma induces human vascular smooth muscle cell proliferation and intimal expansion by phosphatidylinositol 3-kinase dependent mammalian target of rapamycin raptor complex 1 activation. Circ Res 101: 560-569.
52. Li S, Lao J, Chen BPC, Li Y-s, Zhao Y, et al. (2003) Genomic analysis of smooth muscle cells in 3-dimensional collagen matrix. FASEB J 17: 97-99.
53. Peyton SR, Raub CB, Keschrumrus VP, Putnam AJ (2006) The use of poly(ethylene glycol) hydrogels to investigate the impact of ECM chemistry and mechanics on smooth muscle cells. Biomaterials 27: 4881-4893.
54. Peyton SR, Kim PD, Ghajar CM, Seliktar D, Putnam AJ (2008) The effects of matrix stiffness and RhoA on the phenotypic plasticity of smooth muscle cells in a 3-D biosynthetic hydrogel system. Biomaterials 29: 2597-2607.
55. Naito M, Nomura H, Iguchi A (1996) Migration of cultured vascular smooth muscle cells into non-crosslinked fibrin gels. Thromb Res 84: 129-136.
56. Takahashi K, Tanabe K, Ohnuki M, Narita M, Ichisaka T, et al. (2007) Induction of pluripotent stem cells from adult human fibroblasts by defined factors. Cell 131: 861-872.
57. Lee T-H, Song S-H, Kim KL, Yi J-Y, Shin G-H, et al. (2010) Functional recapitulation of smooth muscle cells via induced pluripotent stem cells from human aortic smooth muscle cells. Circulation Research 106: 120-128.

CHAPTER 4 - COMBINING PLURIPOTENT STEM CELL-DERIVED ENDOTHELIAL CELLS WITH DYNAMIC TECHNOLOGY TO ASSESS VASCULAR TOXICITY

Helena Vazão[1,2], Lino Ferreira[1,2]

[1]CNC - Center of Neurosciences and Cell Biology, University of Coimbra, Coimbra, Portugal, [2]Biocant - Center of Innovation in Biotechnology, Cantanhede, Portugal

Manuscript under preparation

ABSTRACT

In this study we describe the combination of arterial ECs derived from human pluripotent stem cells with a dynamic system to create a vascular model for drug screening and toxicology analysis. This technology may find particular use for the identification of drugs that may have a fetal cytotoxic effect. Moreover, the principles defined in this work may be applied to hiPSCs in order to create personalized kits for drug screening in cancer. Here we show that vascular endothelial growth factor ($VEGF_{165}$), thymosin β4 (Tβ4), and TGF-β inhibitor administered at different times over a 18 day-differentiation protocol can give rise to endothelial precursor cells that have the ability to differentiate into arterial ECs. The cells express arterial genes and proteins and respond to arterial flow by aligning in the direction of the flow and further up-regulating the expression of arterial genes. The process is likely mediated by heparan sulfate proteoglycan (HSPG), a component of glycocalyx, which is activated by fluidic shear stress. Overall we demonstrated the relevance of our system formed by arterial ECs cultured under flow conditions for toxicology assessment. Our results further show that hESC-derived ECs cultured under flow conditions can be used to assess vascular toxicity while showing higher sensitivity to vascular toxic compounds than somatic arterial ECs.

KEYWORDS: human embryonic stem cells, endothelial cells, arterial endothelial cells, glycocalyx, shear stress, vascular toxicity, terbinafine.

INTRODUCTION

The development of new technologies and tools for the rapid toxicological profiling of chemical/pharmaceutical substances, at cellular levels, are of great need to reduce and refine the use of animals in research. Vascular cells control the permeability of blood vessels, inflammation and immunity, cell growth, among other key functions, which have an important impact in the homeostasis of the human being. The evaluation of vascular toxicity is of primordial importance in the context of atherosclerosis since endothelial injury is an initial event of the disease.

Vascular cells derived from human pluripotent stem cells represent a potential cell source for vascular kits [1,2]. The use of "embryonic" endothelial cells may represent an opportunity to screen toxicity of compounds that affect fetal vasculature. Endothelial cells (ECs) have been derived from human embryonic stem cells (hESCs) using several methodologies such as embryoid bodies (EBs) which recapitulates *in vivo* embryogenesis [3,4], a mixture of EBs with 2D or 3D culture systems [1,5,6,7] and co-culture with cell lines [8,9,10]. However, to the best of our knowledge, there is no report showing the specification of hESC-derived ECs into arterial, venous, lymphatic or brain-like sub-phenotype either *in vitro* or after transplantation in animal models. This is important for the development of vascular kits with defined features. During embryonic development, specification into arterial-, venous-, lymphatic- or brain-derived ECs is defined at gene level and is mediated by several signaling pathways including VEGF, Notch and ephrin before circulation begins [11,12]**.** Studies in mouse have shown that ephrinB2 and its receptor ephB4 are differentially expressed in arterial and venous endothelial cells, respectively, before the onset of circulation in the developing embryo [13]. After the onset of the circulation, the distinct hemodynamic forces found in arteries and veins, such as blood flow rate, direction and pressure, can be a major driver in the specification of the endothelial cells [11,12]. Indeed, hemodynamic forces as shear stress have the capacity to program or redirect the specification of blood vessel type during development [11,12].

The development of vascular kits requires the development of microfluidic platforms to screen multiple compounds in a high-throughput while the cells are exposed to shear stress forces typically found *in vivo*. Only recently researchers have replicated the circular cross-section of blood vessels in microfluidic devices [14,15,16]. However, so far, these tools have not been used in the context of drug screening/toxicology assessment.

Here we show that vascular endothelial growth factor ($VEGF_{165}$), thymosin β4 (Tβ4), and TGF-β inhibitor administered at different times over a 18 day-differentiation protocol can

give rise to endothelial precursor cells that have the ability to differentiate into arterial ECs. This corresponds to a 2.5-fold enrichment as compared to spontaneous cell differentiation. The cells express arterial genes such as JAG1, ephrin B1 and Hey-2 and the arterial protein EphB2. The cells respond to arterial flow by aligning in the direction of the flow and further up-regulating the expression of arterial genes. The process is likely mediated by heparan sulfate proteoglycan (HSPG), a component of glycocalyx, which is activated by fluidic shear stress. Finally we demonstrated the relevance of our system formed by arterial ECs cultured under flow conditions for toxicology assessment. We show that hESC-derived ECs have higher sensitivity to terbinafine, an antifungal drug, than somatic human umbilical arterial endothelial cells. We further show that cells cultured under physiologic shear stress have higher sensitivity to terbinafine than cells cultured in static conditions.

METHODS

hESC culture and differentiation. Undifferentiated hESCs (passages 33-36; H9, WiCell, Wisconsin) were grown on an inactivated mouse embryonic fibroblast (MEF) feeder layer, as previously described [1,2]. To induce the formation of EBs, the undifferentiated hESCs were treated with 2 mg/mL type IV collagenase (Invitrogen) for 2 h and then transferred (2:1) to low attachment plates (Corning) containing 10 mL of differentiation medium [80% KO-DMEM, 20% fetal bovine serum (FBS, Invitrogen), 0.5% L- glutamine, 0.2% β-mercaptoethanol, 1% nonessential amino acids]. In some cases the EB medium was supplemented with $VEGF_{165}$ (50 ng/mL, Prepotech), Tβ4 (100 ng/mL, Caslo) and SB431542 (100 μM, Tocris). After 4 days in suspension, EBs were plated onto 1% gelatin-coated dishes and grown for 14 additional days. Medium was changed every 2-3 days. The experimental conditions tested were: (i) EB medium only (Prot1), (ii) EB medium supplemented with (ii) $(VEGF_{165})_{days0\text{-}18}$ (Prot2), or (iii) $[(VEGF_{165})_{days0\text{-}18}$ + (SB431542, 100 $mM)_{days7\text{-}18}]$ (Prot3), or (iv) $(VEGF_{165}$ + $T\beta4)_{days0\text{-}18}$ (Prot4), or (v) $[(VEGF_{165})_{days0\text{-}18}$ + $(T\beta4)_{days4\text{-}18}]$ (Prot5), or (vi) $[(VEGF_{165}$ + $T\beta4)_{days0\text{-}18}$ + $(SB431542)_{days7\text{-}18}]$ (Prot6), or (vii) $[(VEGF_{165})_{days0\text{-}18}$ + $(T\beta4)_{days4\text{-}18}$ + $(SB431542)_{days7\text{-}18}]$ (Prot7) (**Fig. 1A**).

Isolation of CD31$^+$ cells. CD31$^+$ cells were isolated from hESCs differentiated under Prot7 at day 18 using MACS (Miltenyi Biotec). Isolated cells were grown on petri dishes (1.5×10^4 cells/cm^2) coated with 0.1% gelatin and containing EGM-2 (Lonza) supplemented with SB431542 (10 μM). HUVECS and HUAECs (both from Lonza) were used as controls for the differentiation studies. Cells were cultured in EGM-2 media or EGM-MV media (both from Lonza; until passage 5) and the medium changed every 2 days.

Flow cytometry analysis. Cells were tripsinized, aliquoted ($1.25\text{-}2.5 \times 10^5$ cells per condition), washed in PBS, centrifuged at 1200 g and then resuspended in PBS containing 5% FBS. Cells were labeled with human CD31 monoclonal antibody (eBioscience), CD34 (Miltenyi Biotec), vwF (Dako), Flk-1/KDR (R&D) and VeCad (Santa Cruz). Cells were characterized on a FACS Calibur (BD) and the data analyzed by Cell Quest software. Twenty thousand events were collected in each run.

Quantitative Reverse Transcription-Polymerase Chain Reaction (qRT-PCR) analysis. Total RNA from experimental groups was isolated using a protocol with TRIzol (Invitrogen) and RNeasy Minikit (Qiagen, Valencia). cDNA was prepared from 1 μg total RNA using Taqman Reverse transcription reagents (Applied Biosystems, CA). Quantitative PCR (qPCR) was performed using Power SYBR Green PCR Master Mix and the detection using an ABI PRISM 7500 Fast System (Applied Biosystems). Quantification of target genes was performed relative to the reference GAPDH gene: relative expression= $2^{[-(Ct_{sample}-Ct_{GADPH})]}$. The mean minimal cycle threshold values (Ct) were calculated from 3-4 reactions. In some cases, gene expression in each experimental group was normalized to the relative gene expression found in HUVECs, HUAECs or undifferentiated hESCs. Primer sequences are published in **Table 1**.

Immunofluorescence analysis and cell staining. Cells were transferred to gelatin-coated slides containing differentiation medium, allowed to attach overnight, and then fixed with 4% paraformaldehyde (Electron Microscopy Sciences) for 15 min at room temperature. In some cases cells were directly fixed in IBIDI slides. Cells were blocked with 1% (w/v) BSA and stained for 1 h with anti-human primary antibodies for CD34 (Dako), CD31 (Dako), vWf (Dako), VECad (Santa Cruz Biotech), a-SMA (Dako), EphB2 (Santa Cruz Biotech), Lefty (Santa Cruz Biotech), and HSPG (US Biological). In each immunofluorescence experiment, an isotype-matched IgG control was used. Binding of

primary antibodies to specific cells was detected with anti-mouse IgG Cy3 conjugate (Sigma), anti-rabbit Cy3 (Jackson Labs) or anti-goat (alexa488, Molecular Probes). If necessary, permeabilization with 0,1% TritonX-100 in PBS was performed. For phalloidin staining, cells were stained with 50 mg/mL FITC-phalloidin (Sigma). Cell nuclei were stained with 4', 6'- diamidino-2-phenylindole (DAPI) (Sigma) and the slides examined with either a Zeiss fluorescence microscope or Zeiss LSM 50 confocal microscope. For uptake of DiI-labeled acetylated low-density lipoprotein (DiI-Ac-LDL), cells were incubated with DiI-labeled Ac-LDL (10 µg/mL, Biomedical Technologies) for 4 h at 37ºC. After incubation, cells were washed three times in EGM-2, fixed with 4 % (w/v) paraformaldehyde for 30 min and visualized in a fluorescent microscope.

Matrigel assay. A 24-well plate was coated with Matrigel (0.4 mL, BD Biosciences) per well and incubated at 37ºC for 30 min. hESC-derived ECs (passage 3) were seeded on top of the polymerized Matrigel at a concentration of 1×10^5 cells per 300 µL of EGM-2 medium. After 1 h of incubation at 37ºC, an extra 1 mL of EGM-2 was added. Cord formation was evaluated by phase contrast microscopy (Carl Zeiss International, Germany), 24 h after cell seeding.

Intracellular Ca^{2+} variation measurements. HUVEC, HUAEC or hESC-derived ECs were loaded with Fura-2 calcium fluorescent indicator by incubation with 5 µM of the membrane permeable acetoxymethyl (AM) derivative FURA- 2/AM (1 mM in DMSO, Molecular Probes) and 0.06% (w/v) Pluronic F-127 (Sigma), using basal medium (M199, Sigma) as a vehicle (35 µL/well, not supplemented with serum nor antibiotics), for 1 h at 37ºC in 5% CO_2 and 90% humidity. The medium was then replaced by the respective basal medium and cells were incubated in the same conditions for 30 min to allow hydrolysis of the acetoxymethyl (AM) esters by cellular esterases, resulting in intracellular capture of the membrane impermeant Fura-2. Afterwards cells were washed twice with 100 µL sodium salt solution (140 mM NaCl, 5 mM KCl, 1 mM $CaCl_2$, 1 mM $MgCl_2$, 10 mM Glucose, 10 mM HEPES-Na^+ pH 7.4). The buffer was replaced again (100 µl/well) immediately prior to incubating or not with test compounds.

Cells located in wells on a plate row were incubated at 25ºC (inside the microplate reader, during basal reading). Cells were then stimulated with 100 µM Histamine [17,18] (Sigma), 100 ng $VEGF_{165}$ (Prepotech, www.peprotech.com) [19], 10 µM Prostaglandin U46619 (Cayman, http://www.caymanchem.com) [20,21] or 2U Thrombin (Sigma) [22] by adding 1 µl of a stock solution. Fluorescence was measured at emission 510 nm using two

alternating excitation wavelengths (340nm and 380nm) [23] using a microplate fluorescence reader (Spectramax Gemini EM, Molecular Devices, with SoftMax® Pro software). The microplate reader was set to "top-read kinetics"; PMT was "high"; temperature was 25ºC; each fluorescence time point was an average of 18 reads; and during basal/inhibitors incubation periods and KCl/Histamine stimulation, each well was read every 3 sec. Fluorescence intensity values (in relative fluorescence units – RFU) measured at 340 nm and 380 nm were taken from the stabilized signal obtained at basal conditions and after incubation or not with the inhibitors. Following stimulation with agonists, the fluorescence values were taken from the time point at the peak of the response. Typically, each experiment consisted of three or four wells plus three or four wells containing cells incubated with inhibitors and all cells were stimulated and read simultaneously. The dose-response curves for the effect of stimuli on the intracellular Ca^{2+} variation were determined using the software GraphPad Prism™.

Fluidic shear stress experiments. HUVECs, HUAECs or hESC-derived ECs (2.6×10^6 cells/mL) were seeded on flow chamber coated-slides (µ-slide 0.4, luer, IBIDI) and grown until confluence. Using a programmed IBIDI pump with positive pressure, the cell monolayer was perfused with EGM-2 medium for 7 days, at flow rate of 15.1 mL/min (corresponding to shear stress of 20 dyne/cm^2), or 3.02 mL/min (corresponding to shear stress of 4 dyne/cm^2). After 7 days the flow was stopped, the cells imaged, and then stained or collected for posterior gene analysis. Medium was collected for ELISA assays. In some experiments, cells were cultured in medium supplemented with terbinafine (0.1 µM or 1 µM) (Sigma) for a maximum of 24 h, under shear stress. Static controls were performed in the chamber coated-slides but without flow. The IBIDI slides allow a laminar perfusion in rectangular flow geometry.

Evaluation of the levels of vascular injury by specific markers. ELISA kits analyzed supernatants collected from the shear stress experiments for vWF and vWFpp (Gen-Probe GTI Diagnostic) and ADMA (Enzo Life Sciences), according to manufacturer's recommendations.

Statistical analysis. An unpaired *t* test or one-way ANOVA analysis of variance with Newman-Keuls post-test was performed for statistical tests using software GraphPad Prism™. Results were considered significant when $P < 0.05$.

Table 1: Primers used for Real Time PCR[1]

	Sense	Antisense
GAPDH [1]	AGCCACATCGCTCAGACACC	GTACTCAGCGCCAGCATCG
PCAM [1]	GCTGTTGGTGGAAGGAGTGC	GAAGTTGGCTGGAGGTGCTC
CD34 [1]	TGAAGCCTAGCCTGTCACCT	CGCACAGCTGGAGGTCTTAT
VECad [1]	ACGGGATGACCAAGTACAGC	ACACACTTTGGGCTGGTAGG
vWF [1]	ATGTTGTGGGAGATGTTTGC	GCAGATAAGAGCTCAGCCTT
Flk-1 [1]	CTGGCATGGTCTTCTGTGAAGCA	AATACCAGTGGATGTGATGGCGG
Oct-4 [24]	GTGGAGGAAGCTGACAACAA	CTCCAGGTTGCCTCTCACTC
EphB4	CTCAGTTCGGATCCTACC	AATGTCACCCACTTCAGAT
Lefty-1	CTGACAAGTTACCTCACCTA	GACACATTGGGCTTTCTG
Lefty-2	GAACTGAATTGCTGTGTTATATG	AACCAGAATCCAGGTATCC
Notch1	ATCTGAAATAGGAAACAAGTGAA	ATAACCAACGAACAACTACATAA
Notch2	AACATCTCATCCATGCTTTG	ACAGTGGTACAGGTACTTC
Notch3	CGCTCGTCAGTTCTTAGA	AAGGAAGGAAGAGACAGAG
Notch4	ATTGACACCCAGCTTCTT	GAGGACAAGGGTCTTCAA
DLL3	TGTCCGTGAAATGAATTGG	AAGAGAAGATGGCAGGTAG
DLL4	GGAGGTATAAGGCAGGAG	AGGTGTGGAAGGGTATTG
JAG1	GTCTCAAAGAAGCGATCAG	ATATACTCCGCCGATTGG
JAG2	ACAATGGAGTATTCTCGGATA	CTGGTAACAAACGCTACG
EFNB1	CAACACTGTCAAGATGGC	CTCTTCTCTTCCTGGTTCA
EFNB2	CCACAGATAGGAGACAAATTG	AGTTGAGGAGAGGGGTAT
ALDH1A1	GAGTTTGTTCATCCAATCGTA	GGTGAGTAGGACAGGTAAG
Hey-2	ACAACTTCAGAAGTGCCT	GACAAGAGAGAGGTGGAG
ICAM-1	CAAGGCCTCAGTCAGTGTGA	CCTCTGGCTTCGTCAGAATC
E-selectin	AGCTTCCCATGGAACACAAC	CTGGGCTCCCATTAGTTCAA
eNOS	GATGCTCCCAACTTGACCTTGACCAT	TAGGTCTTGGGGTTGTCAGG
HO-1	GAAAAGCACATCCAGGCAAT	GCTGCCACATTAGGGTGTCT
DDAH1	GGACAAATCAACGAGGTGCT	TAGCGGTGGTCACTCATCTG
DDAH2	CTGTTGTGGCAGGCAGCAG	GTCAGGGAGGCATATGGGTG

[1] PCR conditions: initial denaturation step at 94ºC for 5 min; 40 cycles of denaturation at 94ºC for 30 sec, annealing at 60ºC for 33 sec and extension at 72ºC for 30 sec. At the end was performed a final 7 minutes extension at 72ºC. After amplification, melting curves were acquired and used to determine the specificity of PCR products.

RESULTS

Derivation of arterial ECs from hESCs

To differentiate hESCs into arterial ECs we screened several protocols using $VEGF_{165}$ [1,25], Tβ4 [26,27] and TGF-β inhibitor (SB431542) [28] as inductive agents of EC differentiation. To determine their inductive effect we examined the expression of CD31 marker overtime by flow cytometry (**Fig. 1B**). CD31 is highly express by differentiated ECs and has been used previously to identify embryonic ECs from human embryoid bodies (EBs) [1]. $VEGF_{165}$ (50 ng/mL) was incorporated in the medium since it induces functional ECs from hESCs [1,25], while TGF-β inhibitor SB431542 stabilizes hESC-derived ECs [28], and therefore was added at the end of some of the differentiation protocols (from day 7 on). FACS results show that expression of CD31 peaked at day 8 for protocols (Prot) 1-5, and at day 18 for Prot 6-7. Differentiation by Prot6 and Prot7 gave the highest percentages of $CD31^+$ cells (4.8%) at the end of the 18 days of differentiation. This is statistically higher ($P<0.05$, n=3) than the percentage obtained using classical EB medium (≈2%). The phenotypic analyses were complemented by gene expression analyses by qRT-PCR (**Fig.1C, and 2**). The genes analyzed included: CD31, CD34, von Willebrand factor (vWF), vascular endothelial cadherin (VE-CAD) and Flk-1/KDR. The gene expression in the hESC-derived cells was normalized by the corresponding gene expression in human umbilical vein endothelial cells (HUVECs). **Figure 1C** shows gene expression in hESC-derived cells differentiated by Prot7. Results indicate that the treatment of cells with $VEGF_{165}$, Tβ4 and SB431542 at different stages over the protocol markedly induced the increase of expression of EC markers, with the exception of CD34 marker. Results also show a decrease in the expression of the pluripotency marker Oct-4 overtime. For subsequent analyses, ECs from Prot7 were used.

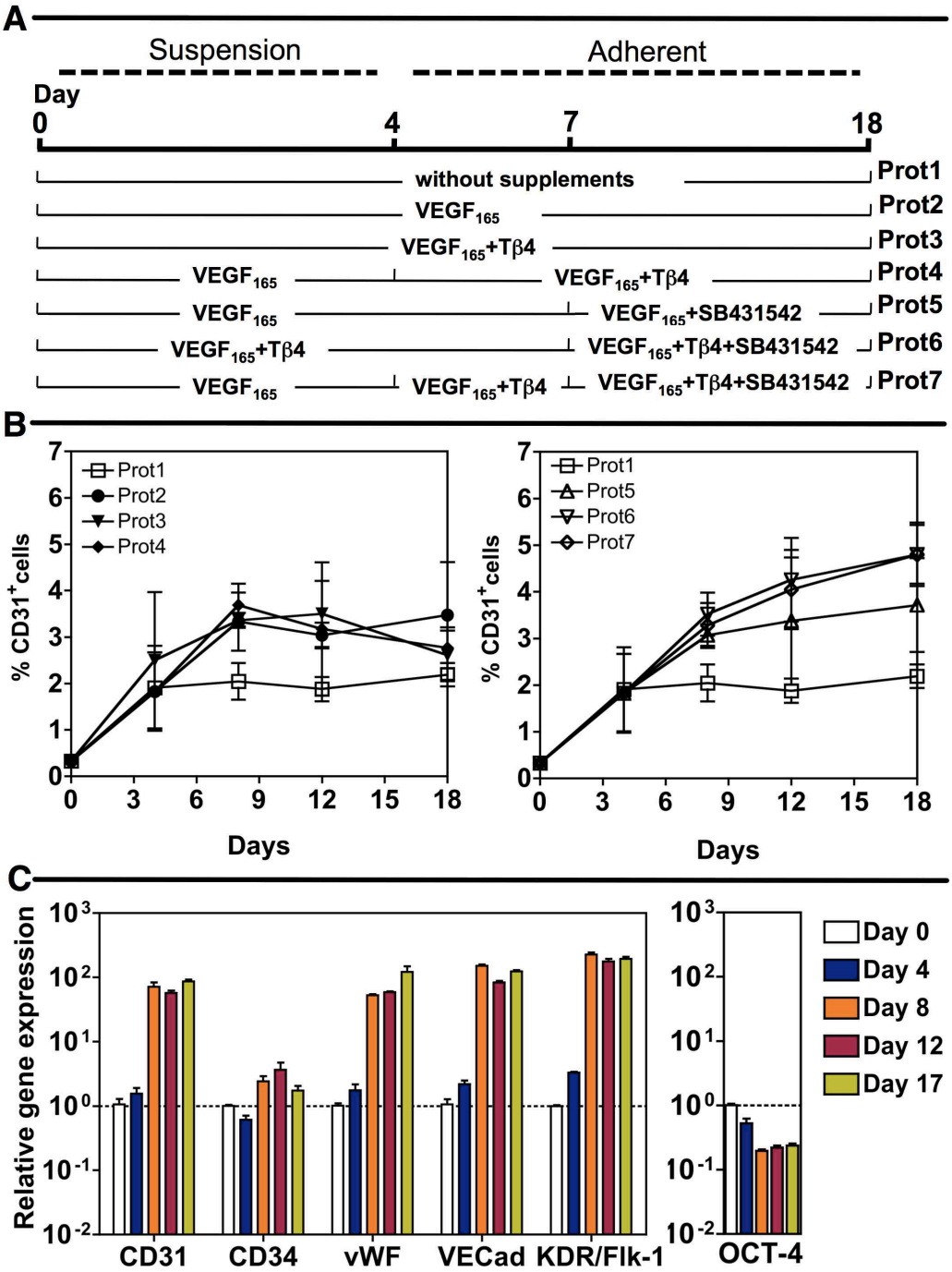

Figure 1- Induction of vascular differentiation on hESCs. (A) Scheme showing the adopted differentiation protocols (Prot1-Prot7). (**B)** Expression of CD31 marker in hESCs differentiated for 18 days, using different protocols. Values indicate mean ± SEM from 3 independent experiments. (**C)** Gene expression in hESC-derived EC cells differentiated by Prot7, as evaluated by qRT-PCR. Gene expression in each experimental group was normalized by the corresponding gene expression observed in HUVECs, with the exception of Oct-4, which was normalized by the corresponding gene expression in undifferentiated hESCs. Results are mean ± SEM (*n*=4).

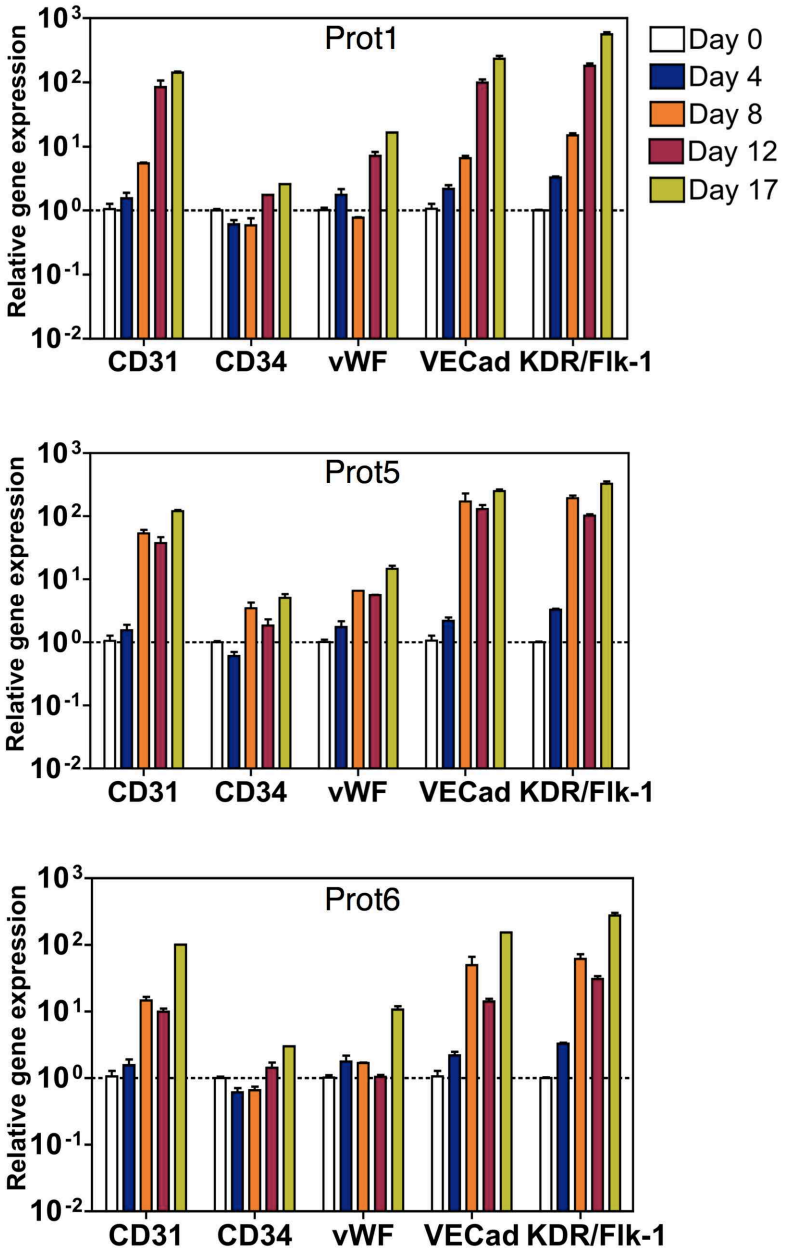

Figure 2- Gene expression in hESC-derived cells differentiated by Prot1, Prot5 and Prot6, as evaluated by qRT-PCR. Gene expression in each experimental group was normalized by the corresponding gene expression observed in HUVECs. Results are Mean ± SEM (*n*=3-4).

To determine whether $CD31^+$ cells could give rise to ECs, $CD31^+$ cells differentiated by Prot7 were isolated by magnetic activated cell sorting (MACS) and cultured in EGM-2 medium supplemented with SB431542 (10 μM). The proliferation rate of $CD31^+$ cells cultured in SB431542-supplemented medium is high, achieving 20 population doublings over a one-month period **(Fig. 3)**. Gene expression analysis in cells differentiated for 3 passages (between 18 and 22 days after cell seeding) indicate that they express CD34,

VECad and Flk-1/KDR at the same or higher level as the one found in HUVECs, albeit have low expression of vWF and CD31 which may indicate different levels of maturation (**Fig. 4C**). Furthermore, the differentiated cells had low expression of Oct-4 confirming their differentiated state. Immunocytochemistry analyses show that $CD31^+$ cells cultured for 3 passages expressed high levels of EC markers (**Fig. 4A)**. Differentiated $CD31^+$ cells stained positively for VECad at cell-cell adherent junctions and produced vWF (**Fig. 4B**). In addition, they do not express the smooth muscle cell marker α-SMA (**Fig. 3**). Overall, our results indicate that $CD31^+$ cells give rise to ECs.

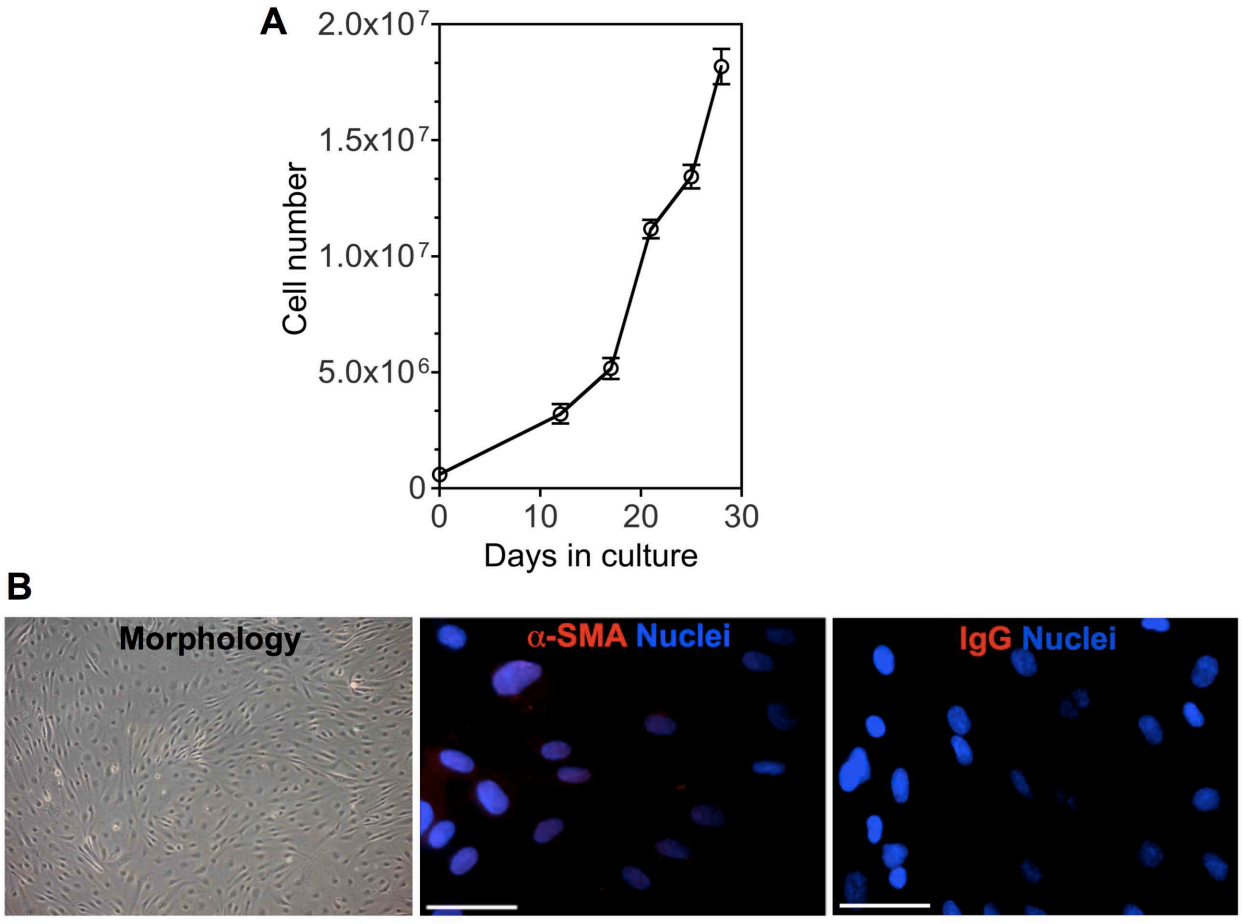

Figure 3- A) Time-course proliferation of hESC-derived ECs (Prot7). (B) hESC-derived ECs (Prot7, passage 3, approximately 22 days after $CD31^+$ cell seeding) have cobblestone morphology and do not express α-SMA, a smooth muscle cell marker.

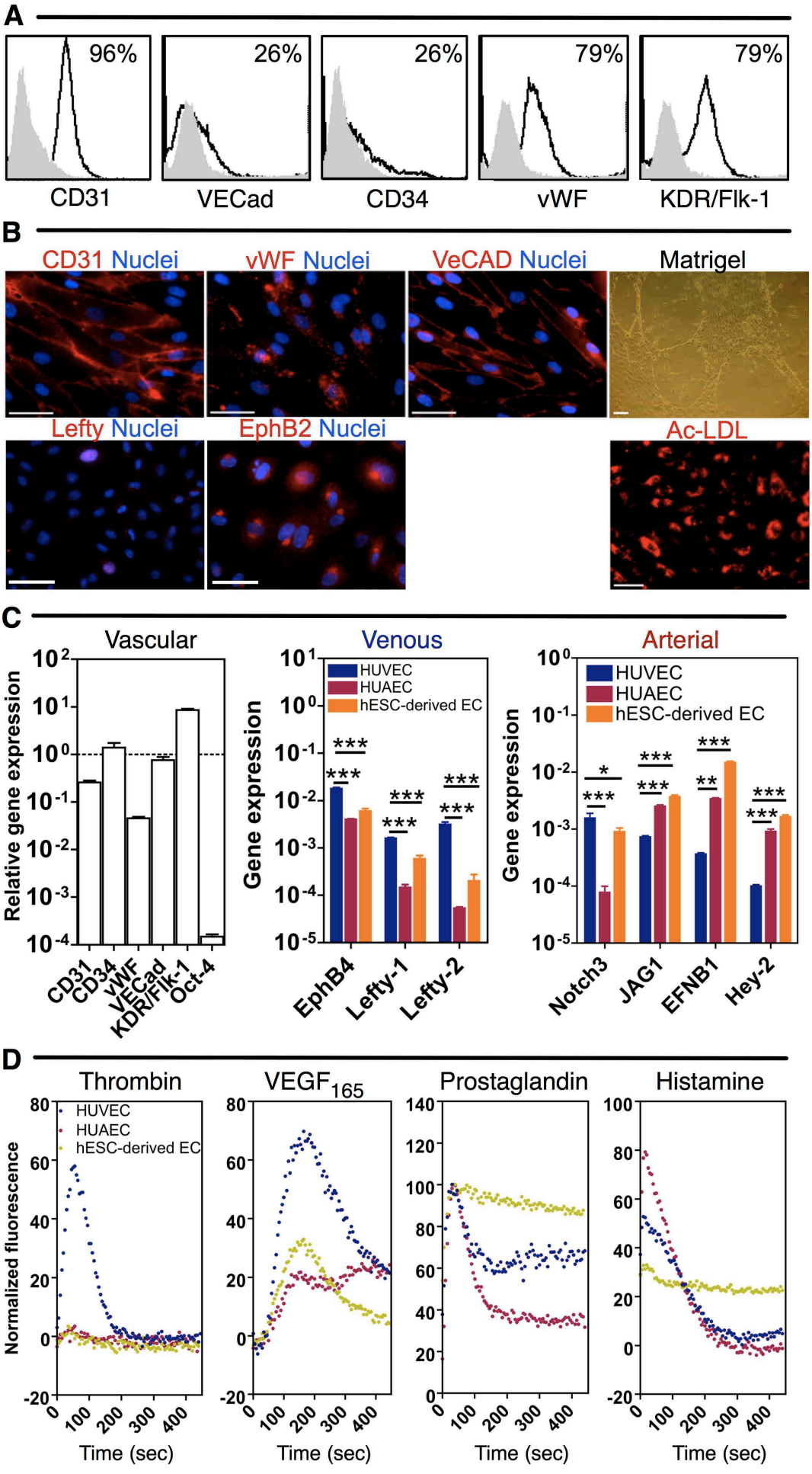
A
96%
26%
26%
79%
79%
CD31
VECad
CD34
vWF
KDR/Flk-1
B
CD31 Nuclei
vWF Nuclei
VeCAD Nuclei
Matrigel
Lefty Nuclei
EphB2 Nuclei
Ac-LDL
C
Vascular
Relative gene expression
CD31
CD34
vWF
VECad
KDR/Flk-1
Oct-4
Venous
Gene expression
HUVEC
HUAEC
hESC-derived EC
EphB4
Lefty-1
Lefty-2
Arterial
Notch3
JAG1
EFNB1
Hey-2
D
Thrombin
VEGF165
Prostaglandin
Histamine
Normalized fluorescence
Time (sec)

Figure 4- Characterization of hES-derived ECs. $CD31^+$ cells isolated by MACS (Prot7) were plated and differentiated for 3 passages (approximately 22 days after cell seeding). **(A)** Flow cytometry analysis of hESC-derived ECs. Percentages of positive cells were calculated based in the isotype controls (grey plot) and are shown in each histogram plot. **(B)** EC marker expression and functionality of hESC-derived ECs. In all figures bar corresponds to 50 µm. **(C)** qRT-PCR analysis for EC markers. Vascular gene expression in each experimental group was normalized by the corresponding gene expression observed in HUVECs, with the exception of Oct-4, which was normalized by the corresponding gene expression in undifferentiated hESCs. In the graphs corresponding to vein and arterial gene expression the genes were normalized by the expression of GAPDH. Results are mean ± SEM (*n*=4). * *P* <0.05, ** *P* <0.01, *** *P* <0.001. **(D)** Concentration of intracellular Ca^{2+} in FURA-2-loaded cultured hESC-derived ECs, HUAECs and HUVECs in response to several agonists. Traces are representative of 6 independent experiments for each condition.

Next, we determine the sub-phenotype of hESC-derived ECs, i.e., whether the ECs have been committed to arterial, venous or lymphatic lineages. We used podoplanin (podocyte membrane mucroprotein [29]), ephrin receptor B2 (EphB2) (a transmembrane ligand [13]) and lefty A/B [30] as a lymphatic, arterial and venous markers, respectively. As expected, human umbilical arterial endothelial cells (HUAECs) express EphB2 but do not express lefty A/B while HUVECs express lefty A/B but do not express EphB2 (**Fig. 5**). HESC-derived ECs stain positive for arterial marker EphB2 but not for the venous marker lefty A/B or the lymphatic marker podoplanin (**Fig. 4B**). Furthermore, hESC-derived ECs have high expression of arterial genes such as JAG1, EFNB1 and Hey-2 and low expression of venous genes such as EphB4, lefty-A and lefty-B (**Fig. 4C**). Together, our results indicate that hESC-derived ECs have been coaxed into arterial ECs.

To determine whether the ECs were functional we evaluate their ability to uptake DiI-labeled acetylated low-density lipoprotein (DiI-Ac-LDL), to form cord-like structures and to respond to vasoactive agonists. **Figure 4B** confirm that hESC-derived ECs are able to take up DiI-Ac-LDL and to form cord-like structures when cultured in the basement membrane Matrigel. Furthermore, the hESC-derived ECs respond to the vasoactive agonists as normal ECs by increasing the intracellular levels of Ca^{2+}(**Fig. 4D**). Cells were loaded with FURA-2, a Ca^{2+} sensitive dye, and their response to known concentrations of vasoactive agonists histamine, $VEGF_{165}$, prostaglandin H2-analogue U46619 and thrombin was monitored by fluorescence. The response profile was compared to the one observed for HUVECs and HUAECs. HESC-derived ECs share a similar response profile to thrombin as HUAECs but different response profiles to $VEGF_{165}$, prostaglandin H2-analogue and histamine. No similarity was found in the response profiles of hESC-derived

ECs and HUVECs. Overall, our results show that hESC-derived ECs are functional but in most cases they show different response profiles to vasoactive agonists as compared to HUAECs and HUVECs. The differences found between hESC-derived ECs and somatic arterial ECs (i.e. HUAECs) are likely ascribed to the different maturation levels of the cells.

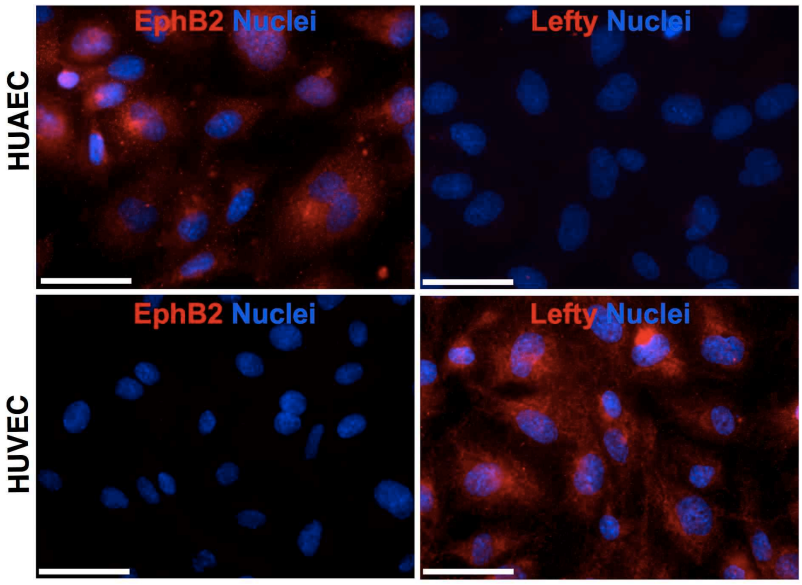

Figure 5- Expression of arterial and venous markers in HUVECs and HUAECs. Expression of the arterial endothelial marker EphB2 and venous marker Lefty in HUAECs and HUVECs. Bar corresponds to 50 µm.

Influence of shear stress in EC morphology, modulation of arterial sub-phenotype and glycocalix expression

Having demonstrated the differentiation of hESCs into arterial ECs we then studied how the differentiated cells responded to arterial (20 dyne/cm^2) and venous (4 dyne/cm^2) shear stress [31]. It has been shown that a mechanosensory complex formed by CD31, VECad and VEGFR2 mediates the responsiveness of ECs to shear stress [16,32]. The activation of this complex leads to integrin activation and alignment which triggers the activation of VEGFR-2 tyrosine kinases, extracellular signal-regulated kinases (ERKs), c-Jun amino-terminal kinases (JNKs), p38 mitogen-activated protein kinase and AKT serine/thronine kinases and transcription factors such as NF-kB. To study the influence of shear stress, hESC-derived ECs (or HUAECs as control) were cultured for 7 days in flow conditions. HESC-derived ECs cultured in arterial flow (20 dyne/cm^2) conditions align morphologically in the direction of the flow and show alignment of the proteins VECad and actin (stained

with phalloidin). Similar results have been obtained for HUAECs (**Fig. 6**). The alignment of the cells is dependent on the magnitude of the shear stress since cells cultured in low (4 dyne/cm^2) or no flow (static conditions) show low or no alignment, respectively. Importantly, cells cultured in flow or static conditions express EphB2 but not lefty A/B (**Fig. 7 and Fig. 8A**). The expression of EphB2 is higher in flow than in static conditions.

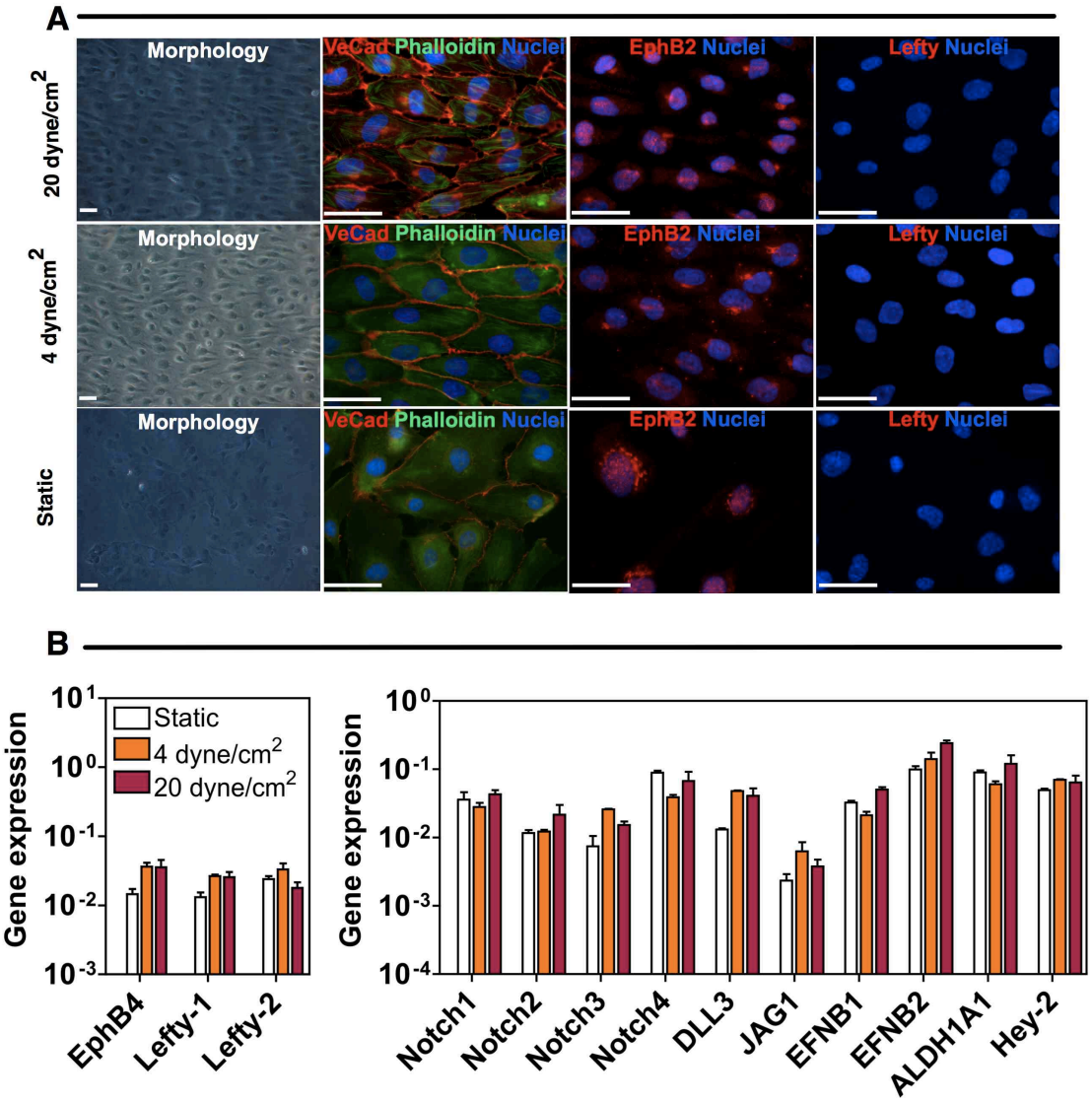

Figure 6- Expression of arterial and venous EC markers in HUAECs cultured on static and flow conditions (7 days), as evaluated by immunocytochemistry (A) and qRT-PCR analysis (B). In A, bar corresponds to 50 μm. In B, results are Mean ± SEM (*n*=3-4).

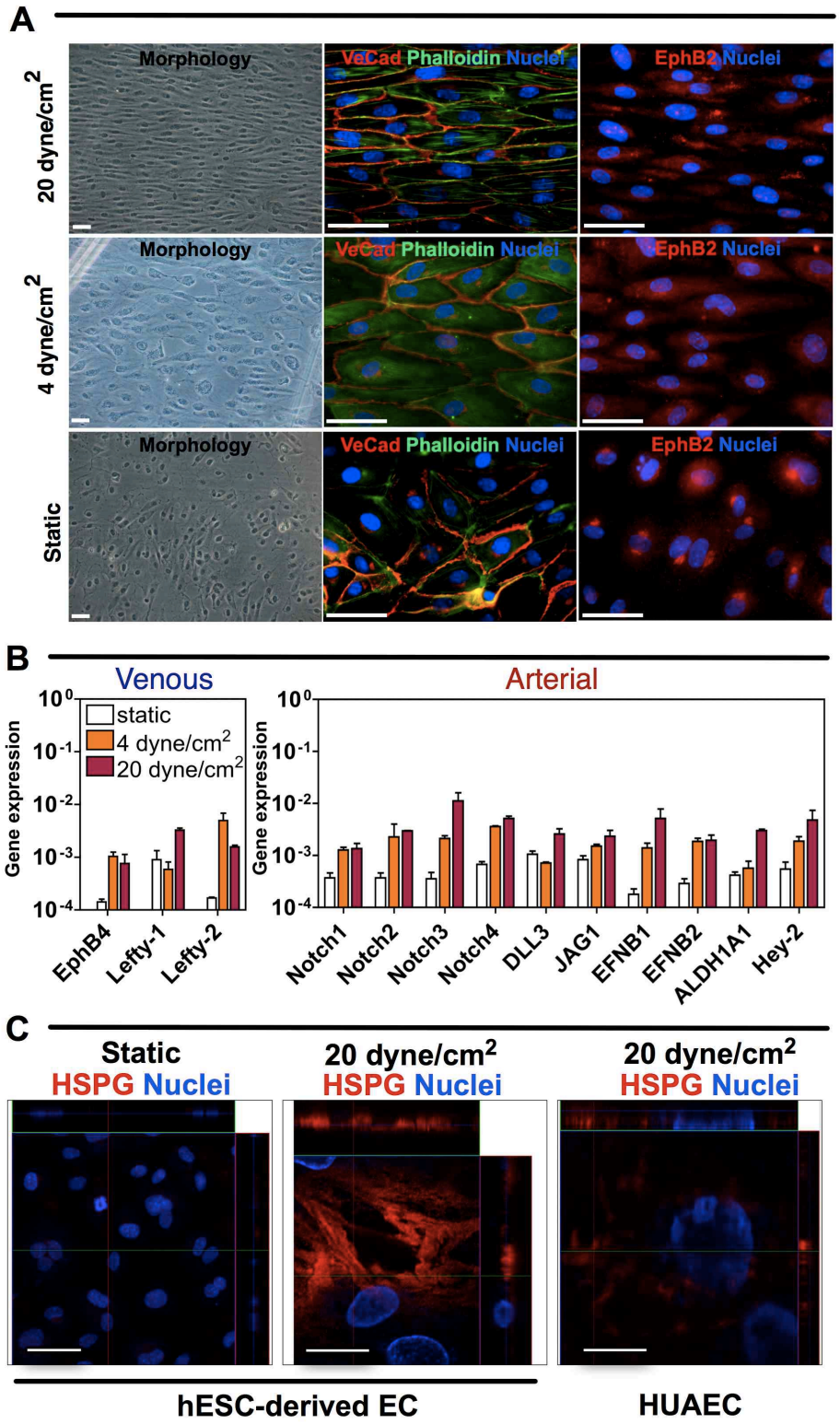

Figure 7- Effect of fluidic shear stress on hESC-derived ECs. **(A)** Cell alignment and expression of endothelial and arterial markers in hESC-derived ECs. Bar corresponds to 50 µm. **(B**) qRT-PCR analysis for venous and arterial markers in hESC-derived ECs (data was normalized by the housekeeping gene GAPDH). Results are mean ± SEM (*n*=4). **(C)** Expression of HSPG in hESC-derived ECs and HUAECs in static and flow conditions. Bar corresponds to 50 µm.

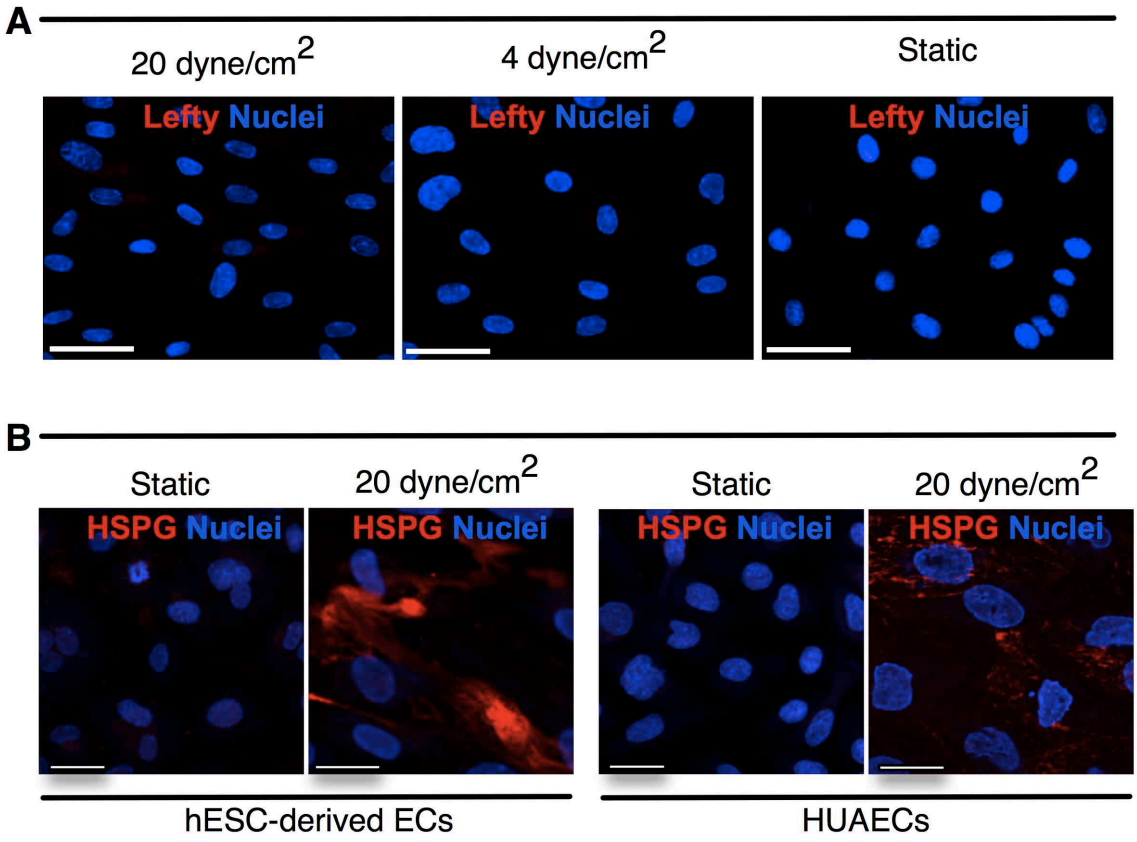

Figure 8- Effect of physiological shear stress in the sub-phenotype of hESC-derived ECs. (A) Cells cultured under static or flow conditions for 7 days do not express the venous EC marker Lefty. Bar corresponds to 50 μm. (B) hESC- derived ECs and HUAECs cultured under static conditions do not express heparan sulfate proteoglycan (HSPG), while both cells express HSPG under flow conditions. Bar corresponds to 50 μm.

Fluidic shear stress contributes for the maturation of hESC-derived ECs into arterial cells. Cells cultured under arterial or venous flow conditions express higher levels of arterial genes such as Notch receptors (1,2,3 and 4), Notch ligands (Dll3 and Jagged-1), Notch transcription factor Hey-2, aldehyde dehydrogenase 1 (ALDH1A1), and ephrin-B1 (EFNB1) and ephrin-B2 (EFNB2), which are ligands of ephrin receptors. Gene expression increased with an increase with flow. An upregulation of venous genes such as EphB4 and lefty-B was also observed when the cells were cultured under flow conditions, yet no lefty protein was observed under these conditions (**Fig. 7B and Fig. 8A**). Interestingly, HUAECs cultured under static or flow conditions have the same gene expression profile (**Fig. 6)**. Therefore, our results indicate that hESC-derived ECs are more prone to respond to shear stress than mature somatic cells.

Heparan sulfate proteoglycan (HSPG), a component of glycocalyx layer of ECs, has been reported to be a fluid stress sensor on ECs [33,34]. A class of HSPG, syndecans, is known to associate with cytoskeletal elements including actin, either directly or through associated actin-binding proteins [33]. Importantly, HSPG is absent on ECs grown and maintained under standard cell culture conditions *in vitro*, i.e. without flow [35]. Therefore we investigated whether hESC-derived ECs express HSPG under flow culture conditions (20 dyne/cm^2). Confocal microscopy analysis show that the surface of hESC-derived ECs or control HUAECs cultured under flow conditions is abundantly decorated with HSPG while no expression of HSPG is observed in static conditions (**Fig. 7C**). The HSPG is detected in the apical region of ECs (XZ view) exposed to flow.

Vascular toxicity assessed in hESC-derived ECs cultured under flow conditions

Terbinafine is an antifungal agent (inhibitor of ergosterol synthesis) that inhibits angiogenesis by suppressing endothelial cell proliferation, inhibits DNA synthesis and activates EC apoptosis [36,37]. Terbinafine is cytotoxic for HUVECs for concentrations above 120 mM [37]. To determine whether the hESC-derived ECs cultured under flow conditions could be used to assess vascular toxicity, cells were cultured for 7 days at 20 dyne/cm^2 after which the culture medium was supplemented or not with terbinafine (0.1 and 1 μM) and cells cultured under the same flow conditions for one more day. No significant changes in terms of EC morphology and cadherin expression were observed in ECs cultured in the presence or absence of the drug at day 8 (**Fig. 9A**). Next, we assess by qRT-PCR the expression of genes involved in inflammation (ICAM-1; E-selectin), oxidative stress sensing (HO-1) and vasculature modulation (eNOS) in hESC-derived cells and control HUAEC after exposition to terbinafine (**Fig. 9B)**. As expected, the expression of these genes increases under fluidic shear stress [38]. Interestingly, the expression of the genes is higher when hESC-derived ECs were cultured in the presence of terbinafine at 0.1 mM. Upregulation of some genes (HO-1 and E-selectin) was only observed for concentrations of 1 mM in HUAECs. We complemented these results by evaluating the expression of two genes related to the expression of dimethylarginine-dimethyl-amino-hydrolases (DDAH), a family of enzymes that metabolizes asymmetric dimethylarginine (ADMA) [39]. ADMA is a naturally occurring amino acid that circulates in plasma and is generated by degradation of methylated proteins. Increase levels of ADMA inhibits nitric oxide (NO) production by competitive inhibition of the physiological substrate L-arginine [40]. Drugs that inhibit NO pathway, upregulate caveolin-1 expression and/or enhance ADMA levels could potentially be associated with drug-induced endothelial dysfunction.

Therefore, increased circulating levels of ADMA may serve as predictive marker of EC dysfunction [40]. To date, two isoforms of DDAH (DDAH1 and DDAH2) have been found in mammals. hESC-derived ECs cultured under flow conditions in medium supplemented with terbinafine show a significant decrease in the expression of DDAH1 and DDAH2 ($P<0.05$ or $P<0.01$, $n=4$). Such effect was not observed for HUAECs cultured under the same conditions. Interestingly, the decrease of DDAH1 and DDAH2 in hESC-derived ECs was only observed when cells were culture under flow conditions. Overall our results indicate that cells cultured under physiologic shear stress have higher sensitivity to terbinafine than cells cultured in static conditions. In addition, hESC-derived ECs are more sensitive to the effect of terbinafine than HUAECs.

Next, we assessed the vascular dyfunction induced by terbinafine in hESC-derived ECs and control HUAECs, in the same conditions as before, by measuring the levels of ADMA and the ratio von Willebrand factor pro-peptide (vWFpp): von Willebrand factor (vWF) secreted by these cells (**Fig. 9C)**. The last 2 proteins with different biological activity are released in equimolar concentrations in plasma and an increased level of both proteins predicts EC activation/injury. Analysis of vWFpp:vWF ratio may discriminate and/or differentiate acute from chronic and progressive vascular injury [41,42]. hESC-derived ECs or HUAECs cultured in static conditions in the presence of the drug have no significant higher secretion of ADMA or vWFpp:vWF than in control conditions (i.e., without the drug). Remarkably, hESC-derived ECs cultured under flow conditions in the presence of terbinafine secrete higher levels of ADMA and vWFpp:vWF than without the drug. Again, the sensitivity of HUAECs to terbinafine was lower than hESC-derived ECs. The concentration of ADMA secreted by hESC-derived cells at 24 h is 3.5 times higher than in basal conditions. Importantly, this shift in concentration is observed in human patients with cardiovascular diseases. Healthy persons have an average of 0.45 ± 0.19 μmol of ADMA per liter of blood and this value increases 2.2 or 2.7 folds when the patient has idiopathic pulmonary arterial hypertension [39]. Furthermore, the secreted concentrations of ADMA correlate with the concentration of terbinafine in the culture medium. The quantification of vWFpp:vWF ratio confirm some of the results obtained by ADMA. Again, no effect of terbinafine was observed in hESC-derived ECs or HUAECs cultured in static conditions. In contrast, both cells cultured in flow conditions and exposed to terbinafine secrete higher levels of vWFpp:vWF, confirming vascular dysfunction.

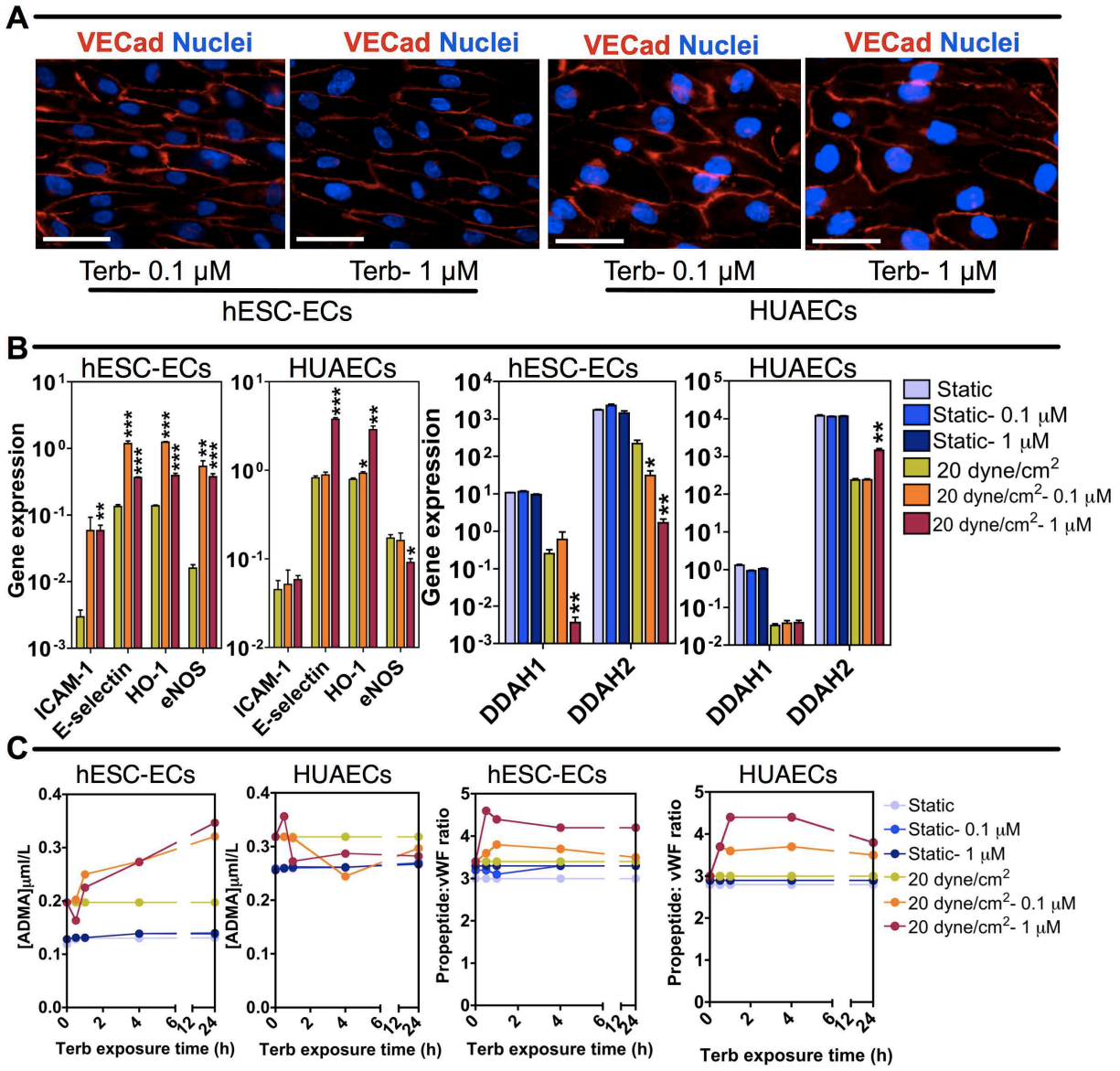

Figure 9- Toxicological effect of terbinafine in hESC-derived cells exposed to physiological shear stress. Cells were cultured under flow (20 dyne/cm^2), in medium without terbinafine, for 7 days, after which the cells were cultured in medium supplemented with terbinafine for 24 h, under flow. **(A)** Expression and localization of VECad in hESC-derived cells and HUAECs cultured in medium supplemented with terbinafine. Bar corresponds to 50 µm. **(B)** Expression of genes involved in inflammation (ICAM-1; E-selectin), oxidative stress sensing (HO-1), vascular modulation (eNOS) and vascular injury sensing (DDAH1 and DDAH2; genes that encode for enzymes that degrade ADMA) in hESC-derived ECs and HUAECs cultured in medium supplemented with terbinafine. Results are mean ± SEM (*n*=4). * *P* <0.05, ** *P* <0.01, *** *P* <0.001. **(C)** Quantification of ADMA and vWFpp:vWF by ELISA in hESC-derived ECs and HUAECs.

DISCUSSION

Herein we describe the combination of arterial ECs derived from human pluripotent stem cells with a dynamic system to create a vascular kit for high-throughput drug screening and toxicology analysis. This technology may find particular use for the identification of drugs that may have a fetal cytotoxic effect. Furthermore, the principles defined in this work may be applied to iPSCs in order to create personalized kits for drug screening in cancer.

Our results show that hESCs can differentiate into arterial ECs. The ECs were characterized at protein level by the expression of ephrin B2 and the absence of venous lefty A/B marker and the lymphatic marker podoplanin. At gene level, the cells express JAG1, EFNB1 and Hey-2 as HUAECs. Our results further indicate that fluidic shear stress contributes for the maturation of hESC-derived ECs into arterial cells since all the arterial genes tested including ephrins (1 and 2), notch receptors (1 to 4), and notch ligands (Jagged1 and delta-like ligand 3), were up-regulated. Previous work has shown that high concentrations of VEGF (50 ng/mL) induces expression of arterial markers such as ephrinB2 and Nrp-1 in embryonic stem cells, whereas low VEGF concentrations (2 ng/mL) lead to expression of venous endothelial markers [43]. Therefore our results agree with these findings since in our differentiation protocol was performed with high concentrations of VEGF (50 ng/mL). However, it should be noted that not always high concentrations of VEGF supports the arterial differentiation in ECs. For example, human endothelial progenitor cells isolated from cord blood or adult bone marrow in the presence of VEGF (50 ng/mL) only adopted a venous phenotype [44]. Developmental studies indicate that at the top of the hierarchy of arterial specification is the ligand sonic hedgehog (Shh). Shh is a pleiotropic molecule, with diverse roles in embryogenesis and patterning. It is expressed in the notochord and results in expression of VEGF by somites bordering the developing vessels. The activation of the Notch pathway by VEGF is also a defining characteristic of arterial EC. The Notch family is composed of 4 receptors (Notch1 to Notch4) and 5 ligands (Jagged-1 and -2 and Delta-like ligands [Dll] 1 to 4). The ephrinB2 ligand and its cognate receptor, EphB4, are differentially expressed in the arterial and venous ECs, respectively [13]. At the moment, it is unclear whether the $CD31^+$ cells collected from EBs are already committed to arterial ECs or whether the arterial specification occurs after their isolation. Our ongoing work will clarify this issue. Furthermore, we aim at understanding the mechanism of arterial specification in medium conditions where Shh and Notch signaling pathway is blocked or enhanced.

We further show in this work that fluidic shear stress impacts the maturation of arterial ECs and the induction of HSPG. Previous studies have supported the idea that hemodynamic forces have the capacity to program or redirect the specification of blood vessel type during development [11,12]. ECs not only have the ability to sense hemodynamic forces, but they have the ability to discriminate between different types of biomechanical stimuli. In this work, we show that hESC-derived ECs cultured in flow conditions (20 dyne/cm^2) aligned in the direction of the flow and express significantly higher levels of arterial markers. Although not demonstrated, HSPGs may mediate this maturation effect. Recent data demonstrated that HSPG is a mechanosensor mediating shear stress-induced EC differentiation from mouse embryonic stem cell-derived ECs [45]. HSPG is a part of the endothelial glycocalyx which is only expressed in flow conditions and absent in static conditions [35]. It is conceivable that HSPGs are physically displaced when exposed to shear and the displacement transmitted to the intracellular machinery. It has been suggested that HSPGs are physically activated (direct or not) to actin and nitric oxide synthetase mediating the mechanotransduction process [33]. These intracellular processes may contribute for the maturation of the cells under shear stress.

Our results further show that hESC-derived ECs cultured under flow conditions can be used to assess vascular toxicity while showing higher sensitivity to vascular toxic compounds than somatic arterial ECs. We hypothesize that the “embryonic” state of hESC-derived ECs might be part of the reason for the higher sensitivity of these cells. We are performing further experiments to elucidate this issue. For proof of concept we have used terbinafine an antifungal drug with anti-angiogenesis and anti-tumoral activity [36,46]. Our results show that hESC-derived ECs cultured under flow respond to very low concentrations of terbinafine (0.1 μM). This was correlated with an up-regulation of oxidative-sensing and inflammatory genes, down-regulation of genes (DDAH1 and DDAH2) encoding enzymes that degrade an inhibitor (ADMA) of nitric oxide synthetase, an increase in the secretion of ADMA and vWF pro-peptide, markers of EC injury.
We envision that the next step of the application of our model would be the development of an effective 3-D dynamic model comprising the possibility of high-throughput screenings of compounds that can affect positively or negatively vascular cells. That application can give us further insights in the applications of new platforms for regenerative medicine in the treatment of vascular and/or cardiovascular injuries.

Acknowledgments

This work was supported by a Marie Curie-Reintegration Grant (Grant nº 230929 to LF), MIT-Portugal program (focus in Bioengineering to LF) and Fundação para a Ciência e a Tecnologia (PTDC/SA-BEB/098468/2008 and PTDC/SAU-TOX/121887/2010 to L.F.; SFRH/BD/40077/2007 to H.V.).

REFERENCES:

1. Ferreira LS, Gerecht S, Shieh HF, Watson N, Rupnick MA, et al. (2007) Vascular progenitor cells isolated from human embryonic stem cells give rise to endothelial and smooth muscle like cells and form vascular networks in vivo. Circulation Research 101: 286-294.
2. Vazão H, das Neves RP, Grãos M, Ferreira L (2011) Towards the maturation and characterization of smooth muscle cells derived from human embryonic stem cells. PLOS one 6: e17771.
3. Levenberg S, Golub JS, Amit M, Itskovitz-Eldor J, Langer R (2002) Endothelial cells derived from human embryonic stem cells. Proc Natl Acad Sci USA 99: 4391-4396.
4. Wang L, Li L, Shojaei F, Levac K, Cerdan C, et al. (2004) Endothelial and Hematopoietic Cell Fate of Human Embryonic Stem Cells Originates from Primitive Endothelium with Hemangioblastic Properties. Immunity 21: 31-41.
5. Li Z, Wilson KD, Smith B, Kraft DL, Jia F, et al. (2009) Functional and transcriptional characterization of human embryonic stem cell-derived endothelial cells for treatment of myocardial infarction. PLoS ONE 4: e8443.
6. Cho S-W, Moon S-H, Lee S-H, Kang S-W, Kim J, et al. (2007) Improvement of postnatal neovascularization by human embryonic stem cell derived endothelial-like cell transplantation in a mouse model of hindlimb ischemia. Circulation 116: 2409-2419.
7. Lu S-J, Feng Q, Caballero S, Chen Y, Moore MAS, et al. (2007) Generation of functional hemangioblasts from human embryonic stem cells. Nat Methods 4: 501-509.
8. Sone M, Itoh H, Yamahara K, Yamashita JK, Yurugi-Kobayashi T, et al. (2007) Pathway for differentiation of human embryonic stem cells to vascular cell components and their potential for vascular regeneration. Arteriosclerosis, Thrombosis, and Vascular Biology 27: 2127-2134.
9. Wang ZZ, Au P, Chen T, Shao Y, Daheron LM, et al. (2007) Endothelial cells derived from human embryonic stem cells form durable blood vessels in vivo. Nat Biotechnol 25: 317-318.
10. Vodyanik MA, Thomson JA, Slukvin II (2006) Leukosialin (CD43) defines hematopoietic progenitors in human embryonic stem cell differentiation cultures. Blood 108: 2095-2105.
11. Kume T (2010) Specification of arterial, venous, and lymphatic endothelial cells during embryonic development. Histol Histopathol 25: 637-646.
12. Swift MR, Weinstein BM (2009) Arterial-venous specification during development. Circulation Research 104: 576-588.
13. Wang H, Chen Z, Anderson D (1998) Molecular distinction and angiogenic interaction between embryonic arteries and veins revealed by ephrin-B2 and its receptor Eph-B4. Cell 93: 741-753.
14. Fiddes LK, Raz N, Srigunapalan S, Tumarkan E, Simmons CA, et al. (2010) A circular cross-section PDMS microfluidics system for replication of cardiovascular flow conditions. Biomaterials 31: 3459-3464.
15. Lee SH, Kang do H, Kim HN, Suh KY (2010) Use of directly molded poly(methyl methacrylate) channels for microfluidic applications. Lab Chip 10: 3300-3306.

16. Tsai M, Kita A, Leach J, Rounsevell R, Huang JN, et al. (2012) In vitro modeling of the microvascular occlusion and thrombosis that occur in hematologic diseases using microfluidic technology. J Clin Invest 122: 408-418.
17. Agasse F, Bernardino L, Kristiansen H, Christiansen SH, Ferreira R, et al. (2008) Neuropeptide Y promotes neurogenesis in murine subventricular zone. Stem Cells 26: 1636-1645.
18. Bernardino L, Agasse F, Silva B, Ferreira R, Grade S, et al. (2008) Tumor necrosis factor-alpha modulates survival, proliferation, and neuronal differentiation in neonatal subventricular zone cell cultures. Stem Cells 26: 2361-2371.
19. Olsson A-K, Dimberg A, Kreuger J, Claesson-Welsh L (2006) VEGF receptor signalling - in control of vascular function. Nat Rev Mol Cell Biol 7: 359-371.
20. Persson B, Boels P, Lövdahl C, Rossi P, Arner A, et al. (2010) Endotoxin Induces Differentiated Contractile Responses in Porcine Pulmonary Arteries and Veins. Journal of Vascular Research 48: 206-211.
21. Gao Y, Zhou H, Ibe BO, Raj JU (1996) Prostaglandins E2 and I2 cause greater relaxations in pulmonary veins than in arteries of newborn lambs. J Appl Physiol 81: 2534-2539.
22. Furchgott R (1999) Endothelium-derived relaxing factor: discovery, early studies, and identification as nitric oxide. Bioscience reports.
23. Grynkiewicz G, Poenie M, Tsien RY (1985) A new generation of Ca2+ indicators with greatly improved fluorescence properties. J Biol Chem 260: 3440-3450.
24. O'connor MD, Kardel MD, Iosfina I, Youssef D, Lu M, et al. (2008) Alkaline phosphatase-positive colony formation is a sensitive, specific, and quantitative indicator of undifferentiated human embryonic stem cells. Stem Cells 26: 1109-1116.
25. Nourse MB, Halpin DE, Scatena M, Mortisen DJ, Tulloch NL, et al. (2010) VEGF Induces Differentiation of Functional Endothelium From Human Embryonic Stem Cells: Implications for Tissue Engineering. Arterioscler Thromb Vasc Biol 30: 80-89.
26. Kraehenbuehl TP, Ferreira LS, Hayward AM, Nahrendorf M, van der Vlies AJ, et al. (2011) Human embryonic stem cell-derived microvascular grafts for cardiac tissue preservation after myocardial infarction. Biomaterials 32: 1102-1109.
27. Smart N, Risebro CA, Melville AAD, Moses K, Schwartz RJ, et al. (2007) Thymosin beta4 induces adult epicardial progenitor mobilization and neovascularization. Nature 445: 177-182.
28. James D, Nam H-s, Seandel M, Nolan D, Janovitz T, et al. (2010) Expansion and maintenance of human embryonic stem cell-derived endothelial cells by TGFbeta inhibition is Id1 dependent. Nat Biotechnol 28: 161-166.
29. Breiteneder-Geleff S, Soleiman A, Kowalski H, Horvat R, Amann G, et al. (1999) Angiosarcomas express mixed endothelial phenotypes of blood and lymphatic capillaries: podoplanin as a specific marker for lymphatic endothelium. Am J Pathol 154: 385-394.
30. Chi J-T, Chang HY, Haraldsen G, Jahnsen FL, Troyanskaya OG, et al. (2003) Endothelial cell diversity revealed by global expression profiling. Proc Natl Acad Sci USA 100: 10623-10628.
31. Malek AM, Alper SL, Izumo S (1999) Hemodynamic shear stress and its role in atherosclerosis. JAMA 282: 2035-2042.
32. Tzima E, Irani-Tehrani M, Kiosses WB, Dejana E, Schultz DA, et al. (2005) A mechanosensory complex that mediates the endothelial cell response to fluid shear stress. Nature 437: 426-431.
33. Florian JA, Kosky JR, Ainslie K, Pang Z, Dull RO, et al. (2003) Heparan sulfate proteoglycan is a mechanosensor on endothelial cells. Circulation Research 93: e136-142.
34. Thi MM, Tarbell JM, Weinbaum S, Spray DC (2004) The role of the glycocalyx in reorganization of the actin cytoskeleton under fluid shear stress: a "bumper-car" model. Proc Natl Acad Sci USA 101: 16483-16488.
35. Potter DR, Damiano ER (2008) The hydrodynamically relevant endothelial cell glycocalyx observed in vivo is absent in vitro. Circulation Research 102: 770-776.
36. Ho P, Zhong W, Lee W (2006) Terbinafine inhibits endothelial cell migration through suppression of the Rho-mediated pathway. Molecular cancer therapeutics 12: 3130-3138.
37. Ho PY, Liang YC, Ho YS, Chen CT, Lee WS (2004) Inhibition of human vascular endothelial cells proliferation by terbinafine. Int J Cancer 111: 51-59.

38. Gaucher C, Devaux C, Boura C, Lacolley P, Stoltz J-F, et al. (2007) In vitro impact of physiological shear stress on endothelial cells gene expression profile. Clin Hemorheol Microcirc 37: 99-107.
39. Pullamsetti S, Kiss L, Ghofrani HA, Voswinckel R, Haredza P, et al. (2005) Increased levels and reduced catabolism of asymmetric and symmetric dimethylarginines in pulmonary hypertension. FASEB J 19: 1175-1177.
40. Böger RH, Cooke JP, Vallance P (2005) ADMA: an emerging cardiovascular risk factor. Vasc Med 10 Suppl 1: S1-2.
41. Louden C, Brott D, Katein A, Kelly T, Gould S, et al. (2006) Biomarkers and mechanisms of drug-induced vascular injury in non-rodents. Toxicologic Pathology 34: 19-26.
42. Tesfamariam B, DeFelice AF (2007) Endothelial injury in the initiation and progression of vascular disorders. Vascul Pharmacol 46: 229-237.
43. Lanner F, Sohl M, Farnebo F (2007) Functional arterial and venous fate is determined by graded VEGF signaling and notch status during embryonic stem cell differentiation. Arterioscler Thromb Vasc Biol 27: 487-493.
44. Aranguren XL, Luttun A, Clavel C, Moreno C, Abizanda G, et al. (2007) In vitro and in vivo arterial differentiation of human multipotent adult progenitor cells. Blood 109: 2634-2642.
45. Nikmanesh M, Shi ZD, Tarbell JM (2012) Heparan sulfate proteoglycan mediates shear stress-induced endothelial gene expression in mouse embryonic stem cell-derived endothelial cells. Biotechnol Bioeng 109: 583-594.
46. Lee W-S, Chen R-J, Wang Y-J, Tseng H, Jeng J-H, et al. (2003) In vitro and in vivo studies of the anticancer action of terbinafine in human cancer cell lines: G0/G1 p53-associated cell cycle arrest. Int J Cancer 106: 125-137.

CHAPTER 5 – VEGF-FUNCTIONALIZED DEXTRAN HAS LONGER INTRACELLULAR BIOACTIVITY THAN VEGF IN ENDOTHELIAL CELLS

João Maia[a,§], **Helena Vazão[b,c,§]**, Dora C.S. Pedroso[b,c], Catarina S.H. Jesus[b,d], Rui M.M. Brito[b,d], Mário Grãos[c], Maria H. Gil[a], Lino Ferreira[b,c,*]

[§]Authors contributed equally

[a] Chemical Engineering Department, Faculty of Science and Technology, University of Coimbra, Coimbra, Portugal, [b] Centre for Neuroscience and Cell Biology, University of Coimbra, Coimbra, Portugal, [c] Biocant, Center for Innovation and Biotechnology, Cantanhede, Portugal, [d] Chemistry Department, Faculty of Science and Technology, University of Coimbra, Portugal.

Published on Biomacromolecules (Research article, published August 2012, doi: 10.1021/bm3009268)

ABSTRACT

Herein, we report that VEGF-functionalized dextran (dexOx-VEGF) is comparatively superior to free VEGF in prolonging the phosphorylation of VEGF receptor 2 (VEGFR-2). Both dexOx-VEGF and free VEGF activate VEGFR-2 and the complexes are internalized into early endosomes ($EEA1^+$ vesicles) and then transported to lysosomes ($Rab7^+$ vesicles). However, after cell activation dexOx-VEGF is preferentially colocalized in early endosomes where VEGF signaling is still active while free VEGF is preferentially transported to late endosomes or lysosomes. We further show that dexOx-VEGF after phosphorylation of VEGF receptor 2 induces an increase of intracellular Ca^{2+} and activates VEGF downstream effectors such as Akt and extracellular signal-regulated kinase (ERK½) proteins. Under specific conditions the activation level is different from the one observed for free VEGF, thus suggesting mechanistic differences, which is illustrated by cell migration and cord-like formation studies. DexOx-VEGF can be cross-linked with adipic acid dihydrazide to form a degradable gel, which in turn can be incorporated in a fibrin gel containing endothelial cells (ECs) to modulate their activity. We envision that these constructs might be beneficial to extend the pro-angiogenic activity of VEGF in ischemic tissues and to modulate the biological activity of vascular cells.

KEYWORDS: vascular endothelial growth factor, oxidized dextran, fibrin, hydrogels, endothelial cells, angiogenesis, umbilical cord blood.

INTRODUCTION

Ischemic diseases, such as myocardial infarction, chronic wounds and stroke, cause a high morbidity with important social impact. Two major angiogenic therapies are being tested to treat patients suffering from these diseases based on the delivery of growth factors [$VEGF_{165}$ (from now on referred to as VEGF), placenta growth factor (PlGF), fibroblast growth factor (FGF), among others] and/or cells (*e.g.* vascular cells, vascular progenitor cells and stem cells). In the first group, VEGF has been extensively examined in the promotion of tissue vascularization. Unfortunately, the bolus delivery of VEGF in phase II human clinical trials failed to demonstrate significant benefits in the approved end points [1]. The fast plasma clearance (19.1 ± 5.7 mL min^{-1} kg^{-1}) and short half-life (33.7 ± 13 min) of VEGF [2] are likely in the origin of the poor therapeutic efficacy observed [3,4].

To overcome this issue, several polymeric matrices have been developed for the efficient delivery of VEGF [5,6,7,8], based on the physical immobilization of VEGF, such as in polyelectrolyte multilayers [9], hydrogels with heparin-based nanoparticles [10] or PLGA based-microparticles [11], and on the chemical immobilization of VEGF to networks formed by collagen, agarose or PEG [6,8,12]. The results indicate that the spatio-temporal presentation of VEGF is essential for a proper therapeutic actuation [13]. Despite these advances, it is important to develop alternative solutions to modulate the effect of VEGF in order to develop more efficient pro-angiogenic therapies.

A well-know strategy to increase the biological life of proteins is by conjugation with polyethylene glycol [14] however, other polymers can be used for the same objective [15]. Dextran has been used successfully for the conjugation of several drugs, including human growth hormone, trypsin and daunomycin [16,17,18]. Typically, dextran is oxidized and

reacted with the amine groups of the protein with the concomitant formation of an imine bond. The nonreduced conjugates were stable for several hours [18] or released relatively small amounts of the drug in physiologic conditions (5% of the drug after 24 h) [16]. Importantly, the bioactivity of VEGF conjugated to dextran and whether this conjugate could be incorporated in scaffolds to modulate the activity of vascular cells is unknown

Herein, we show that the VEGF conjugated to oxidized dextran (dexOx) has different bioactivity properties as compared to free VEGF. We show that VEGF conjugated to dextran delays the clustering of VEGF receptor 2 (VEGFR-2) and it extends the phosphorylation of VEGFR-2 when compared to free VEGF. The VEGF conjugate appears to have longer intracellular bioactivity as suggested by the extended colocalization with the early endosome-associated protein 1 (EEA1), and it modulates differently the intracellular uptake of Ca^{2+} and the signaling pathways mediated by ERK but not Akt. Consequently, this effect reduces endothelial cell migration but not survival. We further show that it is feasible to incorporate this VEGF conjugate in cell constructs. This new approach integrates in the same 3D hydrogel scaffold a VEGF conjugate delivery system and a three-dimensional (3D) matrix able to support cell attachment and being remodelled. Both components can be tailored separately to match different needs. Our results indicate that there is a modulation in endothelial cell (EC) gene expression depending on the percentage of dexOx-VEGF or VEGF released over time.

MATERIALS AND METHODS

Materials.

Adipic acid dihydrazide (AAD), ethyl carbazate (EtC), dextran (from Leuconostoc mesenteroides; Mw 60 kDa, according to Fluka's specification), $NaBH_3CN$ (Fluka), dialysis tubes (MWCO of 12 kDa), human fibrinogen, human thrombin, phosphate-buffered saline (PBS), Tris-buffered saline (TBS), Histopaque-1077 Hybri Max, serum-free medium M199, Pluronic F127, Rhodamine B isothiocyanate (TRITC) and primers for quantitative real time polymerase chain reaction (qRT-PCR) were purchased from Sigma (Sintra, Portugal). Endothelial growth medium (EGM-2) and human umbilical vein endothelial cells (HUVECs) were purchased from Lonza. Slide-a-lyzer (10 kDa) was acquired from Thermo Scientific. N-Succinimidyl-[2,3-^{3}H] Propionate (^{3}HNSP; 1 mCi mL^{-1} with specific activity of 80 mCi $mmol^{-1}$) was purchased from Scopus Research. Scintillation liquid Ultima Gold XR was acquired from Perkin-Elmer, the ELISA kit for VEGF and VEGFR-2 was acquired from R&D Systems and the Fura-2AM was acquired from Molecular Probes. The Bio-Plex phosphoprotein assay kit and the Precision Plus Protein Kaleidoscope Standards were purchased from Bio-Rad. Taqman Reverse transcription reagents and Power SYBR Green PCR Master Mix were from Applied Biosystems. The RNeasy Mini Kit was purchased from Qiagen. CaCl2 was acquired from Merck. Acetylated low-density lipopoprotein (DiI-Ac-LDL) was purchased from Biomedical Technologies. The mini-MACS immunomagnetic separation system was purchased from Miltenyi Biotec. Fetal bovine serum, Trizol reagent, Alexa Fluor 488-conjugated human fibrinogen, Hoescht 34580 and the LIVE/DEAD kit were purchased from Invitrogen. $VEGF_{165}$ was obtained from PeproTech Inc. or from Genentech, Inc., South San Francisco, CA (kind gift). All materials were used as received.

Dextran oxidation and characterization

An aqueous solution of dextran (1 g; 12.5%, w/v) was oxidized with sodium periodate solution (2 mL) with different concentrations (33-165 mg mL^{-1}) to yield theoretical oxidations from 5 to 25%, at room temperature. The reaction was stopped after 4 hours. The resulting solution was dialyzed for 3 days against water, using a dialysis tube with a MWCO of 12 kDa, and then lyophilized (Snidjers Scientific type 2040, Tillburg, Holland). The scale-up of the reaction was done using the same procedure albeit using 30 g of dextran and a calculated amount of periodate to yield a theoretical oxidation of 5, 10 and

25%, referred to as D5, D10 and D25, respectively. The experimental degree of oxidation (DO) was quantified by ^{1}H NMR (Varian 600 NMR spectrometer, Palo Alto, CA) using ethyl carbazate (EtC) as a titrant and taking into account the ratio between the integral of the peak at δ 7.3 ppm and the integral of the anomeric proton at δ 4.9 ppm [19]. The spectra were analyzed with iNMR software, version 2.3.3.

VEGF labeling and characterization of VEGF conjugates by circular dichroism (CD) and Sodium Dodecyl Sulfate Polyacrylamide Gel Electrophoresis (SDS-PAGE).

The ^{3}HNSP solution was transferred to a glass vial with a rubber stopper and the airspace was flushed with N_2 to allow evaporation of the ethyl acetate. A PBS-dialyzed solution of VEGF (2.54 mg mL-1) was moved to the 3HNSP vial and stirred magnetically, at room temperature, for 4 hours. The solution was transferred to a slide-a-lyzer cassette (10 kDa) and dialyzed against PBS. The final ^{3}H-VEGF concentration was 2.1 mg mL-1, as evaluated by measurement of absorbance at 276 nm (ε_{vegf} = 0.37) and the estimated radioactivity was 1.33 ± 0.07 mCi mmol-1, as evaluated by scintillation in a Perkin-Elmer Tri-Carb 2900T Liquid Scintillation Analyzer.

Far-UV CD spectra were collected using an Olis DSM 20 spectropolarimeter equipped with a Peltier temperature controller. Protein samples (~0.6 mg mL-1) were analyzed at 37ºC in a quartz cuvette with a 0.2 mm path-length. Spectra were collected at a resolution of 1 nm with 4 seconds of integration time with a bandwidth of 0.6 mm. To monitor changes in the secondary structure of VEGF bound to dexOx, CD spectra were obtained for VEGF in the presence of a 100-fold weight excess of dextran or the different dexOx. Spectra for VEGF bound to dextrans were background corrected with respect to the same dextran in buffer. Protein secondary structure was estimated from the far-UV CD spectra using the program CONTIN.[[20]]

The SDS-PAGE was performed on a 12.5% (w/v) polyacrylamide gel (0.75 mm thick). Protein was loaded into each well (5 - 10 μg), after denaturing for 5 min at 95ºC. The samples were run at 200 V and then stained with Coomassie Blue. The loaded samples were free VEGF, a mixture of VEGF and dextran, and VEGF conjugates, the last two cases at 100-fold weight excess of dextran.

Evaluation of VEGF conjugates bioactivity

The differentiation of $CD34^+$ cells into ECs was performed according to a methodology described previously by us [21]. HUVECs (passage 7) or UCB-derived ECs (passage 4) were cultured in EGM-2 medium at 37°C and 5% CO_2 until subconfluency was achieved. The cells were tripsinized and plated (20,000 cells per well) on black opaque 96-well plates (Costar). After a period of starvation (20 hours, in M199) the medium was discarded and the wells loaded with a calcium specific fluorescence probe, Fura-2, and a permeabilizer Pluronic F127 reconstituted in M199 (35 µL) and incubated for 1 hour at 37°C in 5% CO_2. Cells were washed 2 times with sodium salt solution (140 mM NaCl, 5 mM KCl, 1 mM $CaCl_2$, 1 mM $MgCl_2$, 10 mM glucose, 10 mM HEPES Na^+, pH 7.4) and again immediately before the incubation or not with test compounds. The reading was performed at 25ºC (Spectramax Gemini EM, Molecular Devices, with SoftMax Pro Software), by measuring emission at 510 nm, using two alternating excitation wavelengths (340 and 380 nm). Cells were then stimulated with VEGF, dexOx-VEGF solutions (VEGF:dexOx was 1:1000, w/w) or histamine (100 µM, Sigma).

The activation of VEGFR-2 receptor, Akt and ERK signaling pathways in HUVECs (80% confluency, in 6-well plates) was induced by starving the cells for 20 hours in serum-free M199 medium (with Earle's Salts and L-glutamine; Sigma-Aldrich) [22] and adding 60 µL of the test solution for a given period of time. Following treatment, the plates were immersed on ice and the medium discarded. Then the proteins were isolated from the cells (total protein concentration of 220-300 µg mL^{-1}) using the Bio-Plex Cell Lysis kit (Bio-Rad). The levels of VEGFR-2 and pVEGFR-2 (phosphorylated VEGFR-2) were determined by ELISA (R&D Systems). The levels of Akt and ERK phosphorylation and total protein were determined using a phosphoprotein and total protein Bio-Plex kit, acquired with a Bio-Plex 200 machine and analyzed using Bio-Plex Manager 5 (all from Bio-Rad), according to the manufacturer's recommendations.

Immunofluorescence analysis

Cells were cultured on gelatin-coated slides until sub-confluency. Starvation was induced in M199 medium for 20 h after which cells were treated according to the different experimental groups. At the end of each experiment, cells were fixed with 4% paraformaldehyde (Electron Microscopy Sciences) for 15 min at room temperature, blocked with 1% (w/v) BSA, and when necessary, permeabilized with 0,1% (v/v) Triton-X.

Cells were then stained for 1 h with anti-human primary antibodies specific for VEGFR-2 (clone: KDR/EIC), Endo180 (clone: B-10, both from Abcam), Early Endosome Antigen 1 (EEA1, clone: C45B10) or Rab 7 (clone: D95F2, both from Cell Signaling). In each immunofluorescence experiment, an isotype-matched IgG control was used. Binding of primary antibodies to specific cells was detected with anti-mouse or anti-rabbit IgG Cy3 conjugate (Sigma). Cell nuclei were stained with 4´,6-diamidino-2-phenylindole (DAPI) (Sigma) and the slides examined with a Zeiss LSM 50 confocal microscope.

Image analysis and quantification of cellular events

For each condition, images were acquired and processed with Fiji/ImageJ.

VEGFR-2 clustering The red channel was transformed in an 8-bit black and white image and the same gray threshold (24 - 255) was applied to every image. A particle analysis was performed while applying a size threshold of 1 μm^2 to infinite. The number of events was counted and used to estimate the degree of VEGFR-2 clustering (**Figure 1**).

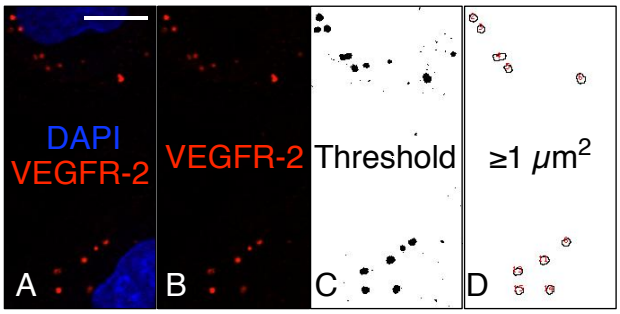

Figure 1 - VEGFR-2 clustering analysis by Fiji/ImageJ. The composite image (A) is first divided into the different channels. The VEGFR-2 channel (B) is transformed into an 8-bit images and the threshold was defined at 24 - 255 (C). The analyze particles tool was used with an area threshold ≥ 1 μm^2.

EEA1 and rab7 co-localization The green channel was transformed in an 8-bit black and white image and a gray threshold was applied to every image. The threshold chosen was established when a homogeneous scattering of black pixels could be observed throughout the image, which would precede a threshold with an essentially white background. A particle analysis was performed while applying a size threshold of 0.1 to 5 μm^2. The generated ROIs were saved. The red channel was treated similarly having the original image as guidance. A threshold was defined and the previously generated ROIs

were overlapped and the filled area fraction was estimated. Each "green" ROI with an occupation percentage >0 by the "red" channel was considered to be “co-localization” (**Figure 2**).

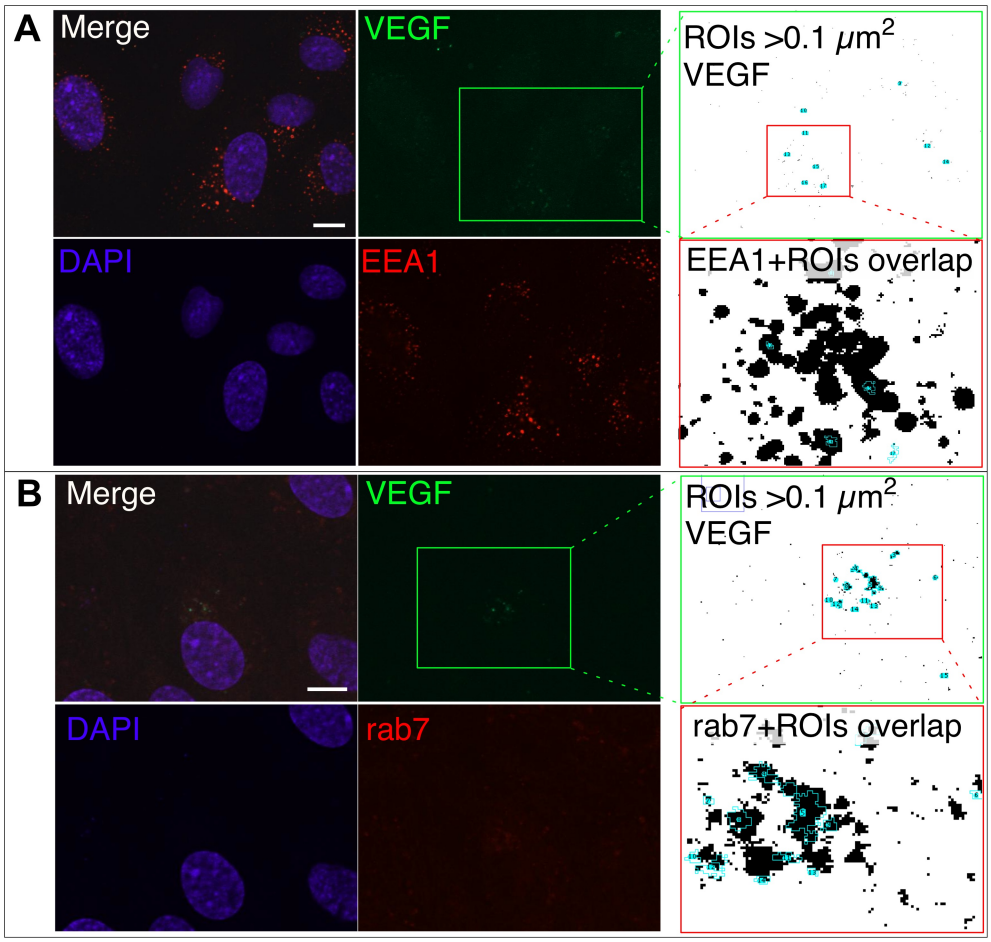

Figure 2 – Methodology adopted to determine VEGF-FITC colocalization with EEA1 or rab-7-labeled vesicles.

Cell survival assay

HUVECs (passage 5) were cultured in EGM-2 medium at 37°C and 5% CO_2 until subconfluency was achieved. The cells were then placed under starvation in M199 for ~20 h, after which were cultured for additional 24 h in M199 medium, M199 medium supplemented with free VEGF (50 ng mL^{-1}), M199 medium supplemented with D25-VEGF (corresponding to 50 ng mL^{-1} of free VEGF), and EGM- 2. At the end, cells were harvested and stained with Annexin/PI kit following the recommendations of the vendor. FACS analysis was performed as reported elsewhere [22]. Briefly, cells were harvested and

incubated for 10 min with Annexin V-FITC conjugate (Invitrogen), and kept on ice until being analyzed by flow cytometry. Propidium iodide (0.1 mg mL^{-1}) was added 5 min before reading the sample. 4 replicates were tested for each experimental condition and 10,000 events were acquired.

Scratch-wound assay

HUVECs were grown in 24-well cell culture plates until confluency. The assay was performed as described elsewhere [23]. A wound was created with a pipette tip, the cells were washed with PBS and then cultured in medium M199 supplemented with 2% FBS, or medium M199 supplemented with 2% FBS and free VEGF (100 ng mL^{-1}) or D25-VEGF (corresponding to 100 ng mL^{-1} of VEGF), or EGM-2 medium. Images were taken on a phase contrast microscope and the wound areas were quantified with Image J. Wound areas were then normalized by the initial area (n = 9 images).

Matrigel assay

A 15-well slide (IBIDI, Germany) was coated with 10 µL of Matrigel (BD Biosciences) per well and incubated for 30 minutes at 37ºC. HUVECs (passage 5) (starved for 20 h in M199 medium) were seeded on top of the polymerized Matrigel at a concentration of 0.2×10^5 cells per 50 µL of medium. Cord formation (length and sprouting) was evaluated by phase contrast microscopy (Zeiss Axiovert 40C, Carl Zeiss International, Germany) 24 h after cell seeding.

Preparation and characterization of dexOx hydrogels

DexOx hydrogels were prepared and characterized as described elsewhere [19]. Briefly, dexOx was dissolved in PBS buffer to obtain a 20% (D25) or 30% (D10 or D5) solutions (w/w) and were stored at 4°C if not used immediately. The hydrogels were prepared by mixing thoroughly dexOx (100 µL) and AAD (100 µL) at different concentrations. The AAD concentration used was calculated based on the desired molar percentage of dextran residues to be cross-linked. The hydrogels were allowed to cure for up to 2 hours and the swelling was performed in 24-well cell culture plates, by immersion in 1 mL of PBS at 37ºC. At regular time intervals, the hydrogels were removed from the aqueous solution, blotted

on filter paper, weighed and returned to the original well while the buffer was replaced. For the in vitro studies, VEGF or ^{3}H-VEGF were added to an aqueous solution of D25 or AAD (10%), depending on the experimental set-up, to obtain a final concentration of 0.2 mg mL^{-1}. Therefore, taking into account the mass of each hydrogel, 20 µg of VEGF could theoretically be released from each gel. The VEGF release study was performed in the same conditions as the swelling study. At regular time intervals, the immersion medium was collected and saved and replaced by new medium. The released VEGF was quantified either by ELISA or scintillation counts.

Isolation of CD34^{+} cells from UCB and their differentiation into ECs

All human umbilical cord blood samples were collected from donors, who signed an informed consent form, in compliance with Portuguese legislation. The collection was approved by the ethical committee of Hospital Infante D. Pedro. CD34^{+} cells were isolated from mononuclear cells, obtained from UCB samples after Histopaque-1077 Hybri Max density gradient separation. CD34^{+} cells were positively selected (2 times) using the mini-MACS immunomagnetic separation system, according to the manufacturer's recommendations. As evaluated by FACS, the cells isolated were > 95% pure for CD34 antigen. CD34^{+} cells were immediately used for cell differentiation studies. The differentiation of CD34^{+} cells was performed according to a methodology described previously by us [21]. Isolated CD34^{+} cells were transferred onto 1% (w/v) gelatin-coated 24-well plates (2 × 105 cells/well) and incubated in endothelial growth medium (EGM-2) with 20% (v/v) fetal bovine serum and 50 ng mL^{-1} VEGF, at 5% CO_2, 37ºC. After 5 days and then every other day, half of the volume of the medium was replaced with fresh one. At the end of the differentiation assay, expression of EC markers was evaluated by fluorescence-activated cell sorting (FACS) and immunofluorescence staining. The functionality of the cells was evaluated by incubation with DiI-Ac-LDL.

Hybrid networks formed by dexOx-VEGF hydrogels within fibrin hydrogels

The dexOx hydrogels (10 µL) were formed with D5, D10 or D25 with 10% cross-linking degree of AAD, by thoroughly mixing equal volumes of dexOx and AAD solutions in PBS, on top of the plungers of 1 mL sterile syringes with cut tips. When required, VEGF was added to the feed solution of dexOx (for gels with either D5 or D10) or AAD (for gels with D25), for a final concentration of 20 µg mL^{-1} (and therefore 100 ng of VEGF per gel), prior to the preparation of the hydrogels. The dexOx hydrogels were allowed to cure for 2 hours,

after which they were washed three times with PBS, allowed to air-dry and immersed in a fibrinogen solution (20 mg mL^{-1}) for 30 min. After removal of the excess fibrinogen solution, the dexOx hydrogels were covered with 50 µL of fibrin gel precursor solution. Human UCB $CD34^+$-derived ECs were encapsulated in the fibrin hydrogels, as previously described [21]. The $CD34^+$-derived ECs (0.35×10^5 per gel) were centrifuged, resuspended in the fibrin gel precursor solution and transferred to the syringes already containing the dexOx hydrogels. Polymerization was initiated at 37ºC and allowed to proceed over 30 min, to yield fibrin hydrogels. The hybrid cell constructs were then removed from the syringes, placed in 96-well plates containing culture medium identical to EGM-2 but without VEGF (unless otherwise stated) and incubated for up to six days, at 5% CO_2, 37ºC. After six days, cell viability was evaluated and the remaining hydrogels were stored at -80°C for subsequent analysis.

Preparation of fluorescent hybrid networks

Fluorescent hybrid networks were formed from D25 modified with TRITC and fibrinogen conjugated with Alexa Fluor 288. For the modification of D25 with TRITC, D25 (100 µL, 20% w/w) was added to TRITC (1 µL of 10 mg mL^{-1} in DMSO) and the final solution was diluted 100-fold with an unlabeled D25 aqueous solution (20% w/w), before the cross-linking with AAD (20%, w/v). In parallel, an aqueous solution of Alexa fluor-conjugated fibrinogen (20 mg mL^{-1} in TBS buffer, pH 7.4) was diluted 1000-fold with an unlabeled fibrinogen solution (20 mg mL^{-1}). The hybrid networks were formed as before between glass slides for better visualization under the fluorescence microscope. Endothelial cells stained with Hoechst were encapsulated within the fibrin hydrogel.

Cell viability analysis on ECs encapsulated in the hybrid networks

Cell viability was determined using a LIVE/DEAD kit. The gels containing the encapsulated cells were washed in PBS, immersed in a working solution of 2 µg mL^{-1} calcein AM and 4 µg mL^{-1} ethidium homodimer-1 in PBS for 30 min at 37°C and visualized under a Zeiss Axiovert 200M fluorescence inverted microscope.

Gene expression analysis on ECs encapsulated in the hybrid networks

Cell constructs were collected at day 6 and stored at -80ºC until further use. Cell constructs were disrupted in Trizol reagent in 2 mL tubes containing a 5 mm diameter

stainless steel bead (Qiagen), in a TissueLyser II aparatus (Qiagen) for 2 min, at 30 Hz. Total RNA was isolated by using the RNeasy Mini Kit, according to manufacturer's instructions. cDNA was synthesized from 1 µg total RNA using Taqman Reverse transcription reagents. Quantitative PCR (qPCR) was performed using Power SYBR Green PCR Master Mix and the detection was carried out in a 7500 Fast Real-Time PCR System (Applied Biosystems). Quantification of target genes was performed relatively to the reference gene (GAPDH): relative expression= $2^{[-(Ct_{sample}-Ct_{GADPH})]}$. The mean minimal cycle threshold values (C_t) were calculated from four to six independent reactions. Primer sequences are shown in **Table 1**.

Statistical analysis

Statistical analyses were performed using Prism software. All data are presented as the mean ± standard error of the mean (SEM) and results were considered significant when $P \leq 0.05$ (*), $P \leq 0.01$ (**) or $P \leq 0.001$ (***).

Table 1 - Primer sequences used for qRT-PCR

Target gene	Primer sequence
Human GAPDH	Forward: AGCCACATCGCTCAGACACC
	Reverse: GTACTCAGCGCCAGCATCG
Human VEGF	Forward: AGAAGGAGGAGGGCAGAATC
	Reverse: ACACAGGATGGCTTGAAGATG
Human Flk-1	Forward: CTGGCATGGTCTTCTGTGAAGCA
	Reverse: AATACCAGTGGATGTGATGGCGG
Human MMP2	Forward: CCCAGAAAAGATTGACGC
	Reverse: CGACAGCATCCAGGTTAT
Human MCP-1	Forward: CCCCAGTCACCTGCTGTTAT
	Reverse: TGGAATCCTGAACCCACTTC

PCR conditions: initial denaturation step at 94ºC for 5 min; 40 cycles of denaturation at 94ºC for 30 sec, annealing at 60ºC for 33 sec and extension at 72ºC for 30 sec. At the end, a 7 min extension at 72ºC was performed.

RESULTS AND DISCUSSION

The conjugation degree of VEGF to dexOx is dependent on the DO of dextran

Although VEGF has been chemically conjugated to several polymers including polyethylene glycol [5,6,7], alginate [24], heparin [25,26] and collagen [8], typically the conjugation of VEGF is by immobilization to polymers already attached to a surface or assembled in a 3D matrix which makes it difficult to assess the amount and bioactivity of immobilized VEGF. Herein, we conjugated VEGF to soluble dextran and the resulting derivative was characterized in terms of immobilized VEGF and bioactivity. We selected dextran as a carrier due to its biocompatibility and ease of chemical modification. For that purpose, dextran was initially oxidized by sodium periodate. The DO of dexOx was determined by ^{1}H-NMR after titration with ethyl carbazate [19]. The dexOx samples used in this study, D5, D10 and D25, have a DO of 3.6 ± 0.1%, 8.6 ± 0.2% and 17.8 ± 1.2%, respectively. The dexOx derivatives were then conjugated with VEGF being the polymer mass 100-fold in excess. The reaction was performed under nonreducing conditions and thus the conjugation of VEGF to dexOx is mediated by an imine bond (Schiff base) (**Fig. 3A**) [16]. Because each molecule of VEGF has 66 amine groups in the outer surface [8], multipoint attachment of VEGF to dexOx is expected in dexOx derivatives with high DO (D10 and D25).

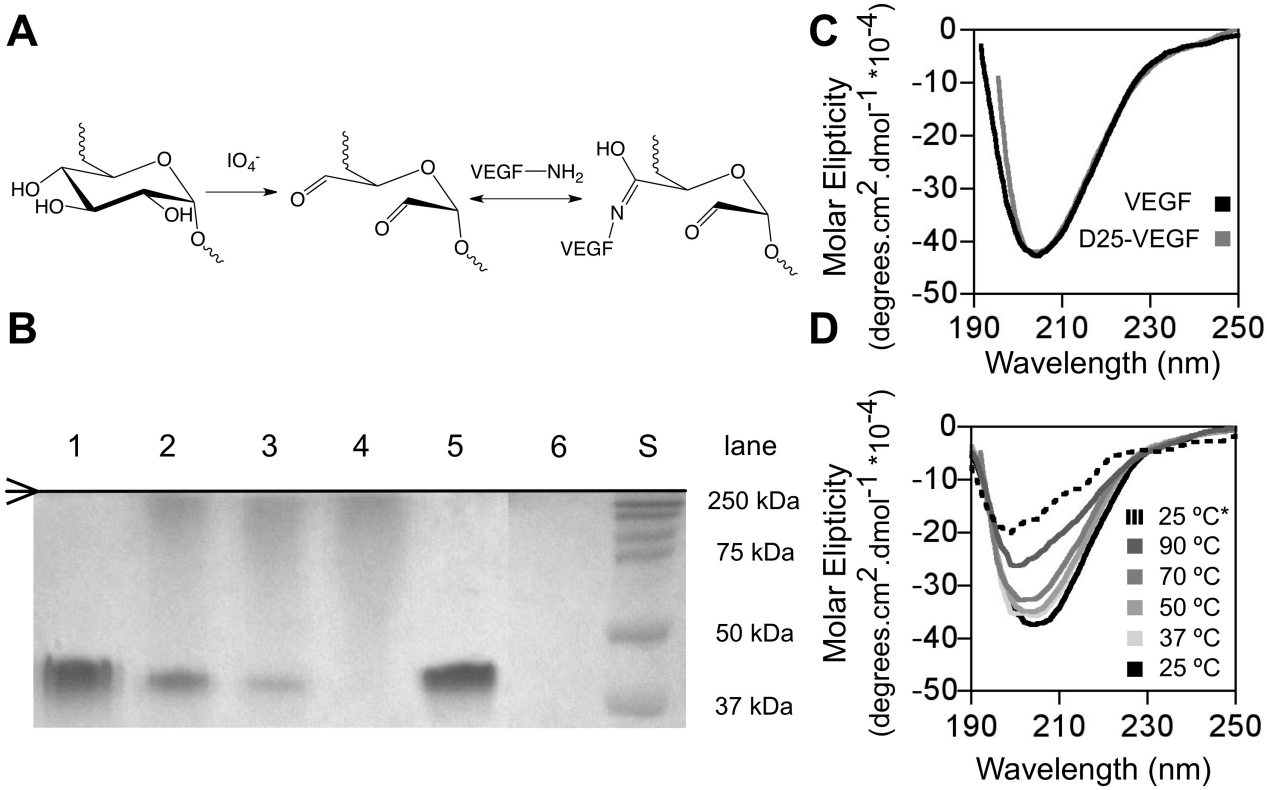

Figure 3 - Quantification of VEGF immobilized to dexOx and secondary structure evaluation of the conjugate. (A) Schematic representation of dextran oxidation and subsequent immobilization of VEGF. (B) Characterization of free VEGF, oxidized dextran and VEGF conjugates by SDS-PAGE: (1) VEGF, (2) D5-VEGF, (3) D10-VEGF, (4) D25-VEGF, (5) dextran + VEGF, (6) D25 and (S) protein standards. (C) Far-UV circular dichroism spectra of free VEGF and D25-VEGF. (D) Far-UV circular dichroism spectra of VEGF at different temperatures. *Spectra run at 25°C after rising temperature to 90°C.

The presence of VEGF in dexOx-VEGF conjugates was characterized by SDS-PAGE (**Fig. 3B**). The presence of unconjugated VEGF contributes to a band with an electrophoretic mobility at approximately 40 kDa (**Fig. 3B**, lane 1), while conjugated VEGF contributes to bands with an electrophoretic mobility above 40 kDa (**Fig. 3B**, lanes 2-4), likely depending on the degree of VEGF immobilization into each polymer chain. Solutions of nonoxidized dextran with VEGF (**Fig. 3B**, lane 5) were used as controls to demonstrate that the presence of dextran does not affect the electrophoretic mobility of unconjugated VEGF. According to Fig. **3B,** the conjugation of VEGF to dexOx is directly proportional to the DO in dexOx (**Fig. 3B,** lanes 2 - 4). DexOx with high DO (**Fig. 3B,** D25, lane 4) is able to immobilize all the supplied VEGF at least up to the detection limit of the SDS-PAGE, while a significant percentage of VEGF remains unreacted in dexOx with low DO (**Fig. 3B,** D5, lane 2). Image analysis by densitometry indicates that 32.6 %, 15.5 % and ~ 0 % of VEGF

is free in D5, D10 and D25 samples, respectively. This corresponds to the immobilization of 6.7, 8.5 and 10 μg of VEGF per miligram of dexOx in D5, D10, and D25, respectively. The presence of free VEGF in D5 and D10 conjugates might be due to the incapacity of dexOx with relatively low oxidation degree to immobilize chemically all the VEGF added initially to the polymeric solution [16]. In subsequent studies we used D25-VEGF to evaluate the biological activity of VEGF after full conjugation with dextran.

VEGF chemically immobilized into dexOx preserves its quaternary structure, as confirmed by CD studies

We investigated the secondary structure of VEGF chemically immobilized into dexOx (D25) by far-UV CD. The spectra for free VEGF and conjugated VEGF are virtually superposable (**Fig. 3C**), indicating that no significant structural changes occur upon protein conjugation to dexOx. This is in line with previous studies showing that the chemical immobilization of proteins on dexOx does not affect its native structure and activity [16]. The CD spectrum of the D25-VEGF conjugate has the same general shape, with a minimum around 205 nm, as the free VEGF (**Fig. 3C)**. Any potential conformational change in VEGF would be observed by shifts in the peak at ca. 205 nm as observed for VEGF heated at 90ºC (**Fig. 3D)**.

To obtain a more quantitative estimate of the secondary structure changes that may occur upon VEGF conjugation to D25, we estimated the secondary structure of VEGF by fitting the CD data with the program CONTIN [20]. The secondary structure percentages were estimated taking into account the number of residues assigned to each structure (α-helix, β-strand and disordered), and compared with previously reported structural studies on two VEGF fragments [one study characterized the fragment corresponding to the KDR-binding domain (95 residues: structure 2VPF from the Protein Data Bank; PDB) [27] and another corresponding to the heparin-binding domain fragment of VEGF (55 residues; PDB code 2VGH) [28]. The remaining residues were considered to be random coil, for a total of 165 residues (**Table 2**). Analysis of the results indicates once again that no significant structural changes are observed upon VEGF conjugation to dexOx. Overall, our results indicate that the structure of VEGF is substantially unaffected by the chemical conjugation to dexOx.

Table 2 – VEGF secondary structure analysis using the program CONTIN to fit the experimental far-UV CD data and comparison with known NMR and X-ray structures.

Entry	α-helix (%)	β-sheet (%)	Unordered (%)	SDE
VEGF[a]	11-12	37-41	48-51	-
VEGF	13	43	44	≤ 0.01
D25 + VEGF	12	43	45	≤ 0.01

[a] Secondary structure based on X-ray and NMR structures [27,28]; 2VPF and 2VGH files from the Protein Data Bank. Estimates were calculated considering 165 residues for the full protein.

VEGF chemically immobilized to dexOx prolongs intracellular VEGFR-2 signaing

In angiogenesis, most of VEGF downstream signalling events require the activation of VEGFR-2 [29] (**Fig. 4A**). Binding of VEGF to VEGFR-2 induces dimerization and subsequent phosphorylation of the receptor. Therefore, to determine the activity of D25-VEGF conjugate, we evaluated its ability to induce VEGFR-2 clustering at the cell surface. HUVECs were starved for 20 h in serum-free M199 medium and then treated for different time periods with M199 medium containing nonconjugated (free VEGF) or conjugated VEGF (D25-VEGF). A VEGF concentration of 100 ng mL^{-1} was used in all experimental groups. We monitored VEGFR-2 clustering by immunocytochemistry (**Fig. 4B**) [30] and quantified the number of clusters above 1 μm^2 (**Fig. 4C1**). VEGFR-2 clustering peaked at 30 min for both free and conjugated VEGF; however, it was statistical higher in free VEGF than on conjugated VEGF (P<0.01, n=10). In contrast, at 60 min, the clustering of VEGFR-2 was statistical higher on conjugated VEGF than on free VEGF (P<0.01, n=10). At 120 min, in both cases, clustering of VEGFR-2 at the cell surface leveled off to baseline levels. Overall, our results indicate that the kinetics of VEGFR-2 clustering was different in free and conjugated VEGF.

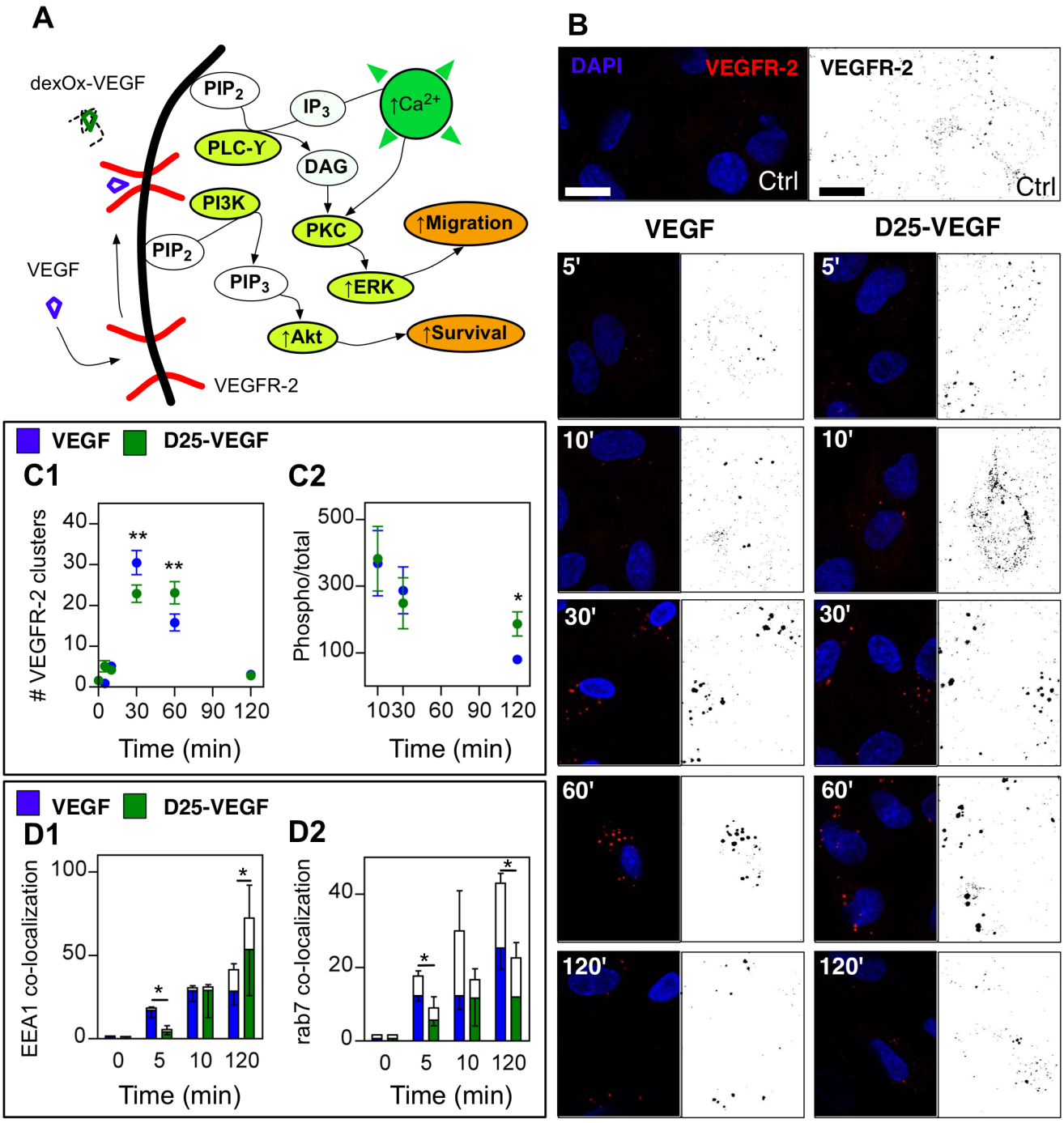

Figure 4 - Bioactivity of free and conjugated VEGF (D25-VEGF). (A) VEGF signaling pathway. Phospholipase C-γ (PLC-γ); phosphatidylinositol 3'-kinase (PI_3K); protein kinase C (PKC); phosphatidylinositol-3,4,5-trisphosphate (PIP_3); phosphatidylinositol 4,5-bisphosphate (PIP_2); inositol 1,4,5-trisphosphate (IP3) and diacylglycerol (DAG). (B) Confocal images of VEGFR-2 clustering. HUVECs were starved for 20 h and then cultured in medium supplemented with free or conjugated VEGF (D25-VEGF) at a final concentration of 100 ng mL^{-1} (Scale bar: 10 μm). (C1) Number of VEGFR-2 clusters (≥ 1 μm^2) in cells cultured in medium with free or conjugated VEGF as a function of time. Results are average ± SEM, n = 10. In some cases, the error bars are smaller than the size of the symbol. Statistical analyses were performed by ANOVA followed by a Bonferroni post-test (treatment vs baseline (time 0 h)). (C2) Phosphorylation levels (phospho/total protein) of VEGFR-2 induced by free and conjugated VEGF are represented as a percentage of the control. Results are average ± SEM, n = 4-8. (D1-D2) Co-localization of VEGF-FITC (blue) or D25-VEGF-FITC (green) with vesicles

immunostained for EEA1 (D1) or rab7 (D2), while empty bars represent no co-localization events. The VEGF-FITC concentration was 1 μg mL^{-1}. Results are average ± SEM, n = 3-6. Statistical analyses in C2, D1 and D2 were performed by an unpaired t-test.

Next, we evaluated whether D25-VEGF had the same capacity to phosphorylate VEGFR-2 (both at cell surface and intracellular) as VEGF. Again starved HUVECs were exposed to both inductive agents and the phosphorylation of the receptor was quantified by ELISA. Both VEGF and D25-VEGF were able to induce phosphorylation of VEGFR-2 at similar levels in HUVECs after 10 and 30 min ($P>0.05$, n=4-8) (**Fig. 4C2**). However, the phosphorylation level in cells treated for 2 h was higher for D25-VEGF than for nonconjugated VEGF ($P<0.05$, n=4-8). These results suggest that D25-VEGF conjugate has extended activity as compared to soluble VEGF.

Stimulation of VEGFR-2 by VEGF leads to the removal of the receptor from the plasma membrane by endocytosis, followed by a downregulation of VEGF signalling through lysosomal proteolysis of the receptors [31]. Therefore, we next examined the intracellular trafficking of D25-VEGF and VEGF covalently labeled with FITC. It has been reported that receptors entering the cell through endocytosis are contained in early endosomes which then fuse with an early sorting endosomal compartment that is marked for EEA1 protein [32]. Therefore we monitored the initial trafficking of VEGF by confocal microscopy through the co-localization of VEGF or D25-VEGF with $EEA1^+$ vesicles (**Fig. 4D1**). Our results show that the co-localization of VEGF with $EEA1^+$ vesicles progresses over time for both VEGF and D25-VEGF peaking at 2 h (last time assessed). Interestingly, the co-localization of D25-VEGF with $EEA1^+$ vesicles at time 2 h was statistical higher than VEGF ($P<0.05$, n=6). Finally, we monitored the trafficking of VEGF and D25-VEGF from early to late endosomes ($Rab7^+$ vesicles). In this case, the co-localization of D25-VEGF with $Rab7^+$ vesicles at time 2 h was statistical lower than VEGF ($P<0.05$, n=3) (**Fig. 4D2**).

Overall our results indicate that D25-VEGF extended VEGF signaling likely because it affects intracellular trafficking. It has been shown that in resting ECs, 60% of VEGFR-2 is present at the cell surface and available for interaction with VEGF while the remaining 40% of receptors are present in vesicles (that stain for EEA1) that can fuse with cell membrane, once the cell is activated by VEGF, in a time frame of 5 min [31]. Our results show that the clustering of VEGFR-2 is rapid, peaking at 30 min, followed by a decrease in the number of clusters to basal levels at time 2 h. The higher colocalization of D25-VEGF with $EEA1^+$ vesicles than VEGF at 2 h might explain the higher phosphorylation of

VEGFR-2. It is known that the internalization of the complex VEGF: VEGFR-2 in early endosomal compartments does not terminate its signalling [33]. In addition, the lower phosphorylation of VEGFR-2 in cells activated by VEGF than D25-VEGF might be due to the fact that VEGF is faster transported to late endosomes ($Rab7^+$ vesicles) than D25-VEGF. The reasons for this phenomenon are still unknown. The accumulation of VEGF at late endosomes will likely be followed by its degradation at the lysosomes. Approximately 40% of VEGFR-2 is degraded within 30 min of stimulation [31]. The differences found in the intracellular trafficking kinetics of D25-VEGF and VEGF might be explained by the interaction of dextran in D25-VEGF with carbohydrate receptors including lectin-type receptor Endo180 [34]. This is a 180-kDa transmembrane glycoprotein receptor highly expressed in HUVECs (**Fig.5**). Endo180 internalizes glycosylated ligands via clathrin-coated pit mediated endocytosis. We found that 10 min after adding medium supplemented with D25-VEGF labeled with FITC to HUVECs ca. 40% (n=3) of the VEGF conjugate co-localized with Endo180 receptor. Multiple interactions of D25-VEGF with either VEGFR2 or carbohydrate receptors might explain the differences in the internalization kinetics between D25-VEGF and VEGF.

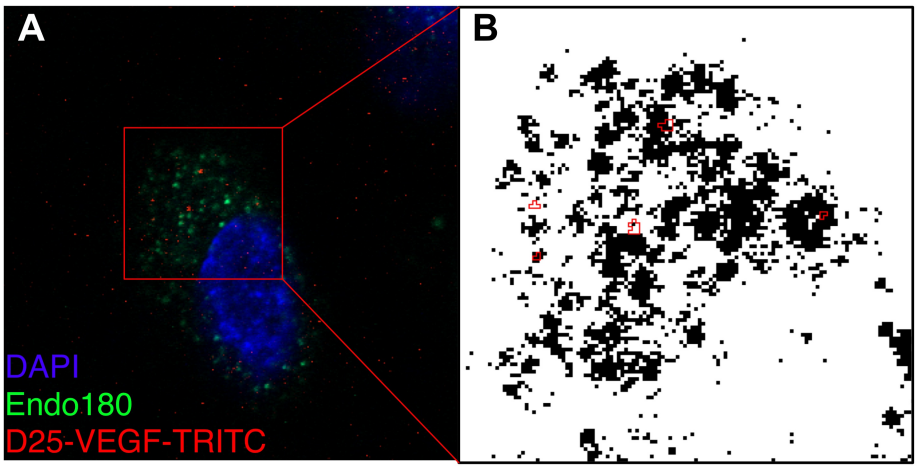

Figure 5 – Representative confocal image showing the co-localization of Endo180 with D25-VEGF-TRITC. HUVECs were exposed to D25-VEGF-TRITC for 10 min. Image analysis was performed as before.

VEGF chemically immobilized into dexOx induces the increase of cytosolic free Ca^{2+} in ECs but at a different rate as compared to free VEGF

To further assess the bioactivity of VEGF conjugated to dexOx, we evaluated its ability to induce an increase in intracellular free Ca^{2+} in ECs, mediated by the activation of VEGFR-

2 (**Fig. 6A**). Initially, we tested the ability of VEGF conjugates to induce an increase of intracellular Ca^{2+} in HUVECs. Previous results have shown that free VEGF activates the transient increase in cytosolic calcium in HUVECs through VEGFR-2 [35]. This cytosolic free calcium increase is initially due to mobilization from intracellular Ca^{2+} stores and only afterward is due to extracellular calcium influx [35]. In this work, HUVECs were cultured in serum-free medium for 20 h to minimize the influence of VEGF present in the serum and loaded with a fluorescent dye to monitor the free intracellular Ca^{2+} concentration. As a first step, cells were activated by different concentrations of free VEGF to determine a dose response profile (**Fig. 6A**). Histamine and bovine serum albumine (BSA) were used to set the variation interval in Ca^{2+} uptake. The administration of VEGF induces an increase in intracellular free Ca^{2+} uptake (first 5 min), followed by a plateau phase where Ca^{2+} remains constant for the remainder of the experiment. As expected, the levels of cytosolic free Ca^{2+} increased in direct correlation with an increase of the VEGF concentration.

Next, we evaluated the inductive effect of D25-VEGF conjugate (corresponding to a concentration of VEGF of 100 ng mL^{-1}) in the intracellular concentration of free Ca^{2+} in HUVECs (**Fig. 6A2**). Interestingly, D25-VEGF induces an initial increase of intracellular free Ca^{2+} corresponding to the effect of 25 ng mL^{-1} of free VEGF (taking into account the slope of the curve), reaching a plateau after 7-8 min with an intracellular Ca^{2+} concentration similar to the one observed for 100 ng mL^{-1} of free VEGF. Our results indicate that although D25-VEGF loses approximately 75% of the initial induction effect (taking into account that D25-VEGF contains 100 ng mL^{-1} of VEGF), the later response is, however, similar to 100 ng mL^{-1} VEGF.

Because Ca^{2+} uptake is likely affected by the type of cells used, we extended the studies to UCB $CD34^{+}$-derived ECs previously characterized by us [21] (**Fig. 6B**). These cells respond faster to free VEGF than HUVECs (**Fig. 6B1**) and the temporal profile of intracellular levels of Ca^{2+} is different in both types of cells. Despite the initial slow increase in intracellular Ca^{2+} mediated by D25-VEGF, the intracellular levels of Ca^{2+} after 5 min are superior to the ones observed for 100 ng mL^{-1} of free VEGF.

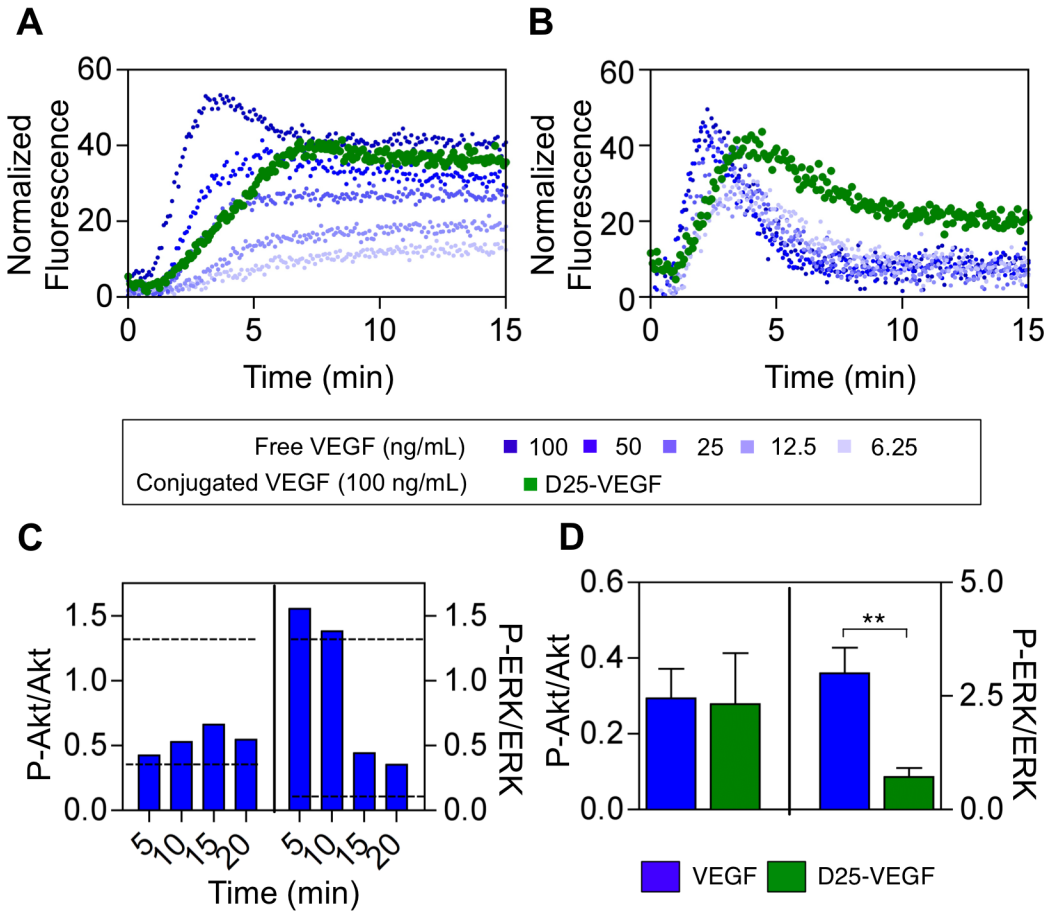

Figure 6 - Bioactivity of free and conjugated VEGF as assessed by their ability to induce Ca^{2+} accumulation in the cytoplasm and activate Akt and ERK signaling pathways. HUVECs (A) and ECs derived from cord blood stem cells (B) were loaded with Fura-2 dye and exposed to free or conjugated VEGF. Histamine (100 μM) and BSA (1%, w/v) were used to set the limits (100% and 0%, respectively) and to normalize the experimental data of cytosolic free Ca^{2+}. (C) Phosphorylation levels (phospho/total protein) of Akt and ERK over time mediated by free VEGF. Dashed lines represent positive control (*i.e.* starved cells exposed to EGM-2 medium) and negative control (*i.e.* starved cells maintained in M199 medium) (n = 1). (D) ERK and Akt phosphorylation levels after 10 min of stimulation with free VEGF and D25-VEGF (100 ng mL^{-1}). Results are average ± SEM, n = 4-8. Statistical analyses were performed by an unpaired t-test.

The differences found in the initial intracellular Ca^{2+} profiles between free and conjugated VEGF (D25-VEGF) in both types of ECs are unlikely due to the accessibility of VEGF to interact with VEGFR-2 since the same level of phosphorylation was observed for cells treated with both ligands for short period of times (≤30 min) (**Fig. 4C2**). Indeed, our results indicate that the level of intracellular Ca^{2+} is different in D25-VEGF and free VEGF despite their ability to phosphorylate VEGFR-2 at the same level. One of the explanations for the differences found is related to differences in the kinetics of endocytic trafficking of VEGF:

VEGFR-2 complex for short times (5 min) (**Fig. 4D1 and 4D2**). Another explanation for the differences found in the intracellular levels of Ca^{2+} is related to differences in the association of VEGFR-2 with coreceptors, including carbohydrate receptors such as Endo180 (**Fig. 5**). A recent study has shown that the association of VEGFR-2 with neuropilin-1 was enhanced by soluble VEGF, while the association of VEGFR-2 with integrin β1 was enhanced by VEGF bound to a collagen gel [30]. Therefore, it is possible that the differences in the intracellular levels of Ca^{2+} might be ascribed to the modulation of VEGFR-2 by other receptors.

VEGF chemically immobilized to dexOx affects distinctively the phosphorylation of Akt and ERK signaling pathways in ECs as compared to free VEGF

To further confirm the activation of HUVECs by D25-VEGF, the activation of Akt [22] and ERK [36,37], downstream effectors of VEGF signaling pathway (**Fig. 4A**), was evaluated by phosphoprotein analysis. The activation of any of these effectors has been reported to promote cell migration [37] and cell survival when cells are cultured under stress conditions [22,36]. Activation of Akt and ERK signaling pathways was evaluated in HUVECs, in the same way as described earlier for the VEGFR-2. The levels of phosphorylated and total Akt and ERK proteins were determined using a Bio-Plex kit.

Phosphorylation of Akt in HUVECs exposed to free VEGF was relatively low and peaked at 15 min after administration, decreasing thereafter (**Fig. 6C**). Akt phosphorylation mediated by D25-VEGF conjugate was not statistically different ($P>0.05$, n=4) to the one observed for free VEGF, in both cases at similar VEGF concentrations (**Fig. 6D**). On the other hand, ERK½ signaling was highly activated when HUVECs were exposed to VEGF. Free VEGF increased ERK½ phosphorylation as early as 5 min, followed by a decrease in the effect up to 20 min. A similar profile has been reported elsewhere for the activation of ERK by free VEGF [38]. Importantly, cells exposed to free VEGF for 10 min have statistically higher ERK phosphorylation than the ones exposed to D25-VEGF conjugate ($P<0.01$, n=4) (**Fig. 6D**).

In line with our intracellular Ca^{2+} data, the downstream effects of the activation of VEGFR-2 are different in free VEGF and D25-VEGF. Both VEGF ligands activate Akt signalling pathways (calcium-independent pathway) at similar levels; however, higher activation of ERK signalling was observed for free VEGF than for D25-VEGF. Importantly, the high

levels of ERK phosphorylation mediated by free VEGF agree with the rapid and high intracellular levels of Ca^{2+} observed by us in the previous section (**Fig. 6A**), which can potentiate PKC activity and then ERK phosphorylation (**Fig. 6A**).

Next, functional assays have been performed to assess the bioactivity of free and conjugated VEGF. In one set of tests, HUVECs were starved for 20 h and then cultured in one of the following conditions for 24 h: M199 medium (without serum and VEGF) (i), M199 medium supplemented with free VEGF (50 ng mL^{-1}) (ii) or D25-VEGF (corresponding to 50 ng mL^{-1} of VEGF) (iii), and EGM-2 medium (containing serum and VEGF). Cell survival was evaluated by flow cytometry after staining the cells with Annexin/propidium iodide (**Fig. 7A**). Annexin V is a phospholipid-binding protein with specificity for phospatidyl serine, one of the earliest markers of cellular transition to an apoptotic state. This phospholipid is translocated from the inner to the outer leaflet of the plasma membrane. PI enters in necrotic cells and binds to double-stranded nucleic acids, but is excluded from cells with normal integrity. As expected, cells cultured in EGM-2 and M199 medium show the highest (live cells: 87.1 ± 3.6, n=4) and lowest (live cells: 35.0 ± 3.4, n=4) survival, respectively. Cells treated with free VEGF or D25-VEGF showed intermediate levels of cell survival (between 54 and 61% of live cells). Importantly, no statistical difference (P>0.05) was observed between cells treated with free (live cells: 60.6 ± 4.5, n=4) and conjugated VEGF (live cells: 53.5 ± 6.4, n=4). This agrees with the fact that both free and conjugated VEGF have similar activation of Akt signaling (**Fig. 6D**), the pro-survival signaling pathway.

In another set of tests, the impact of free and conjugated VEGF on cell migration was examined by a scratch-wound assay (**Fig. 7B**). In this assay, HUVECs were cultured in M199 medium, M199 medium supplemented with free and D25-VEGF (in both cases having 100 ng mL^{-1} VEGF) and EGM-2 medium. Cells cultured in EGM-2 and M199 medium show the highest (16 h) and lowest (>42 h) healing time, respectively. Importantly, cells cultured in M199 medium supplemented with free VEGF have lower healing time (24 h) than cells cultured in M199 medium supplemented with D25-VEGF (42 h). Previous studies have shown that cell migration is modulated by the activation of ERK signaling [37]. Our results agree with the fact that cells exposed to free VEGF have higher ERK phosphorylation than the ones exposed to D25-VEGF (**Fig. 6D**). We complement these studies by evaluating the impact of free and conjugated VEGF on cord-like structure formation by ECs seeded on top of Matrigel (**Fig. 6D**). The length and sprouts of the cords

were evaluated by microscopy after 24 h. No statistical differences ($P>0.05$, n=6) were observed in the length of the cords for HUVECs treated with D25-VEGF or VEGF; however, HUVECs treated with D25-VEGF had a statistically lower number of sprouts than cells treated with VEGF ($P<0.001$, n=6). These differences are likely ascribed to differences in ERK activity as previously demonstrated [39].

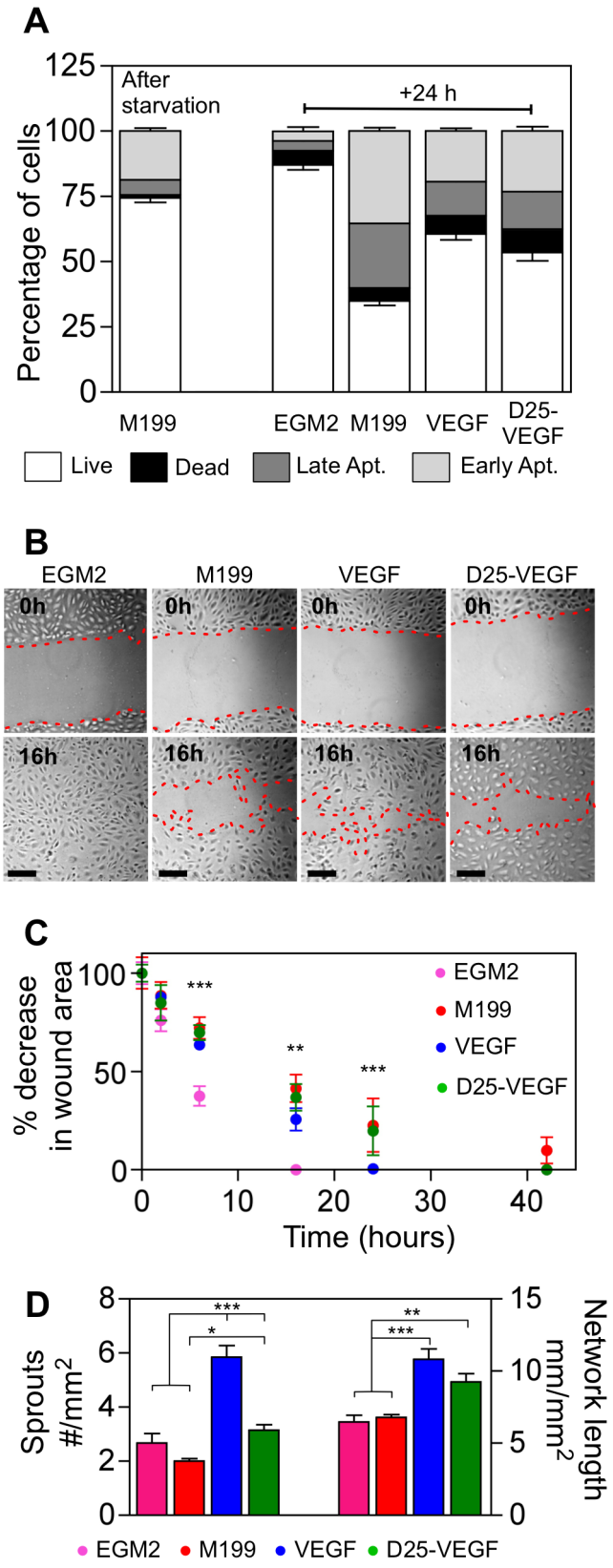

Figure 7 - Effect of free and conjugated VEGF (D25-VEGF) in EC survival, migration and capacity to form cord-like structures. (A) Cell survival under starvation conditions as assessed by annexin/PI staining followed by flow cytometry analysis. HUVECs were starved for ~20 h and then cultured in medium M199, or in medium supplemented with free VEGF or D25-VEGF (50 ng mL^{-1} VEGF) or in EGM-2 medium. Live cells ($Annexin^-/PI^-$), death cells ($Annexin\ V^-/PI^+$), early apoptotic cells ($Annexin^+/PI^-$) and late apoptotic cells ($Annexin^+/PI^+$). Results are average ± SEM, n = 4. Statistical analyses were performed by

an unpaired t-test. (B) Cell migration studies by a scratch-wound assay. HUVECs were cultured in the same conditions as before. (C) Quantification of wound closure. Wound area at each time was normalized by initial wound area. Results are average ± SEM, n = 9. Statistical analyses were performed for free VEGF and D25-VEGF groups by an unpaired t-test. (D) Capacity of ECs to form cord-like structures on top of Matrigel. Tube length and sprouts were evaluated after 24 h of HUVECs seeding. Results are average ± SEM, n = 6. Statistical analyses were performed by ANOVA followed by a Bonferroni post-test.

Preparation and characterization of a hybrid construct containing dexOx-VEGF releasing system and ECs derived from UCB stem cells

Inspired by the unique properties of dexOx-VEGF conjugates, we decided to prepare gels, which in turn could be integrated in a cell supportive 3D fibrin matrix (see below). VEGF was chemically conjugated to dexOx and the remaining aldehyde groups reacted with AAD to form a hydrogel. The gel was formed within minutes, depending on the feed concentration of dexOx and/or AAD [19,40]. Hydrogels with or without VEGF have similar degradation profile (**Fig. 8A**).

To determine the release of VEGF from hydrogels we used two methodologies: (i) quantification by ELISA and (ii) quantification by tritium (^{3}H-VEGF). ELISA results showed that only a tiny amount (< 4%) of VEGF is released from the D25-VEGF gels (**Fig. 8B**). In contrast, D10-VEGF and D5-VEGF hydrogels release high concentration of VEGF, as assessed by ELISA (**Fig. 8B**). The D5-VEGF hydrogels degrade in less than 2 days and release approximately 30% of the initial VEGF over that time while D10-VEGF hydrogels degrade in 4 days and release approximately 7% of the initial VEGF over the same time. In a subsequent step, radiolabeled VEGF (^{3}H-VEGF) was used for the release studies (**Fig. 8C**). In contrast to the ELISA results, a significant release of VEGF was observed for all the experimental groups. This might be due to the fact that VEGF released from D25 and D10 gels is conjugated to chains of oxidized dextran or nanoparticles and thus unable to bind to the ELISA kit.

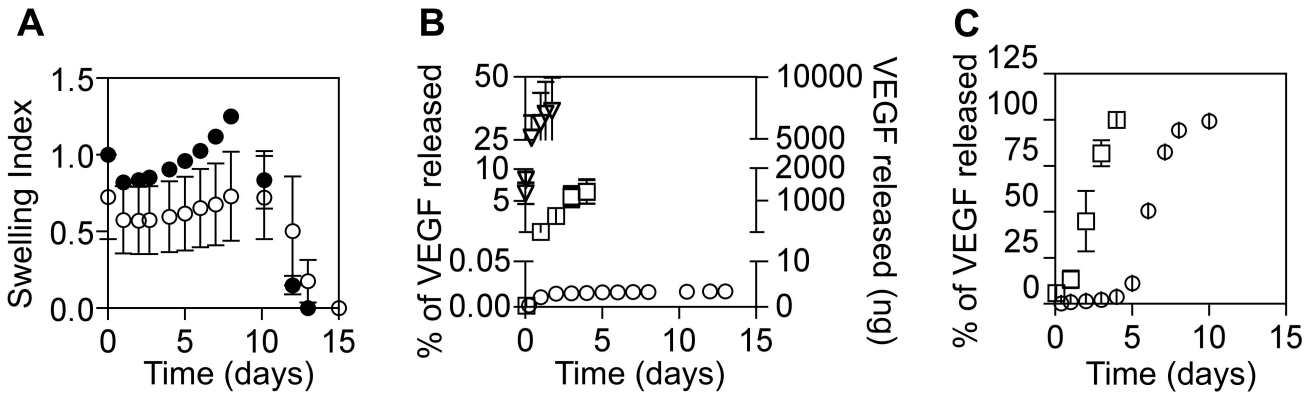

Figure 8 - Characterization of hydrogels containing VEGF conjugates. (A) Swelling index of D25 hydrogels, loaded (○) or not (●) with VEGF. (B) Release of VEGF from D5 (▽), D10 (□) and D25 (○) hydrogels as quantified by ELISA. Results are either in percentage or total mass released. (C) Release of VEGF from D10 (□) and D25 hydrogels (○) as quantified by scintillation. Results are average ± SEM, *n* = 3.

The hybrid constructs were formed by two components: (i) a hydrogel of dexOx-VEGF cross-linked with AAD and (ii) a fibrin hydrogel embedding the dexOx-VEGF hydrogel (**Fig. 9A**). Fibrin gels were selected because in a previous study we showed that these gels provide a permissive environment for EC adhesion, migration and 3-D organization [21]. The dexOx hydrogels containing VEGF (10 µL volume) were prepared initially in a syringe plunger, after which a mixed aqueous solution of fibrinogen and thrombin (50 µL in total) was placed on top of the dexOx hydrogel (**Figs. 9A and 9B**). UCB-derived ECs ($CD34^+$), previously characterized by us [21], were immersed in the fibrin gel precursor solution, prior to application to the syringe. These cells have a typical cobblestone morphology, and express high levels of EC markers, including CD31, von Willebrand factor (vWF), CD34 and Flk-1/KDR over time [21]. After the curing of the fibrin gel, the hybrid constructs were placed in EGM-2 medium and incubated at 37°C. Cell viability was quantified by a LIVE/DEAD assay at the 6^{th} day. D5 hydrogels located within fibrin gels were completely degraded before the 6^{th} day, while partial degradation or no macroscopic degradation were observed for the remaining hydrogels, D10 and D25, respectively. The survival of the ECs was high (> 80%) for all the experimental groups tested (**Fig. 10**).

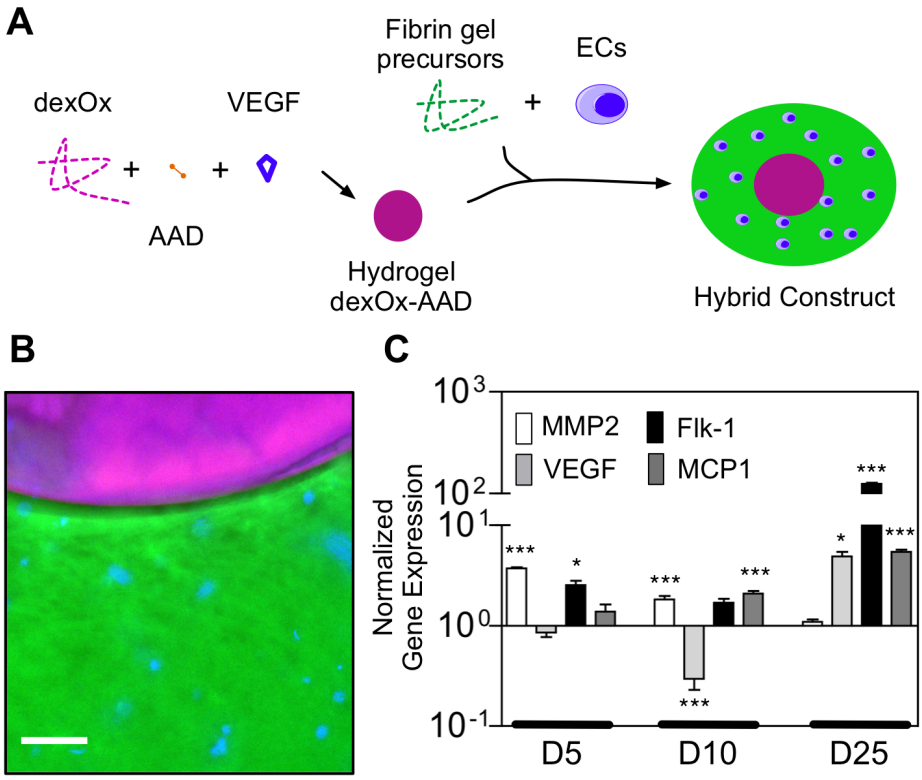

Figure 9 - Modulation of the activity of ECs derived from umbilical cord blood stem cells in a hybrid construct. (A) Scheme showing the preparation of the hybrid construct. (B) Fluorescence image showing the interface between dexOx hydrogel and fibrin hydrogel. DexOx hydrogel (labeled with TRITC) containing immobilized VEGF is in red/purple; fibrin hydrogel is in green (Alexa 488-labeled), and the nuclei of cells are in blue (Hoechst 34580-labeled). Scale bar is 200 μm. (C) Gene expression on ECs encapsulated in hybrid networks for 6 days, as assessed by qRT-PCR. Gene expression of ECs in hybrid networks containing VEGF was normalized by gene expression of the same cells in hybrid networks without VEGF. Results are average ± SEM, *n* = 4. Each gene of experimental group was compared to the same gene in the control group (*i.e.*, cells encapsulated in a hybrid construct without VEGF) by an unpaired t-test.

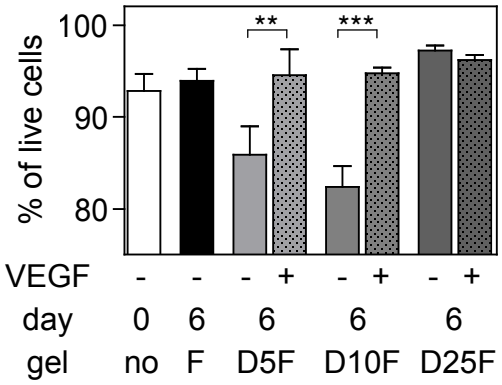

Figure 10 - Viability of ECs encapsulated in hybrid constructs as assessed by a LIVE/DEAD assay at day 6 (n=9).

The effect of dexOx-VEGF on the encapsulated ECs was evaluated by qRT-PCR analysis. We analyzed the expression of VEGF; the receptor of VEGF [Flk-1 (VEGFR-2)]; matrix metallo-proteinase 2 (MMP-2), which is involved in the remodelling of the extracellular matrix (ECM) and cell migration and which has been shown to be stimulated by VEGF *in vitro*;[41] and MCP-1, an endogenous cytokine with chemotactic properties toward smooth muscle cells (SMCs) and upregulated when ECs are exposed to certain conditions.[42] Gene expression in cells encapsulated in constructs with VEGF was normalized by the corresponding gene expression in cells encapsulated in fibrin hydrogels without VEGF (**Fig. 9C**). The expression of MMP-2 was higher for gels that have the ability to rapidly release VEGF (D5 and D10). The constructs with D25-VEGF have no statistically significant upregulation of the MMP-2 gene at day 6, as compared to the control. These results are in line with the fact that VEGF induces the migration and invasion of endothelial cells.[43] For invasion, cells secrete metalloproteases to allow cleavage of matrix proteins. The secretion of MMP-2 in VEGF-activated endothelial cells is mediated by integrins in a phosphatidylinositol 3-kinase-dependent way.[43]

Constructs that rapidly release VEGF have cells showing a down-regulation in VEGF gene expression. By contrast, constructs that slowly release VEGF (D25-VEGF hydrogels) have cells showing an upregulation of VEGF and VEGFR-2 gene expression. The down-regulation of VEGF expression in constructs having D5 and D10 was expected since exogenous VEGF tightly regulate VEGF gene expression.[44] The up-regulation of VEGF and VEGFR2 genes in constructs having D25 hydrogels is likely due to the unique inductive properties of VEGF conjugate (*i.e.*, immobilized to dextran). Cells encapsulated in constructs with D25 hydrogels express high levels of MCP-1, a chemotactic protein, specific for SMCs, which would benefit the survival of the ECs, by secreting EC-specific cytokines and growth factors.[45] Collectively, our results indicate that it is feasible to prepare constructs that can modulate EC gene expression and ultimately cell activity depending in the release of soluble or VEGF conjugate. Further work is required to study the effects of this technology *in vivo* for the neovascularization of ischemic tissues.

CONCLUSIONS

This work shows that VEGF conjugated to dextran has different properties as compared to free VEGF. Like free VEGF, D25-VEGF is able to interact with VEGFR-2; however, at different kinetics. Both VEGF and D25-VEGF were able to induce phosphorylation of VEGFR-2 at similar levels in HUVECs after 10 and 30 min of treatment; however, D25-VEGF induces higher levels of phosphorylation at 2 h than free VEGF. The higher levels of VEGFR-2 phosphorylation in D25-VEGF than free VEGF is likely due to the retention of high concentrations of D25-VEGF in early endosomes, which are still active in terms of signaling. Differences in the intracellular trafficking kinetic in free and D25-VEGF do not affect Akt but do affect ERK½ signalling pathway. Lower expression of ERK½ protein, slower accumulation of intracellular Ca^{2+}, lower cell migration in a scratch-wound assay and lower sprouts formation in a Matrigel assay are observed in cells exposed to D25-VEGF compared to free VEGF. We also show that it is possible to integrate dexOx-VEGF in gel matrices and to modulate EC gene expression according to the dexOx-VEGF/VEGF release profile from the gels. We envision that these constructs might be beneficial to modulate the pro-angiogenic activity of vascular cells in ischemic tissues.

ACKNOWLEDGMENTS

The authors would like to acknoweldge the financial support of Crioestaminal (project nº CENTRO-01-0202-FEDER-005476 “INJECTCORD”), Marie Curie Grant (Grant nº 230929 to LF), MIT-Portugal Program (focus in Bioengineering to LF; BPD 000081/CMIT to DP), Fundação para a Ciência e Tecnologia (PTDC/SAU-BEB/098468/2008 to LF; SFRH/BD/40077/2007 to HV) and Instituto de Investigação Interdisciplinar (III/BIO/20/2005 to JM); we also thank Hélder Pinto for assistance on the Multiplex analysis; Attila Köfalvi for assistance on the radioactivity measurements.

REFERENCES

1. Lee K, Silva EA, Mooney DJ (2011) Growth factor delivery-based tissue engineering: general approaches and a review of recent developments. J R Soc Interface 8: 153-170.
2. Eppler SM, Combs DL, Henry TD, Lopez JJ, Ellis SG, et al. (2002) A target-mediated model to describe the pharmacokinetics and hemodynamic effects of recombinant human vascular endothelial growth factor in humans. Clin Pharmacol Ther 72: 20-32.
3. Hanft JR, Pollak RA, Barbul A, van Gils C, Kwon PS, et al. (2008) Phase I trial on the safety of topical rhVEGF on chronic neuropathic diabetic foot ulcers. J Wound Care 17: 30-37.
4. Henry TD, Annex BH, McKendall GR, Azrin MA, Lopez JJ, et al. (2003) The VIVA trial: Vascular endothelial growth factor in Ischemia for Vascular Angiogenesis. Circulation 107: 1359-1365.
5. Leslie-Barbick JE, Moon JJ, West JL (2009) Covalently-Immobilized Vascular Endothelial Growth Factor Promotes Endothelial Cell Tubulogenesis in Poly(ethylene glycol) Diacrylate Hydrogels. J Biomat Sci, Polym Ed 20: 1763-1779.
6. Phelps EA, Landázuri N, Thulé PM, Taylor WR, García AJ (2010) Bioartificial matrices for therapeutic vascularization. Proc Natl Acad Sci USA 107: 3323-3328.
7. Porter AM, Klinge CM, Gobin AS (2010) Biomimetic Hydrogels with VEGF Induce Angiogenic Processes in Both hUVEC and hMEC. Biomacromolecules 12: 242-246.
8. Shen YH, Shoichet MS, Radisic M (2008) Vascular endothelial growth factor immobilized in collagen scaffold promotes penetration and proliferation of endothelial cells. Acta Biomat 4: 477-489.
9. Müller S, Koenig G, Charpiot A, Debry C, Voegel J-C, et al. (2008) VEGF-Functionalized Polyelectrolyte Multilayers as Proangiogenic Prosthetic Coatings. Adv Funct Mat 18: 1767-1775.
10. Chung Y-I, Kim S-K, Lee Y-K, Park S-J, Cho K-O, et al. (2010) Efficient revascularization by VEGF administration via heparin-functionalized nanoparticle-fibrin complex. J Control Rel 143: 282-289.
11. Ferreira LS, Squier T, Park H, Choe H, Kohane DS, et al. (2008) Human embryoid bodies containing nano- and microparticulate delivery vehicles. Adv Mat 20: 2285-2291.
12. Aizawa Y, Wylie R, Shoichet M (2010) Endothelial Cell Guidance in 3D Patterned Scaffolds. Adv Mat 22: 4831-4835.
13. Chen RR, Silva EA, Yuen WW, Brock AA, Fischbach C, et al. (2007) Integrated approach to designing growth factor delivery systems. FASEB J 21: 3896-3903.
14. Harris J, Martin N, Modi M (2001) Pegylation: A Novel Process for Modifying Pharmacokinetics. Clinical Pharmocokinetics 40: 539-551.
15. Pasut G, Veronese FM (2007) Polymer-drug conjugation, recent achievements and general strategies. Progress in Polymer Science 32: 933-961.

16. Battersby J, Clark R, Hancock W, Puchulu-Campanella E, Haggarty N, et al. (1996) Sustained release of recombinant human growth hormone from dextran via hydrolysis of an imine bond. J Control Rel 42: 143-156.
17. Bernstein A, Hurwitz E, Maron R, Arnon R, Sela M, et al. (1978) Higher antitumor efficacy of daunomycin when linked to dextran: in vivo and in vitro studies. J Natl Cancer Inst 60: 379-384.
18. Kobayashi M, Takatsu K (1994) Cross-linked Stabilization of Trypsin with Dextran-dialdehyde. Biosci Biotechnol Biochem 58: 275-278.
19. Maia J, Ribeiro MP, Ventura C, Carvalho RA, Correia IJ, et al. (2009) Ocular injectable formulation assessment for oxidized dextran-based hydrogels. Acta Biomat 5: 1948-1955.
20. Provencher S (1982) CONTIN: A general purpose constrained regularization program for inverting noisy linear algebraic and integral equations. Comput Phys Commun 27: 229-242.
21. Pedroso DCS, Tellechea A, Moura L, Fidalgo-Carvalho I, Duarte J, et al. (2011) Improved Survival, Vascular Differentiation and Wound Healing Potential of Stem Cells Co-Cultured with Endothelial Cells. Plos One 6: e16114.
22. Gerber H, McMurtrey A, Kowalski J, Yan M, Keyt B, et al. (1998) Vascular endothelial growth factor regulates endothelial cell survival through the phosphatidylinositol 3 '-kinase Akt signal transduction pathway - Requirement for Flk-1/KDR activation. J Biol Chem 273: 30336-30343.
23. Liang C-C, Park AY, Guan J-L (2007) In vitro scratch assay: a convenient and inexpensive method for analysis of cell migration in vitro. Nature Protocols 2: 329-333.
24. Silva EA, Mooney DJ (2007) Spatiotemporal control of vascular endothelial growth factor delivery from injectable hydrogels enhances angiogenesis. J Thromb Haemost 5: 590-598.
25. Anderson SM, Chen TT, Iruela-Arispe ML, Segura T (2009) The phosphorylation of vascular endothelial growth factor receptor-2 (VEGFR-2) by engineered surfaces with electrostatically or covalently immobilized VEGF. Biomaterials 30: 4618-4628.
26. Yamaguchi N, Zhang L, Chae B-S, Palla CS, Furst EM, et al. (2007) Growth factor mediated assembly of cell receptor-responsive hydrogels. J Am Chem Soc 129: 3040-3041.
27. Muller YA, Christinger HW, Keyt BA, de Vos AM (1997) The crystal structure of vascular endothelial growth factor (VEGF) refined to 1.93 A resolution: multiple copy flexibility and receptor binding. Structure 5: 1325-1338.
28. Fairbrother WJ, Champe MA, Christinger HW, Keyt BA, Starovasnik MA (1998) Solution structure of the heparin-binding domain of vascular endothelial growth factor. Structure 6: 637-648.
29. Matsumoto T, Claesson-Welsh L (2001) VEGF Receptor Signal Transduction. Sci STKE 2001: re21.
30. Chen TT, Luque A, Lee S, Anderson SM, Segura T, et al. (2010) Anchorage of VEGF to the extracellular matrix conveys differential signaling responses to endothelial cells. J Cell Biol 188: 595-609.
31. Gampel A, Moss L, Jones MC, Brunton V, Norman JC, et al. (2006) VEGF regulates the mobilization of VEGFR2/KDR from an intracellular endothelial storage compartment. Blood 108: 2624-2631.
32. Mu F-T, Callaghan JM, Steele-Mortimer O, Stenmark H, Parton RG, et al. (1995) EEA1, an Early Endosome-Associated Protein. J Biol Chem 270: 13503-13511.
33. Lampugnani MGM, Orsenigo FF, Gagliani MCM, Tacchetti CC, Dejana EE (2006) Vascular endothelial cadherin controls VEGFR-2 internalization and signaling from intracellular compartments. J Cell Biol 174: 593-604.
34. Sheikh H, Yarwood H, Ashworth A, Isacke CM (2000) Endo180, an endocytic recycling glycoprotein related to the macrophage mannose receptor is expressed on fibroblasts, endothelial cells and macrophages and functions as a lectin receptor. Journal of Cell Science 113: 1021-1032.
35. Dawson NS, Zawieja DC, Wu MH, Granger HJ (2006) Signaling pathways mediating VEGF165-induced calcium transients and membrane depolarization in human endothelial cells. FASEB J 20: 991-993.
36. Gupta K, Kshirsagar S, Li W, Gui L, Ramakrishnan S, et al. (1999) VEGF prevents apoptosis of human microvascular endothelial cells via opposing effects on MAPK/ERK and SAPK/JNK signaling. Exp Cell Res 247: 495-504.

37. Rousseau S, Houle F, Landry J, Huot J (1997) p38 MAP kinase activation by vascular endothelial growth factor mediates actin reorganization and cell migration in human endothelial cells. Oncogene 15: 2169-2177.
38. Pedram A, Razandi M, Levin ER (1998) Extracellular signal-regulated protein kinase/Jun kinase cross-talk underlies vascular endothelial cell growth factor-induced endothelial cell proliferation. J Biol Chem 273: 26722-26728.
39. Shankar S, Chen Q, Srivastava RK (2008) Inhibition of PI3K/AKT and MEK/ERK pathways act synergistically to enhance antiangiogenic effects of EGCG through activation of FOXO transcription factor. J Mol Signal 3: 7.
40. Maia J, Ferreira L, Carvalho R, Ramos M, Gil MH (2005) Synthesis and characterization of new injectable and degradable dextran-based hydrogels. Polymer 46: 9604-9614.
41. Burbridge MF, Cogé F, Galizzi JP, Boutin JA, West DC, et al. (2002) The role of the matrix metalloproteinases during in vitro vessel formation. Angiogenesis 5: 215-226.
42. Rollins B, Yoshimura T, Leonard E, Pober J (1990) Cytokine-activated human endothelial cells synthesize and secrete a monocyte chemoattractant, MCP-1/JE. Am J Pathol 136: 1229-1233.
43. Prager GW, Breuss JM, Steurer S, Mihaly J, Binder BR (2004) Vascular endothelial growth factor (VEGF) induces rapid prourokinase (pro-uPA) activation on the surface of endothelial cells. Blood 103: 955-962.
44. Lee S, Chen TT, Barber CL, Jordan MC, Murdock J, et al. (2007) Autocrine VEGF signaling is required for vascular homeostasis. Cell 130: 691-703.
45. Heydarkhan-Hagvall S, Helenius G, Johansson BR, Li JY, Mattsson E, et al. (2003) Co-culture of endothelial cells and smooth muscle cells affects gene expression of angiogenic factors. J Cell Biochem 89: 1250-1259.

CHAPTER 6 – General conclusions

The first goal of this thesis was to develop new differentation and maturation protocols of hESCs into vascular cells (endothelial and smooth muscle cells). In most cases, the application of hESC-derived vascular cells in regenerative medicine, drug screening and toxicology studies requires the use of mature and specialized cells. These cells are vital for accurate assessment and therapeutic discovery. Furthermore, it is believed that regenerative medicine platforms requires cells that are derived from the same embryonic lineage as in the affected tissue or organ [1].

Prior to this thesis, although several studies have reported the differentiation of human pluripotent stem cells into SMCs [2,3], no study has truly addressed the maturation of SMCs. The maturation here means complete organization of the contractile machinery of the cells. In this thesis (**chapter 3**) we show that hESC-derived SMCs contractility is mediated by Ca^{2+}, which involves the activation of RhoA/Rho kinase- and Ca^{2+}/Calmodulin (CaM)/myosin light chain kinase (MLCK)-dependent pathways. Our work shows for the first time part of the mechanism underlining the maturation of hESC-derived SMCs, and has identified endothelin-1 as a major player in that process. Due to time constraints, we did not characterize the sub-type of SMCs obtained in our study. In fact, only recently, protocols to differentiate human pluripotent stem cells into different sub-types of SMCs [1] have been reported. Because SMCs were derived from $CD34^{+}$ cells, we believe that the SMCs obtained in this work are mesodermic vascular SMCs, although it is unclear whether they are derived from lateral plate mesoderm or paraxial mesoderm.

Another particular innovative aspect in **chapter 3** is related to the impact of the 3D environment at the geno- and phenotype of the differentiated SMCs [4]. Gene expression studies have demonstrated that human aortic SMCs encapsulated in a 3D collagen matrix have significantly less focal adhesions, lower proliferation, and lower α-SMA expression than cells in 2D [5]. However, to our knowledge, no study has compared the gene expression of smooth muscle progenitor cells (SMPCs) with fully differentiated SMCs when cultured in 2D or 3D systems. Our results show that hESC-derived SMPCs encapsulated for 3 days in fibrin gels express similar gene levels of α-SMA, SM-MHC, and SMα22 as encapsulated hVSMCs. Therefore, our results highlight the importance of a 3D environment to modulate the differentiation/maturation of hESC-derived SMPCs.

In **chapter 4**, we developed a protocol to differentiate hESCs into arterial ECs. This specialization has not been described before for hESCs. Only recently, it has been demonstrated the differentiation of human pluripotent stem cells (hPSCs) into a sub-type of ECs, in this case into ECs with blood brain barrier (BBB) properties [6]. The method involved the differentiation of hPSCs into endothelial and neural cells followed by purification of the BBB-like endothelial population on selective matrix. Our results indicate that hESCs exposed to $VEGF_{165}$, thymosin β4 and TGFβ inhibitor administered at different times over a 18-day differentiation protocol give rise to arterial ECs. These cells further maturate after exposure to fluidic shear stress of 20 dyne/cm^2.

An innovative aspect of this study was the demonstration that arterial ECs derived from hESCs cultured in flow conditions express HPSG as somatic arterial ECs express in vivo. We speculate that HPSGs mediate the upregulation of arterial genes and therefore EC maturation. Furthermore, we show that arterial ECs are much more sensitive to the action of terbinafine in flow than in static conditions.

The second goal of this thesis was the identification of new strategies to modulate vascular cell activity (second part). We show that VEGF conjugated with dextran has a prolonged bioactivity than unconjugated VEGF (**chapter 5**). Our results indicate that this effect is at least in part mediated by the accumulation of VEGF in early endosomes (EEA1+ organelles). It is known that membrane trafficking and degradation along the endocytic pathway is regulated by a wide array of regulatory molecules including GTPases, ubiquitin ligases and clthrin- and ubiquitin-binding effectors [7]. Recent data indicate that VEGFR-2 after activation by VEGF is trafficked to Rab5a and EEA1 positive organelles. Furthermore, Rab7a GTPase regulates early to late endosome trafficking [7]. The mechanism underlining the accumulation of VEGF conjugated to dextran in EEA1+ organelles is still unclear but it may involve the formation of multiple complexes of the VEGF conjugate with VEGFR-2 and physical hindrances because of the size of dextran. These aspects should be further investigated in the near future. The differences in the trafficking of the unconjugated and conjugated VEGF had consequences in the activation of the signaling pathways and in the activity of the cells. We further demonstrate the incorporation of the VEGF conjugate in a 3D matrix and its effect in the modulation of the activity of ECs derived from cord blood hematopoietic stem cells.

Perspectives and future work

The hESC-derived vascular cells reported here have tremendous potential for the design of cellular kits for drug screening and toxicology assessment. However, further advances are needed to develop high-throughput microfluidic systems that mimic the 3-D environment of vascular living systems. A recent study of Hsiao has reported a microfluidic system with 28 side chambers that could harbour spheroids of prostate cancer cells and endothelial cells [8]. Perhaps one day this type of system can be adapted for the culture of endothelial cells, enabling the high-throughput screening of multiple drugs in culture conditions that mimic physiologic conditions.

The recent advances in the generation of iPSCs and the possibility to create in vitro models of diseases open excellent opportunities for the platforms investigated in this thesis. It will be interesting to extend the studies performed in hESCs to iPSCs (obtained from healthy and ill patients) and compare the differences in terms of kinetics of differentiation, stability of the vascular phenotype, response to fluidic shear stress, etc… It will be also very important to understand in more detail the mechanism underlining the differentiation of hESCs (and potentially iPSCs) into the different sub-types of ECs. Our ongoing studies are focused in determining the relevance of Shh and Notch signaling pathways in the specification of hESCs into arterial phenotype. Furthermore, we are conducting experiments in order to elucidate whether the $CD31^+$ cells isolated from EBs at day 18 are already specified in arterial ECs or whether the specification occurs afterwards. Finally, the use of vascular cells derived from human pluripotent stem cells in microfluidic systems gives us an opportunity to evaluate the embryonic toxicity of libraries of chemical compounds at levels not possible until now.

Further experiments are also required to demonstrate the biological activity of VEGF conjugated to dextran. Conjugated VEGF may be useful in guiding the differentiation of transplanted endothelial precursor cells into mature endothelial cells in several contexts of ischemic diseases. Specifically, the conjugated VEGF may find application in the treatment of chronic wounds.

References

1. Cheung C, Bernardo AS, Trotter MWB, Pedersen RA, Sinha S (2012) Generation of human vascular smooth muscle subtypes provides insight into embryological origin-dependent disease susceptibility. Nature Biotechnology 30: 165-173.
2. Hill KL, Obrtlikova P, Alvarez DF, King JA, Keirstead SA, et al. (2010) Human embryonic stem cell-derived vascular progenitor cells capable of endothelial and smooth muscle cell function. Experimental Hematology 38: 246-257.e241.
3. Vo E, Hanjaya-Putra D, Zha Y, Kusuma S, Gerecht S (2010) Smooth-Muscle-Like Cells Derived from Human Embryonic Stem Cells Support and Augment Cord-Like Structures In Vitro. Stem Cell Rev and Rep.
4. Ross JJ, Hong Z, Willenbring B, Zeng L, Isenberg B, et al. (2006) Cytokine-induced differentiation of multipotent adult progenitor cells into functional smooth muscle cells. J Clin Invest 116: 3139-3149.
5. Li S, Lao J, Chen BPC, Li Y-s, Zhao Y, et al. (2003) Genomic analysis of smooth muscle cells in 3-dimensional collagen matrix. FASEB J 17: 97-99.
6. Lippmann ES, Azarin SM, Kay JE, Nessler RA, Wilson HK, et al. (2012) Derivation of blood-brain barrier endothelial cells from human pluripotent stem cells. Nature biotechnology.
7. Jopling HM, Odell AF, Hooper NM, Zachary IC, Walker JH, et al. (2009) Rab GTPase regulation of VEGFR2 trafficking and signaling in endothelial cells. Arterioscler Thromb Vasc Biol 29: 1119-1124.
8. Hsiao AY, Torisawa Y-s, Tung Y-C, Sud S, Taichman RS, et al. (2009) Microfluidic system for formation of PC-3 prostate cancer co-culture spheroids. Biomaterials 30: 3020-3027.